Copyright is owned by the Author of the thesis. Permission is granted for an individual to download a copy for research and private study only. The thesis may not be reproduced elsewhere without the permission of the Author.



Exploring the prevalence and molecular basis of tomato leaf mould caused by *Fulvia fulva* on disease-resistant tomato cultivars in commercial New Zealand glasshouses

A thesis presented in partial fulfilment
of the requirements for the degree of
Master of Science
in
Plant Breeding
at Massey University, Palmerston North, New Zealand.

Francisco Ferrada-Hartley
2026

Abstract

Leaf mould disease, caused by the fungus *Fulvia fulva* (formerly *Cladosporium fulvum*), can significantly reduce tomato yields in commercial glasshouses. Protection against this disease has predominantly been based on the introgression of one or two *Cf* resistance genes from wild tomato species. For example, most resistant cultivars contain the *Cf-9* locus, which harbours the resistance genes *Cf-9B* and *Cf-9C*. In all cases, these *Cf* genes encode immune receptors that recognise specific virulence factors of *F. fulva* called effectors. Unfortunately, however, resistance conferred by *Cf* genes can be overcome through mutation or deletion of the genes encoding the recognised effectors. This has led to the global emergence of *F. fulva* strains capable of overcoming all deployed *Cf* genes. As such, currently deployed *Cf* genes no longer provide reliable control against leaf mould disease. Recently, wild tomato plants with one or more of 10 new *Cf* resistance genes were identified, suggesting that these genes could be stacked in commercial tomato cultivars through breeding to provide durable resistance. However, before these *Cf* genes can be introduced into commercial tomato cultivars, it must first be determined whether they have already been overcome by *F. fulva* through mutation of the corresponding effector genes.

In the current study, I aimed to address this knowledge gap by investigating *F. fulva* strains present in commercial tomato glasshouses across New Zealand. Specifically, this project sought to determine the prevalence of leaf mould on various cultivars currently grown in the country, particularly those carrying *Cf*-derived resistance genes (including cultivars marketed as “Ff:A–E”, which harbour the *Cf-9* locus). Initial glasshouse observations revealed apparent leaf mould symptoms on cultivars previously considered to be resistant. Establishing whether these cultivars remain protected, or whether their resistance genes have been widely overcome, is essential for informing future breeding programmes.

To address this aim, a field survey was conducted across 20 tomato growing sites in New Zealand, encompassing mostly commercial glasshouses, during which leaf mould-infected samples were collected, for the most part, from tomato cultivars considered to be resistant. Leaf mould was recorded on all four resistant cultivars sampled, indicating that these cultivars did not remain reliably protected under the

conditions encountered, though confirming this pattern nationally would require wider scrutiny across more cultivars and locations.

F. fulva was isolated from three samples (one from a resistant cultivar and two from *F. fulva* collections), visually characterised, stored, and prepared for genomic DNA extraction. The three isolates spanning a temporal range (collected in the 1980s, 2022 and 2025) were whole-genome sequenced, and the coding sequences of 20 known avirulence (*Avr*) and extracellular protein (*Ecp*) effector genes were reconstructed and compared against published reference alleles to identify mutations, truncations and gene-loss events. The effector repertoire was largely conserved, with changes concentrated in the *Avr* genes: a mutation profile consistent with the predicted evasion of several deployed *Cf* genes. In contrast, the effectors recognised by the recently identified resistances were largely intact across all isolates, indicating that these new *Cf* genes are predicted to remain effective and represent viable candidates for deployment.

Together, these findings provide a first genomic assessment of the current status of leaf mould resistance in commercially grown tomato cultivars in New Zealand. By clarifying which *Cf* resistance genes appear to have been overcome and which are predicted to remain effective, this research supports evidence-based cultivar deployment, reduces the risk of resistance breakdown, and strengthens Integrated Pest Management (IPM) strategies within the New Zealand tomato industry.

Acknowledgments

I would like to express my sincere gratitude to the individuals and organisations who made this research possible.

First, I am deeply grateful to Dinah Cohen from Tomatoes New Zealand for her commitment and support, and to the team at Te Ahikawariki / Vegetable Industry Centre of Excellence (VICE) for their generous funding and support. Their commitment to advancing the New Zealand tomato industry has been the cornerstone of this research. Special thanks to T&G Global for awarding the Edward Turner Horticulture Futures Grant, which significantly facilitated this research and my postgraduate studies.

Special thanks must go to my academic supervisors, Associate Professor Carl Mesarich and Dr Marianna Tarallo, Dr Svetla Sofkova-Bobcheva and Keith Thorburn from Massey University, and Dr Joanna Bowen from the Bioeconomic Science Institute, for their invaluable guidance, time, and consistent engagement throughout this endeavour. Your expertise and mentorship have been instrumental in shaping this work.

I would also like to extend my thanks to my colleague and friend Wanda O'Meara, Mark Christensen (Heritage Food Crops Research Trust), Shane McCulloch (Shane's Greenhouses), Peter Mundy and Jordie (Castle Rock Orchard), Robert Wu (Rosy Red Produce), Yubo and Rofl (Gourmet New Zealand), Albert Shih (Vegefresh Growers) and Chris and Renata (Bioforce), who contributed their time, facilities, and samples to this study; this research would not have been possible without your cooperation.

Additionally, I am immensely grateful to the T&G Covered Crops team, especially my colleagues Andrew Hutchinson, Chris Cowie, Nilesh Patel, Dave Naicker, Warren Frost, and Ben Smith, for their ongoing encouragement and for providing the professional environment necessary to conduct this research.

On a personal note, I wish to thank my family. To my parents, Jose and Patricia, and my brother, Pablo, in Chile: thank you for always believing in me, despite the distance

between us. To my relatives-in-law, Trish, Rebecca, and Tim, thank you for your constant help and unwavering support throughout this journey.

Finally, to my wife, Wendy, and my beautiful children, Liam and Tristan: thank you for your love, patience, and support. This achievement is as much yours as it is mine, and I am profoundly grateful for the sacrifices you made to allow me to complete this endeavour.

Table of Contents

1. Introduction 20
1.1. An Overview of New Zealand's Fresh Tomato Industry 20
1.2. The Local Greenhouse Environment 20
1.3. Open-field Tomatoes and the Processed Tomato Industry 21
1.4. Varietal Diversity and Consumer Preferences 22
1.5. Economic Value and Market Structure 22
1.6. Industry Challenges 23
1.7. Biosecurity Concerns 24
2. *Fulvia fulva*, the Causal Agent of Tomato Leaf Mould 26
2.1. Pathogenic Lifestyle and Host Range 26
2.2. Colonisation Mechanism and Infection Process 27
2.3. Life Cycle and Environmental Conditions 29
2.4. Visual Symptoms 30
2.5. Genome Overview 33
2.5.1. Genomic Architecture and the Two-Speed Genome of Fulvia fulva 33
2.5.2. Mating-Type Loci and the Potential for Heterothallism in Fulvia fulva 35
2.6. Dissection of the *Fulvia fulva*–tomato interaction at the molecular level 37
2.6.1. Compatible Interactions (Disease Susceptibility) 37
2.6.2. Incompatible Interactions (Disease Resistance) 38
2.6.3. Cf Immune Receptor (Resistance) Proteins 39
2.7. Resistance to *Fulvia fulva* in Commercially-Grown Tomatoes 40
2.8. New Resistances to Leaf Mould Identified in Wild Tomato 41
2.9. Emerging Challenges in New Zealand's Leaf Mould Management 42
3. Research Objectives and Hypotheses 44
3.1. Objectives 44
3.2. Research Hypotheses 44
3.3. Thesis structure and overview 45
4. Materials and Methods 48
4.1. Stakeholder Engagement and Participant Recruitment Strategy 48
4.2. Sample Collection Protocol 48
4.2.1. Operational Procedure 49
4.2.2. Specimen Recovery and Biosecurity 49
4.3. Fungal Isolation 50
4.4. Cryopreservation and Long-Term Storage 51

4.5. Genomic DNA Extraction from Fungal Isolates 52
4.6. DNA Extraction Protocol 53
4.6.1. CTAB DNA Extraction Method 53
4.6.2. High Molecular Weight DNA Extraction Protocol 54
4.7. Assessment of DNA Quality and Concentration 55
4.7.1. Fluorometric and Spectrophotometric Quantification 55
4.7.2. Agarose Gel Electrophoresis for DNA Integrity 55
4.8. Bioinformatic Pipeline 56
4.8.1. Genome Sequencing 56
4.8.2. Reference and Isolate gDNA Alignment and Output Overview 57
4.8.3. Sequence Preparation and Intron Excision 58
4.8.4. Multiple Sequence Alignment 58
4.8.5. Variant Calling and Integrity Classification 59
4.8.6. Conservation and Divergence Metrics 59
4.8.7. Data Outputs and Structured Validation 60
4.8.8. Literature Metadata Extraction 60
4.8.9. Literature Cross-Referencing 61
4.8.10. Visualisation 62
4.8.11. Software and Availability 62
5. Results 64
5.1. Field Collection and Geographic Distribution 64
5.2. Leaf Mould Occurrence on Resistant and Non-Resistant Cultivars 65
5.3. Fungal Isolation and Culture Viability 70
5.4. Morphological Characterisation and Diagnostic Identification 73
5.5. Single Spore Isolation and Purified Culture Development 77
5.6. Biomass Augmentation and DNA Extraction Outcomes 78
5.7. Pathogen Isolation and DNA Extraction Efficiency 78
5.8. An Overview on Effector Integrity Across the *F. fulva* Isolate Panel 79
5.9. Summary of Sequence Variation 82
5.10. Truncation of *Avr2* in CM1 and CO1 Isolates 82
5.11. Amino-acid Substitutions in Avr4 and Avr6 84
5.12. Substitutions in *Ecp* Effectors 86
5.13. Effector Absence 87
5.14. Conservation and Divergence Profiles 88
6. Discussion 91
6.1. Logistical Constraints and Methodological Challenges in *F. fulva* Sampling 91
6.2. Participant-Led Sampling Limitations 92

6.3. Procedural Fidelity Audit 92
6.4. Operational and Biological Constraints on Genome Sequencing 93
6.5. Understanding how Protected Crop Conditions Influence Pathogenesis 94
6.5.1. Temperature and Humidity Gradients 95
6.5.2. Hydraulic Feedback and Stomatal Dynamics 96
6.5.3. Strategic Management Dilemmas and the New Zealand Context 96
6.6. Host Resistance Erosion and Claims of the Breakdown of Commercial “Ff: A-E” Cultivars 97
6.7. The Chemical Deficit and the Necessity of Polygenic Breeding Strategies 98
6.8. Predicted Breakdown of *Cf*-Mediated Resistance in New Zealand Isolates 100
6.8.1. Cf-2 / Avr2 100
6.8.2. Cf-4 / Avr4 101
6.8.3. Cf-4E / Avr4E 101
6.8.4. Cf-5 / Avr5 102
6.8.5. Cf-9 / Avr9 102
6.8.6. Cf-9B / Avr9B 103
6.8.7. Cf-6 / Avr6 104
6.9. Novel Mutations Not Previously Described in the Literature 104
6.9.1. Changes at Previously-Reported Positions 105
6.10. Incursion Events and Mutation Origins in New Zealand: Are mutations or mutation profiles unique to New Zealand? 105
6.11. Mutations Profile: Did These Mutations Arise After the Incursion, or Were They Present in the Founding Population? 106
6.12. Mating Types: Are Both Mating Types Present — and is Sexual Reproduction Occurring? 107
6.13. Clonal Profile: Is the New Zealand Population Clonal? 107
6.14. Concordance with Previous PCR-based Genotyping 108
6.15. Genomic Location and Structural Context of Effector Mutations 110
6.15.1. Avr2 110
6.15.2. Avr4 110
6.15.3. Avr4E 110
6.15.4. Avr5 111
6.15.5. Avr6 111
6.15.6. Avr9 111
6.15.7. Avr9B 112
6.15.8. Ecp genes: Ecp Effectors with New Zealand Changes 112
6.16. Ongoing Genomic Characterisation and Future Directions 113
7. Conclusion 115

7.1. Genome Sequencing Conclusions 116
7.2. Limitations 120
7.3. Future Directions 121
8. References 123
Appendix I: Tomato Leaf Mould Sampling Guidelines 142
Appendix II: Leaf Mould (*Fulvia fulva*) 2024 Project Symptoms Guideline 143
Appendix III: Factsheet – Tomato Leaf Mould 144
Appendix IV: Leaf Mould (*Fulvia fulva*) 2024 Project Sampling Form 145
Appendix V: Statement on the Use of Large Language Model and Generative Artificial Intelligence 146
Appendix VI: Code Availability 147

Figures

Figure 1. Number of registered tomato growers in each New Zealand region (TomatoesNZ, 2025)..... 23
Figure 2. Progressive development of chlorotic lesions on the adaxial (upper) leaf surface of tomato caused by the leaf mould fungus, *Fulvia fulva*. a) Incipient stage of infection, characterised by localised, early-onset chlorosis before widespread cellular disruption. b) Advanced infection showing extended, diffuse, pale-yellow chlorotic spots corresponding to fungal colonisation of the underlying mesophyll. These symptoms result from the death of palisade parenchyma cells due to the pathogen's hemibiotrophic nature, eventually leading to the collapse of leaf tissue. 31
Figure 3. Dense sporulation of *Fulvia fulva* on the abaxial (lower) leaf surface of tomato. These close-up image captures the characteristic velvet-like appearance of the pathogen. The brownish (a), olive-green to brownish (b), greyish (c) and greyish to brownish (d) fungal masses consist of a high density of conidiophores and conidia emerging through the stomata. This stage marks the peak reproductive phase, during which the pathogen is primed for secondary dispersal via wind or water. 31
Figure 4. Progression of *Fulvia fulva* infection of tomato leaves. A series of three consecutive leaves illustrating the transition from incipient to well-developed sporulation, both for the adaxial (a) and abaxial (b) side of these leaves. a) From left to right, the mild stage shows sparse, pale fungal patches; the intermediate stage demonstrates expanding, darkening colonies; and the well-developed stage exhibits a thick, confluent velvety mass covering a significant portion of the leaf underside. b) The sequence highlights the evolution of chlorosis, beginning with faint, indistinct yellowing (incipient), progressing to clearly defined yellow lesions (developed), and concluding with necrotic browning and leaf curling in the most advanced stage of the disease. 32
Figure 5. MaxQ™ 4000 Benchtop Orbital Shaker (Thermo Fisher Scientific, Waltham, MA, USA) containing Potato Dextrose Broth cultures of Fulvia fulva. 52
Figure 6. Leaf mould symptoms on tomato cultivar ‘Grandice’ in Reporoa in November 2024. Different infection stages are seen in the abaxial (lower) side of these leaves. The central leaf shows the highest concentration of velvety sporulation bodies, covering approximately 2/3 of the area. 66

Figure 7. Leaf mould symptoms on tomato landrace (landrace locally bred by the grower) ‘Oley’ in Whanganui in February 2025. a) Scattered, pronounced brownish sporulation bodies are observed across the abaxial (lower) side of the leaf; b) Multiple chlorotic-diffuse spots extend across the majority of the adaxial (upper) side of the leaf. 66
Figure 8. Leaf mould symptoms on tomato cultivar ‘Grandice’ in Tuakau in February 2025. a) The majority of the abaxial (lower) side of the leaf has been overtaken by a greyish-purple clump of sporulation bodies. b) Despite advanced fungal presence in the opposite side of the leaf, the adaxial (upper) side of the leaf appears green, with mild chlorosis symptoms. 67
Figure 9. Leaf mould symptoms on tomato cultivar ‘Duelle’ in Heathcote Valley in February 2025. The picture shows the abaxial (lower) side of the leaf, with seven relatively scattered brown sporulation bodies across the leaf area. 67
Figure 10. Leaf mould symptoms on tomato cultivar ‘Avalantino’ in Clarville in February 2025. a) Mild-difusse chlorosis is present in the adaxial (upper) side of the leaf. b) A single small incipient brownish formation can be seen in the abaxial (lower) side of the leaf. 68
Figure 11. Leaf mould symptoms on tomato cultivar ‘Clobogo’ in Ohaupo in June 2025. In this abaxial (lower) view, a single, relatively condensed point of infection towards the tip of the leaf extends from the midrib to the margin. 68
Figure 12. Variation in culturing and isolation outcomes for *Fulvia fulva* from leaves of tomato cultivars from diverse New Zealand localities. a) Successful isolation of a compatible *F. fulva* colony from surface-disinfected 'Clobogo' leaf tissue (isolate CO1) after 15 days of incubation on Potato Dextrose Agar (PDA) + chloramphenicol (100 mg/L). b) Established *F. fulva* colonies (ICMP 7320) cultured at Massey University, approximately five weeks of age. c) Extensive microbial and fungal contamination from 'Oley' leaf tissue sample (origin: Whanganui) after three weeks of growth in PDA + Lactic Acid (LA; 1%); no *F. fulva* colonies were identified. d) Contamination, presumably by Cladosporium spp., from 'Duelle' leaf tissue samples (Tuakau) samples (isolate DT1) two weeks post-inoculation on PDA + chloramphenicol (100 mg/L).... 71
Figure 13. Single-spored culture derived from a leaf lesion on tomato cultivar Clobogo, Ōhaupō (isolate CO1). Morphological characteristics are consistent with Fulvia fulva. Image shows: a) conidiophore; b) catenated conidia; and c) a conidium. 74

Figure 14. Single-spored culture derived from a leaf lesion on tomato cultivar Grandice, Reporoa (isolate GR1). Morphological characteristics are consistent with Fulvia fulva. Image shows: a) conidiophore, stained with lactophenol blue..... 74
Figure 15. Single-spored culture derived from a leaf lesion on tomato cultivar Duelle, Tuakau (isolate DT1). Morphological characteristics are consistent with *Fulvia fulva*. Image shows conidiophores, stained with lactophenol blue. 75
Figure 16. Single-spored culture sourced from isolate ICMP 7320. Morphological characteristics are consistent with *Fulvia fulva*. Image shows: a) conidiophore; and b) catenate conidia, both stained with lactophenol blue. 75
Figure 17. Single-spored culture derived from a leaf lesion on tomato cultivar Campari, Mokai (isolate CM1). Morphological characteristics are consistent with *Fulvia fulva*. Image shows: a) conidiophore; and b) catenate conidia, both stained with lactophenol blue. 76
Figure 18. Example of contaminant conidia on conidiophores found during single-sporulation culture (Lactophenol blue stain; Compatible with *Penicillium*). 76
Figure 19. Comparative biomass development of single-spore (SS) cultures for *Fulvia fulva*. Left: Isolate ICMP 7320; Right: Isolate CO1. Both isolates were photographed following 17 days of incubation on Potato Dextrose Agar (PDA). Both colonies exhibit a characteristic circumscribed, rounded morphology with typical olive-green pigmentation..... 77
Figure 20. Comparative biomass development in single-spore (SS) cultures of *Fulvia fulva* after 20 days of incubation on Potato Dextrose Agar (PDA) supplemented with chloramphenicol (100 mg/L). a) GR1 exhibiting multiple discrete colonies clustered around a central biomass, characterised by a pale olive-green pigmentation. b) Close-up of isolate GT1 showing a single, significantly larger colony. The morphology remains circumscribed with a complex mosaic of olive-green, grey, and brown pigmentation..... 78
Figure 21. Effector gene integrity across the three New Zealand Fulvia fulva isolates. Each cell shows the integrity status of one effector gene (rows) in one isolate (columns). Integrity was determined by whole-genome sequencing, reconstructing each coding sequence and comparing it against the reference allele (strain 0WU, except *Avr4E*, strain R5). Isolates are ordered left to right by collection date: ICMP 7320 (1980s), CM1 (2022) and CO1 (2025). Cells are coloured by integrity class: intact (green, protein identical to the reference), missense (amber, full-length with one or

more amino-acid substitutions), truncated (orange, coding sequence not spanning the full gene), and absent (grey, effector not detected). Each cell is annotated with percentage protein identity to the reference (100% for intact; — for absent). Of the 60 effector–isolate combinations, 46 were intact, 6 missense, 2 truncated and 6 absent. 81
Figure 22. a) *Avr2* substitution (ICMP 7320). Cropped CDS alignment centred on codon 43 of *Avr2*. The reference allele (0WU) is shown at the top, with isolates ICMP 7320 (1980s), CM1 (2022), and CO1 (2025) below; the Clustal conservation line marks fully conserved columns (*). ICMP 7320 carries a single substitution (c.127T>G) altering codon 43 from TTG to GTG (L43V, boxed); CM1 and CO1 match the reference at this position. Numbers at right indicate cumulative coding nucleotides; b) Avr2 protein, substitution (ICMP 7320). Cropped protein alignment centred on residue 43 of Avr2. Reference (0WU) on top; isolates ICMP 7320 (1980s), CM1 (2022), CO1 (2025) below. ICMP 7320 carries a Leu→Val substitution (L43V, boxed); the conservation line marks this as a strong-group (conservative) change (:). CM1 and CO1 match the reference at this residue. ; c) *Avr2* truncation (CM1, CO1). Cropped CDS alignment at the exon 1–exon 2 junction of *Avr2*. CM1 and CO1 are identical to the reference through exon 1 but lack the second exon (deletion from c.160, shown as dashes), predicting a 53-residue product; ICMP 7320 and the reference retain the full coding sequence; d) Avr2 protein, truncation (CM1, CO1). Cropped protein alignment at the truncation boundary of Avr2. CM1 and CO1 terminate after 53 residues, lacking the C-terminal region present in the reference and ICMP 7320 (missing residues shown as dashes)..... 83
Figure 23. a) *Avr4* substitution (ICMP 7320). Cropped CDS alignment centred on codon 86 of *Avr4*. ICMP 7320 carries a single substitution (c.257G>T) altering codon 86 from TGT to TTT (C86F, boxed); CM1 and CO1 are identical to the reference; b) Avr4 protein, substitution (ICMP 7320). Cropped protein alignment centred on residue 86 of Avr4. ICMP 7320 carries a Cys→Phe substitution (C86F, boxed), a non-conservative change (blank conservation); CM1 and CO1 are identical to the reference. 84
Figure 24. a) *Avr6* substitution (CM1, CO1). Cropped CDS alignment centred on codon 30 of *Avr6*. Both recent isolates, CM1 (2022) and CO1 (2025), carry a single substitution (c.89G>A) altering codon 30 from TGC to TAC (C30Y, boxed); ICMP 7320 is identical to the reference; b) Avr6 protein, substitution (CM1, CO1). Cropped protein

alignment centred on residue 30 of Avr6. CM1 (2022) and CO1 (2025) carry a Cys→Tyr substitution (C30Y, boxed), a non-conservative change; ICMP 7320 is identical to the reference. 85
Figure 25. a) *Ecp4* substitution (ICMP 7320). Cropped CDS alignment centred on codon 127 of *Ecp4*. ICMP 7320 carries a single substitution (c.380T>G) altering codon 127 from GTT to GGT (V127G, boxed); CM1 and CO1 are identical to the reference; b) Ecp4 protein, substitution (ICMP 7320). Cropped protein alignment centred on residue 127 of Ecp4. ICMP 7320 carries a Val→Gly substitution (V127G, boxed), a non-conservative change; CM1 and CO1 are identical to the reference. 86
Figure 26. a) *Ecp12* substitution (ICMP 7320). Cropped CDS alignment centred on codon 124 of *Ecp12*. ICMP 7320 carries a single substitution (c.370G>A) altering codon 124 from GGG to AGG (G124R, boxed); CM1 and CO1 are identical to the reference; b) Ecp12 protein, substitution (ICMP 7320). Cropped protein alignment centred on residue 124 of Ecp12. ICMP 7320 carries a Gly→Arg substitution (G124R, boxed), a non-conservative change; CM1 and CO1 are identical to the reference. . 87
Figure 27. Sequence conservation and divergence across *Avr2* in three New Zealand Fulvia fulva isolates. Per-column Shannon entropy (bits) and percentage identity to the reference allele (0WU) are plotted against reference coordinate position for the Avr2 [coding sequence / protein] alignment of isolates ICMP 7320 (1980s), CM1 (2022) and CO1 (2025). Shannon entropy quantifies variability at each position ($H = -\Sigma\, p_i \log_2 p_i$, with the alignment gap treated as an additional character state), such that invariant positions score zero and higher values indicate greater divergence; percentage identity gives the proportion of isolate sequences matching the reference at each position. Divergence is concentrated in the 3′/C-terminal region corresponding to the second exon, which is absent in CM1 and CO1 (see Figure 22); the remainder of the gene is highly conserved. Avr2 was the only effector showing substantial divergence (mean identity 77.9% nucleotide / 78.2% protein; mean entropy 0.333 bits nucleotide)..... 89

Tables

Table 1. The 22 commercial tomato cultivars available in New Zealand that are marketed as resistant to leaf mould, showing the resistance designation and supplier for each. Designations are Ff:A-E or Pf:A-E, denoting cultivars bred to carry the *Cf-2*, *Cf-4*, *Cf-5*, *Cf-6* and *Cf-9* resistance genes (see Section 2.7); no cultivar in this list carries the Cf:A-E designation. Modified from Bayer Vegetables New Zealand (2026a, b, c, d, e, f), Enza Zaden New Zealand (n.d.), Terranova Seeds New Zealand (2026a, b, c, d) and Syngenta (2026). 43

Table 2. Assembly statistics for the three sequenced *Fulvia fulva* isolates. Genome assemblies were generated with SPAdes v4.0.0 (--careful), filtered to remove contigs shorter than 1 kb (SeqKit v2.12.0), and assessed for completeness with BUSCO v5.8.2 against the dothideomycetes_odb10 lineage dataset. BUSCO (%) is the proportion of complete single-copy orthologues recovered; N50 is the contig length at which half the total assembly length is contained in contigs of that size or longer. Length is the total assembled length in base pairs. Isolates are ordered by collection date: ICMP 7320 (1980s), CM1 (2022), CO1 (2025). 57

Table 3. Field collection log outcomes for the 2024–2026 tomato leaf mould survey. 69

Table 4. Summary of *Fulvia fulva* sampling efforts: temporal data, geographic distribution, and isolation success. 72

Table 5. Morphological Dimensions and Characteristics of *Fulvia fulva* Isolates (adapted from Videira et al., 2017). 73

Table 6. Purity and concentration of genomic DNA extracted from *Fulvia fulva* isolates. DNA concentration (ng/µL) and purity ratios were measured with a DeNovix DS-11 FX+ Spectrophotometer/Fluorometer. The A_{260}/A_{280} ratio indicates protein contamination (≈1.8 expected for pure DNA) and the A_{260}/A_{230} ratio indicates contamination by salts, phenol or carbohydrates (≈2.0–2.2 expected). Values within these ranges indicate DNA of suitable purity for library preparation and downstream whole-genome sequencing. 79

Table 7. Effector integrity per *Fulvia fulva* isolate (protein identity to reference in parentheses; “absent” = effector not detected in that isolate). 80

List of abbreviations

Avr	Avirulence
CDS	Coding Sequence
Cf	*Cladosporium fulvum*
CTAB	Cetyltrimethylammonium bromide
Ecp(s)	Extracellular protein(s)
EDTA	Ethylenediaminetetraacetic acid
IPM	Integrated Pest Management
HR	Hypersensitive Response
PCR	Polymerase Chain Reaction
PDA	Potato Dextrose Agar
PDB	Potato Dextrose Broth
RH	Relative Humidity
RIP	Repeat-induced Point Mutation
RLP(s)	Receptor-Like Protein(s)
RO	Reverse Osmosis
SDS	Sodium dodecyl sulfate
T°	Temperature
TAE	Tris-acetate-EDTA
TES	2-{[1,3-Dihydroxy-2-(hydroxymethyl)propan-2-yl]amino}ethane-1-sulfonic acid
TM	Transmembrane
ToBRV	Tomato Brown Rugose Virus
VPD	Vapour Pressure Deficit
mL	millilitre(s)
µL	microlitre(s)

Chapter 1

1. Introduction

1.1. An Overview of New Zealand's Fresh Tomato Industry

The tomato industry is a cornerstone of New Zealand's horticultural economy, yielding a farm-gate value exceeding $161.6 million per annum as of March 2024 (Tomatoes New Zealand [TomatoesNZ], 2026d). According to TomatoesNZ (2026a), market stability is maintained through a dual production framework: a high-tech greenhouse sector that provides year-round fresh table tomatoes, and an open-field sector that supplies the processing industry. This structural division allows the industry to balance high-value retail demand with the volume requirements of the manufacturing sector. Currently, the industry is undergoing intense consolidation; high entry barriers have limited the expansion of experienced growers and the entry of new players over the last decade, leading smaller family partnerships (3,000–10,000 m²) to be absorbed by large-scale, investor-partnered units. Some operations now encompass 20 hectares of protected crops, a strategic shift necessary to gain bargaining power within a market dominated by a supermarket duopoly where a limited number of retailers dictate terms (TomatoesNZ, 2021; United States Department of Agriculture - Foreign Agricultural Service, 2025).

1.2. The Local Greenhouse Environment

Modern greenhouse production in New Zealand is a highly technical discipline requiring substantial initial capital, starting at approximately $2 million per hectare for basic infrastructure and rising significantly for facilities equipped with automated climate control, supplementary lighting, and advanced irrigation systems (TomatoesNZ, 2025). The covered cropping sector, which utilises approximately 120 hectares of land under glass or plastic, continues to support roughly 140 businesses and provides steady employment for approximately 1,000 workers (TomatoesNZ, 2025; Te Puni Kōkiri, 2024).

Such modern facilities are primarily clustered in Auckland—the region with the largest number of growers—followed by the Central North Island, Nelson, and Christchurch, with secondary hubs in Northland, the Bay of Plenty, and Canterbury (TomatoesNZ, 2026a).

While the fresh market remains more geographically diverse than processing, regional nuances persist; for example, North Island retailers typically prefer tomatoes picked without the calyx, whereas South Island consumers often view the retained calyx as a marker of freshness (TomatoesNZ, 2026a).

The technical efficiency of these systems allows for extraordinary productivity; high-tech glasshouses can produce up to 100 kilograms of tomatoes per square meter annually (1,000 tonnes per hectare), a figure 10 to 20 times higher than field-grown crops (EECA, 2026; Tomatoes NZ, 2021). This intensity is further supported by atmospheric CO_2 enrichment, which can boost yields by 20% to 30% (Heuvelink & Dorais, 2005; Horticulture New Zealand [Horticulture NZ], 2021).

While growers typically capture carbon dioxide (CO_2) as a byproduct of burning natural gas for heat, the closure of the Marsden Point Refinery has introduced fragility into the secondary supply of industrial CO_2 (Horticulture NZ, 2024), generating speculation and uncertainty among growers.

1.3. Open-field Tomatoes and the Processed Tomato Industry

In contrast to intensive indoor environments, tomatoes for the processing sector are cultivated in open fields, primarily in Hawke's Bay and Gisborne, with approximately 60,500 tonnes of field-grown tomatoes being produced annually for canning, sauces, and paste (TomatoesNZ, 2026). This regional concentration is the result of decades of rationalisation. At the same time, processing was distributed across Auckland, Gisborne, Hawke's Bay, and Nelson in the 1950s; it eventually consolidated on the East Coast, where favourable climates and centralised infrastructure favoured consolidation (Nichols & Bussel, 1980). However, recent market trends indicate that

demand for locally grown tomatoes has decreased after Cyclone Gabrielle's impact (Steele, 2025).

Traditional pockets of outdoor fresh production continue to persist in Northland, Horowhenua, Otaki, and Marlborough (TomatoesNZ, 2024).

1.4. Varietal Diversity and Consumer Preferences

The rapid diversification of varieties has largely driven the growth of the New Zealand tomato industry. While standard round loose tomatoes remain a market staple, specialty tomatoes (such as vine-ripened, cherry, cocktail, and plum varieties) have captured an increasing share of consumer interest (TomatoesNZ, 2026). This shift reflects a broader trend toward premiumisation, where consumers are willing to pay more for fruit that offers superior flavour, texture, and visual appeal.

In the commercial space, Dutch varieties predominate due to their high yields and suitability for greenhouse climates (TomatoesNZ, 2026). The processing sector continues to rely on specialised Heinz seeds, which are bred globally to ensure consistency in the rich red colour and acidity required for products such as ketchup and soup (Australian Press Association New Zealand, 2012).

1.5. Economic Value and Market Structure

As of March 2024, the sector comprised approximately 140 registered members (Figure 1) who produced fresh tomatoes, with an annual combined farm-gate value exceeding $161.6 million (TomatoesNZ, 2025).

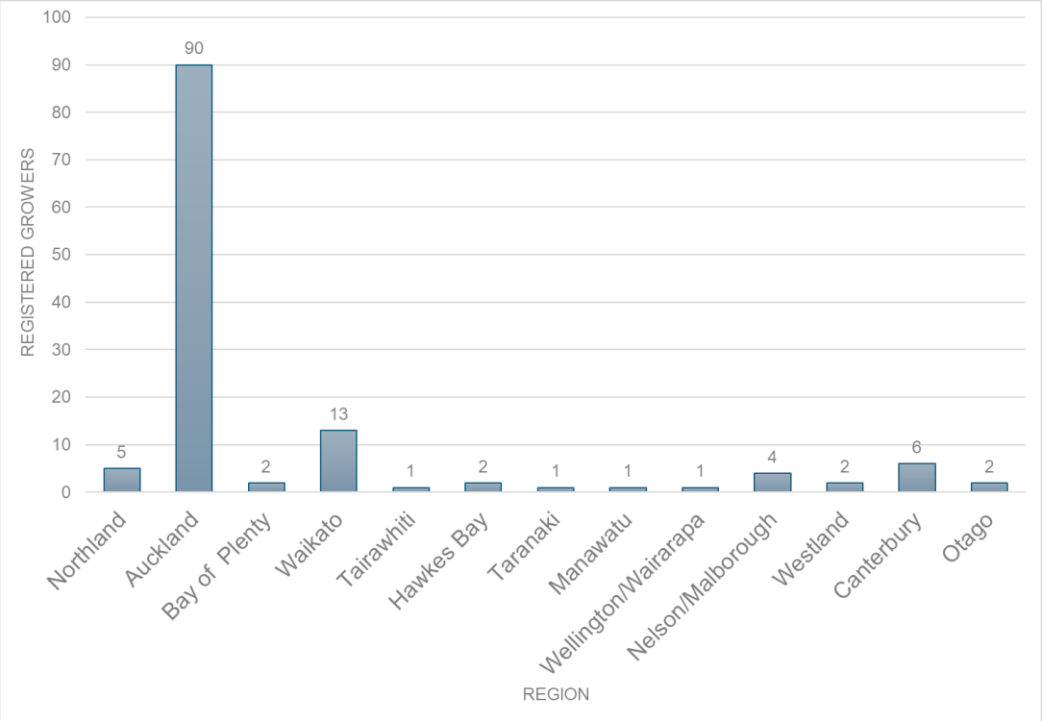

Figure 1. *Number of registered tomato growers in each New Zealand region (TomatoesNZ, 2025).*

While the domestic tomato market remains the bedrock of the industry (TomatoesNZ, 2026a), the export sector has undergone significant recalibration, reaching a historical high volume in 2019, with New Zealand growers sending 3,316.5 metric tonnes of fresh tomatoes overseas. However, by the 2023 calendar year, this volume had contracted to approximately 902 metric tonnes (TomatoesNZ, 2026b). This sharp decline is attributed to a confluence of factors, most notably disruptions to sea freight and logistics caused by the COVID-19 pandemic, as well as increased competition in Asian markets. Japan remains the primary export destination for New Zealand tomatoes, consistently accounting for nearly half of total export volume, followed by Pacific Rim neighbours such as New Caledonia and Fiji (TomatoesNZ, 2026b; TomatoesNZ, 2026e).

1.6. Industry Challenges

According to TomatoesNZ (2023), the fresh tomato industry faces several critical challenges. A primary concern is decarbonisation and the energy transition; while the sector is committed to transitioning from greenhouse gas heating to non-fossil fuels by 2037, the high capital costs of fuel switching and energy reduction present a significant barrier. Furthermore, rising production costs have placed immense pressure on

operational margins. The industry is contending with high inflation and significant price hikes for fertiliser, seeds and logistics. Energy volatility is particularly critical, with gas and coal prices surging by 50% and 85%, respectively, between 2021 and 2022, whereas labour expenditure has risen to 33% of total production cost.

The bureaucracy and regulation burdens exacerbate these economic strains. The sector operates in a progressively restrictive environment due to water-use constraints, land-use limitations, and building consent requirements that significantly inflate production costs. Additionally, biosecurity issues have cost growers over $200,000 in tomato levy fees by 2023 (TomatoesNZ, 2023).

1.7. Biosecurity Concerns

Biosecurity threats pose a significant long-term source of uncertainty for the New Zealand tomato industry. Of particular concern is the unregulated sale of seeds online, which bypasses established safety protocols (TomatoesNZ, 2023), alongside the critical risk posed by the Tomato Brown Rugose Virus (ToBRV) outbreak detected in Australia in August 2024 (Department of Agriculture, Fisheries and Forestry, 2024; Ministry for Primary Industries, 2024; TomatoesNZ, 2025). The reported global decrease in the efficacy and availability of pesticides has reached a critical point in protected cropping environments, where the contained nature of the facilities often results in high selection pressures, accelerating the development and spread of pesticide resistance within glasshouse populations (Veronesi et al., 2022).

Greenhouse whitefly (*Trialeurodes vaporariorum*) remains the most prevalent and challenging threat to the New Zealand greenhouse tomato industry. The management of this pest is notably problematic due to documented, worldwide pesticide resistance (Dearlove et al., 2024). This global trend appears to be mirrored domestically, where, anecdotally, resistance to all commercially available pesticides has been consistently observed; however, formal studies have yet to quantify the exact levels of this resistance in New Zealand (D. Cohen, personal communication, September 12, 2025).

Other major pests posing a significant risk include the Tomato-Potato Psyllid (*Bactericera cockerelli*), which serves as a vector for *Candidatus Liberibacter* transmission and has been reported to show increased pesticide resistance in recent years (Veronesi et al., 2022, 2025).

Regarding fungal diseases, reports of leaf mould (*Fulvia fulva*) prevalence and incidence have increased among industry players in the last decade (Vogrincic, 2018, 2020, 2026).

2. *Fulvia fulva*, the Causal Agent of Tomato Leaf Mould

Fulvia fulva (basionym *Cladosporium fulvum*, syn. *Passalora fulva*) is a highly specialised fungal pathogen classified within the *Mycosphaerellaceae* family of the Ascomycota phylum (de Wit et al., 2012; Dixon et al., 1996; Gül et al., 2024; Thomma et al., 2005). As the causal agent of tomato leaf mould, it represents a significant threat primarily to greenhouse-grown tomato crops (Gül et al., 2024; Kawaguchi & Suenaga-Kanetani, 2014; Lucentini et al., 2021).

Although traditionally categorised as an asexual fungus, contemporary molecular evidence and the identification of functional mating-type genes suggest the potential for cryptic sexual recombination within the species (de la Rosa et al., 2024; Stergiopoulos et al., 2007; Zaccaron et al., 2022).

2.1. Pathogenic Lifestyle and Host Range

F. fulva is a hemibiotrophic pathogen that is specifically adapted to the genus *Solanum* (de Wit et al., 2012; Mesarich et al., 2023; Stergiopoulos et al., 2007; Sudermann et al., 2022; Thomma et al., 2005). Hemibiotrophs are defined by their ability to initially colonise living host tissue as biotrophs before transitioning to a necrotrophic phase, during which they kill host cells (Liao et al., 2022). The infection strategy of *F. fulva* is characterised by a strictly extracellular existence, colonising the apoplast between leaf mesophyll cells. To sustain itself in the apoplast, the fungus manipulates host metabolism to induce the release of essential nutrients, including GABA (gamma-aminobutyric acid) and sucrose (Thomma et al., 2005).

While recognised predominantly as a foliar pathogen, severe outbreaks may occasionally involve other tissues such as stems, blossoms, petioles, and fruit (Bahoch et al., 2025; Gül et al., 2024; Thomma et al., 2005). Furthermore, the fungus exhibits a preference for well-nourished hosts, as its proliferation is markedly constrained on starved or senescent plant material (Sudermann et al., 2022). Notably, *F. fulva* can be successfully cultured *in vitro* using relatively simple artificial media,

such as potato dextrose broth or agar (Stergiopoulos et al., 2007; Sudermann et al., 2022; Thomma et al., 2005).

For the majority of its disease cycle on tomato, *F. fulva* is a biotroph, residing within living host tissue during a prolonged latent, asymptomatic period—typically lasting 10 to 14 days—without inducing visible cellular damage (de Wit et al., 2012; Gül et al., 2024; Kawaguchi & Suenaga-Kanetani, 2014; Stergiopoulos et al., 2007; Sudermann et al., 2022; Thomma et al., 2005). However, the transition to a necrotrophic state occurs in the later stages of infection when the fungus deploys plant cell wall-degrading carbohydrate-active enzymes (de Wit et al., 2012; Hane et al., 2020; Ökmen et al., 2019). This shift leads to the collapse and eventual death of host tissue, manifesting on the adaxial (upper) leaf surface as chlorotic yellow spots caused by the necrosis of palisade parenchyma cells (Iida et al., 2015; Stergiopoulos et al., 2007; Thomma et al., 2005).

2.2. Colonisation Mechanism and Infection Process

The infection process of *F. fulva* is defined by its strictly extracellular lifestyle in the apoplast (Bahoch et al., 2025; Bernal-Cabrera et al., 2021; Enya et al., 2009; Stergiopoulos et al., 2007; Thomma et al., 2005). Pathogenesis begins when asexual spores called conidia germinate on the abaxial (lower) leaf surface, after which the fungus enters the host exclusively through open stomata (Gül et al., 2024; Stergiopoulos et al., 2007; Thomma et al., 2005).

Remarkably, the pathogen does not employ mechanical force or form specialised infection structures, such as appressoria, to penetrate the epidermis (Gül et al., 2024; Mesarich et al., 2023; Meyer & Gärber, 2021; Stergiopoulos et al., 2007; Thomma et al., 2005). Once internal access is gained, the hyphae colonise the mesophyll intercellular spaces – the extracellular compartment collectively termed as the apoplast (Gül et al., 2024; Lucentini et al., 2021; Van Esse et al., 2008).

During colonisation, the fungus secretes a suite of small proteins into the apoplast known as effectors, which promote infection by suppressing host defences, protecting

the fungus from plant-derived hydrolytic enzymes, and otherwise facilitating establishment in host tissue (Stergiopoulos & de Wit, 2009; de Wit et al., 2009).

Despite the lack of other specialised infection structures like haustoria, which enter plant cells and are produced by certain fungi like rusts and powdery mildews for nutrient extraction, the fungus maintains intimate contact with mesophyll cells to withdraw nutrients, concentrating its growth around vascular tissues to exploit sucrose gradients near the phloem (Iida et al., 2015; Novak et al., 2021; Thomma et al., 2005; Van Esse et al., 2008).

The recognition of these effectors by tomato is governed by a gene-for-gene relationship, in which resistance depends on the matched presence of a pathogen avirulence gene and a corresponding host resistance (*R*) gene (Flor, 1971). In the tomato–*F. fulva* interaction, these *R* genes are the *Cf* genes (named for *Cladosporium fulvum*), most of which were introgressed into cultivated tomato from wild *Solanum* relatives (Rivas & Thomas, 2005; Kruijt et al., 2005). *Cf* genes encode receptor-like proteins (RLP) — membrane-anchored receptors carrying an extracellular leucine-rich repeat domain that mediates recognition of the cognate effector but lacking an intracellular signalling domain, such that signal transduction requires association with partner kinases (Jones et al., 1994; Dixon et al., 1996; Rivas & Thomas, 2005). When a *Cf* protein recognises its cognate effector, it activates effector-triggered immunity, typically culminating in a localised hypersensitive response — a form of programmed cell death that arrests the biotrophic pathogen (Jones & Dangl, 2006; de Wit, 2016). An effector recognised in this way renders the strain carrying it avirulent on plants possessing the corresponding *Cf* gene; hence the historical designation of the recognised effectors as “avirulence” proteins (Rivas & Thomas, 2005).

This recognition system establishes a coevolutionary arms race between the pathogen and the host (de Wit et al., 2009; de Wit, 2016). The deployment of a *Cf* gene in commercial cultivars imposes strong selection on *F. fulva* to evade recognition, which it achieves by losing or altering the recognised effector — through complete deletion of the effector gene, or through mutations that abolish recognition while, ideally for the pathogen, retaining the effector's contribution to virulence (Stergiopoulos et al., 2007; de Wit, 2016; Mesarich et al., 2023). Such escape events break the corresponding *Cf*-

mediated resistance and have repeatedly rendered deployed *Cf* genes ineffective in the field (Stergiopoulos et al., 2007; Iida et al., 2015). More recently, cognate resistances have also been identified for several Ecp effectors (the *Cf-Ecp* genes), extending the pool of potential resistance sources beyond the classical Avr-recognising *Cf* genes (Laugé et al., 2000; Mesarich et al., 2018). Because the durability of any deployed resistance therefore depends directly on the integrity and dispensability of its cognate effector in the pathogen population, the genomic context in which effector genes reside — and the mechanisms by which they are lost or mutated — is central to understanding resistance breakdown. The following section considers how the architecture of the *F. fulva* genome shapes these processes; the effectors themselves, and their recognition, are described in more detail in section [2.6.].

2.3. Life Cycle and Environmental Conditions

Development of leaf mould disease is acutely sensitive to environmental variables, requiring high relative humidity (RH; exceeding 85%) and warm temperatures, with an optimum range of 22–24°C (Gül et al., 2024; Kawaguchi & Suenaga-Kanetani, 2014; Sudermann et al., 2022).

Following stomatal penetration and the subsequent 10- to -14-day colonisation phase, the fungus completes its cycle by forming hyphal aggregations, or stromata, within the substomatal spaces (de Wit et al., 2012; Iida et al., 2015; Mesarich et al., 2023; Thomma et al., 2005).

Conidiophores are then projected back through the stomata to release massive quantities of olive-green to brown conidia, facilitating secondary dispersal via wind or water to fresh abaxial leaf surfaces (Bahoch et al., 2025; Enya et al., 2009; Sudermann et al., 2022; Thomma et al., 2005).

Tomato is the only known host of *F. fulva*, so there is no alternative-host reservoir to bridge the crop-free interval (Thomma et al., 2005). As a hemibiotroph, the fungus survives in crop residues or as conidia and sclerotia in the soil (Jones and Jones,

1991). These sclerotia can produce new conidia, which can survive for a year or longer in greenhouse environments (Babadoost, 2011).

2.4. Visual Symptoms

Symptoms generally start on the lower foliage and progress acropetally (Enya et al., 2009). On the adaxial surface, initial pale green or yellowish spots evolve into distinct yellow chlorotic lesions, while corresponding abaxial patches develop a velvety fungal mass ranging in colour from olive-green to greyish-purple (Figures 2, 3 and 4) (Enya et al., 2009; Meyer & Gärber, 2021; Sudermann et al., 2022; Yoshida et al., 2021).

In severe instances, infection results in leaf curling, wilting, premature defoliation, and potential host death (Gül et al., 2024; Novak et al., 2021; Thomma et al., 2005).



***Figure 2**. Progressive development of chlorotic lesions on the adaxial (upper) leaf surface of tomato caused by the leaf mould fungus,* Fulvia fulva*. a) Incipient stage of infection, characterised by localised, early-onset chlorosis before widespread cellular disruption. b) Advanced infection showing extended, diffuse, pale-yellow chlorotic spots corresponding to fungal colonisation of the underlying mesophyll. These symptoms result from the death of palisade parenchyma cells due to the pathogen's hemibiotrophic nature, eventually leading to the collapse of leaf tissue.*

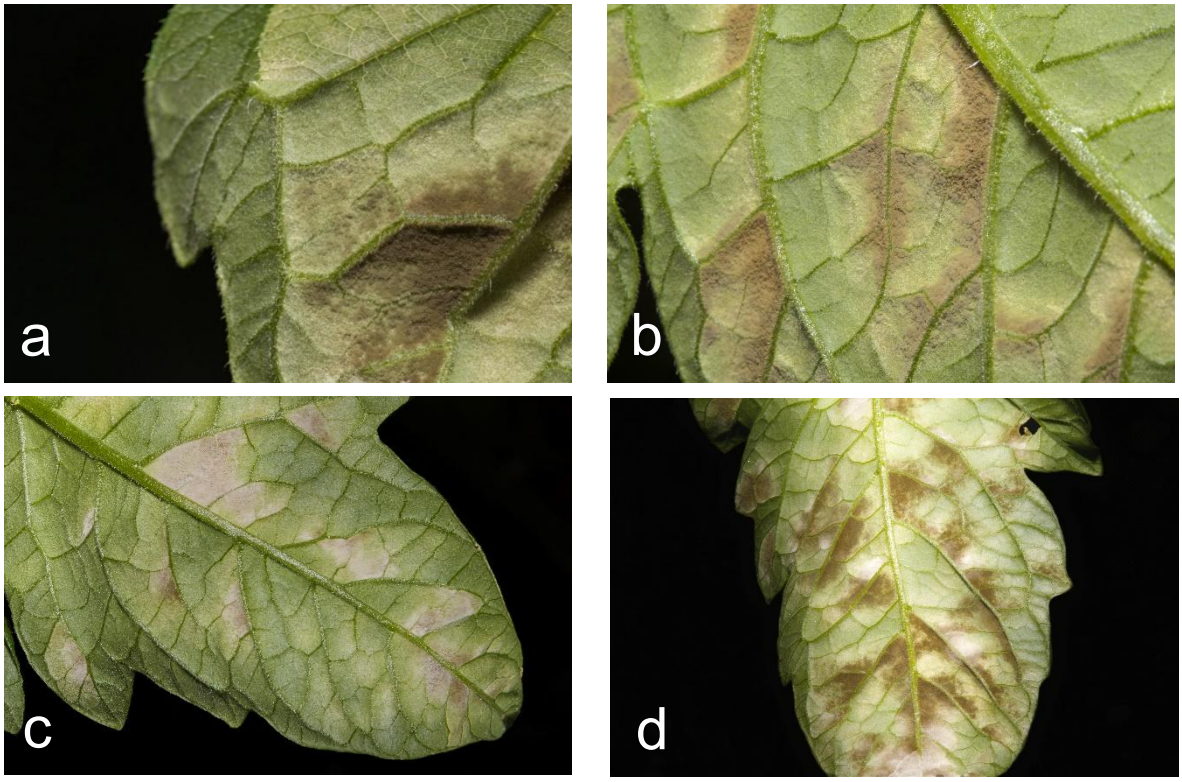

***Figure 3.** Dense sporulation of* Fulvia fulva *on the abaxial (lower) leaf surface of tomato. These close-up image captures the characteristic velvet-like appearance of the pathogen. The brownish (a), olive-green to brownish (b), greyish (c) and greyish to brownish (d) fungal masses consist of a high density of conidiophores and conidia emerging through the stomata. This stage marks the peak reproductive phase, during which the pathogen is primed for secondary dispersal via wind or water.*

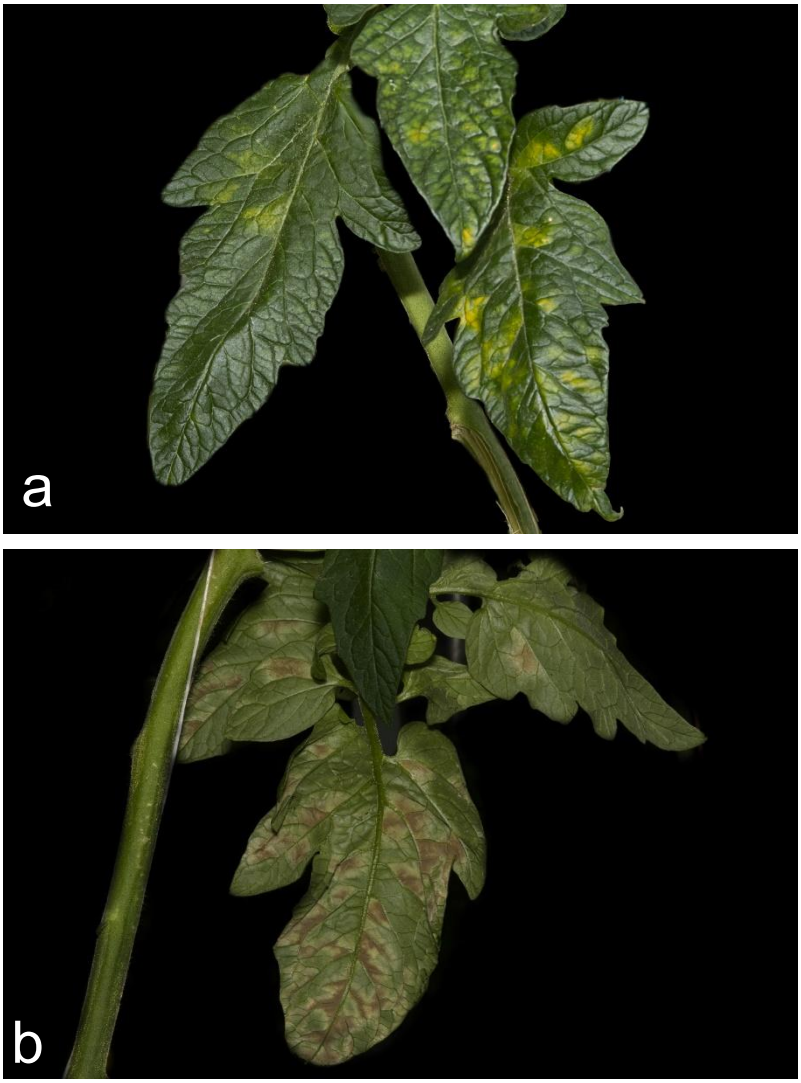

Figure 4. *Progression of* Fulvia fulva *infection of tomato leaves. A series of three consecutive leaves illustrating the transition from incipient to well-developed sporulation, both for the adaxial (a) and abaxial (b) side of these leaves. a) From left to right, the mild stage shows sparse, pale fungal patches; the intermediate stage demonstrates expanding, darkening colonies; and the well-developed stage exhibits a thick, confluent velvety mass covering a significant portion of the leaf underside. b) The sequence highlights the evolution of chlorosis, beginning with faint, indistinct yellowing (incipient), progressing to clearly defined yellow lesions (developed), and concluding with necrotic browning and leaf curling in the most advanced stage of the disease.*

2.5. Genome Overview

2.5.1. Genomic Architecture and the Two-Speed Genome of Fulvia fulva

The genomic architecture of *F. fulva* is defined by a highly compartmentalised structure consistent with the “two-speed genome” model of fungal pathogen evolution (Torres et al., 2020; Zaccaron et al., 2022). This model describes genomes partitioned into distinct territories operating at divergent evolutionary rates: gene-dense, repeat-poor regions harbouring conserved housekeeping functions, and gene-sparse, repeat-rich regions disproportionately enriched in genes encoding virulence factors, called effectors, and other pathogenicity-related factors (de Wit et al., 2012; Torres et al., 2020). This bipartite organisation is understood to facilitate rapid adaptation to host immune pressure while preserving the integrity of core biological processes (Torres et al., 2020; Zaccaron et al., 2022).

Repetitive DNA accounts for approximately 47–50% of the total *F. fulva* genome assembly, and these elements are not randomly dispersed but are instead highly clustered, forming extended intergenic tracts that punctuate otherwise gene-dense areas (Mesarich et al., 2023; Zaccaron et al., 2022). Core compartments are characterised by elevated GC content and compact intergenic sequences, with a median intergenic size of only 646 bp, of which approximately 87.8% are repeat-free, conferring structural stability to conserved loci (Zaccaron et al., 2022). Gene-sparse regions, by contrast, contain intergenic sequences frequently exceeding 10–60 kb in length, composed of more than 80–90% repetitive DNA, and generally exhibit reduced GC content relative to core regions (de Wit et al., 2012; Zaccaron et al., 2022). At a broader scale, the genome is organised into approximately 500 gene clusters; intergenic regions within clusters are repeat-poor (mean <3%), whereas the intervals separating clusters are overwhelmingly repeat-rich (>90%), establishing discrete boundaries between genomic zones of stability and plasticity (Zaccaron et al., 2022).

The adaptive significance of this compartmentalisation is most apparent in the distribution of effectors. These are secreted proteins that play central roles in host colonisation and are frequent targets of plant immune recognition (see subsections [2.6.1.] and [2.6.2.] for more details). Consequently, genes encoding effectors are

significantly enriched in the highly flexible, gene-sparse and subtelomeric regions of the genome (de Wit et al., 2012; Zaccaron et al., 2022). Effector genes including *Avr9*, *Avr4E*, and *Avr5* are situated within repeat-rich compartments and are flanked by some of the longest intergenic sequences in the genome (de Wit et al., 2012). The proximity of these loci to structurally unstable repetitive DNA facilitates their complete deletion as a mechanism of immune evasion, a strategy exemplified by the absolute correlation between *Avr9* deletion and the breakdown of *Cf-9*-mediated resistance (de Wit et al., 2012; Mesarich et al., 2023). Notably, however, not all effector genes occupy gene-sparse regions; *Avr2*, *Avr4*, *Ecp2*, and *Ecp6* reside in gene-rich, repeat-poor compartments and evolve predominantly through point mutations and small indels rather than large-scale structural rearrangements (de Wit et al., 2012). This observation suggests that genomic location may be a deterministic factor in the mode of effector evolution under host-imposed selection pressure (Torres et al., 2020; Zaccaron et al., 2022).

Several molecular mechanisms operate within the repeat-rich compartments to generate and sustain genomic variability. Transposable element accumulation is favoured in gene-sparse regions, where insertions are comparatively buffered from purifying selection (de Wit et al., 2012; Torres et al., 2020). Repeat-Induced Point (RIP) mutations have extensively shaped the genome, with nearly 40% of the assembly bearing RIP signatures; while predominantly confined to repetitive sequences, RIP frequently leaks into adjacent single-copy regions, elevating the mutation rate of flanking genes, including those encoding effectors (de Wit et al., 2012; Zaccaron et al., 2022). However, a caveat applies to the interpretation of RIP in this pathogen. RIP is a meiosis-associated process present during the sexual cycle, and its extensive footprint sits uneasily with the historical characterisation of F. fulva. This apparent contradiction has been taken to indicate a cryptic or ancestral sexual cycle, consistent with recent mating-type evidence (de la Rosa et al., 2024). An extreme manifestation of compartmentalisation is observed on chromosome 14 (Chr14; 460 kb), the smallest chromosome in *F. fulva*. This accessory element is gene-poor, composed of approximately 80% repeats, heavily RIPed, and dispensable, being absent from the majority of global isolates (Zaccaron et al., 2022). Its properties are consistent with a role as a reservoir for rapid genetic experimentation, decoupled from

the selective constraints governing core chromosomes (Torres et al., 2020; Zaccaron et al., 2022).

Comparative genomic analysis with the closely related pine needle blight pathogen, *Dothistroma septosporum*, further underscores the functional logic of this architecture (de Wit et al., 2012; Mesarich et al., 2023). Despite sharing a conserved core of 13 mesosyntenic chromosomes, *F. fulva* possesses a markedly larger genome attributable to the expansion of its repeat-rich compartments (de Wit et al., 2012). Syntenic regions, corresponding to core compartments, harbour approximately 70% of all predicted genes and exhibit high inter-species conservation (de Wit et al., 2012; Mesarich et al., 2023). Non-syntenic, repeat-rich regions, by contrast, are disproportionately enriched for secreted proteins and candidate effectors, reinforcing the conclusion that the “fast-speed” dynamic compartments represent the primary substrate for species-specific host adaptation in this pathosystem (de Wit et al., 2012; Mesarich et al., 2023; Torres et al., 2020).

2.5.2. Mating-Type Loci and the Potential for Heterothallism in Fulvia fulva

F. fulva has long been classified as an asexual fungus, given that its sexual teleomorph has never been observed under natural or laboratory conditions (Thomma et al., 2005). Despite this, molecular investigations have revealed that the fungus possesses a genetic repertoire fully consistent with a heterothallic mating system (Stergiopoulos et al., 2007) and a substantial proportion of its genome bears RIP signatures, raising the possibility that sexual reproduction occurs cryptically in nature (Zaccaron et al., 2022). Such a possibility is further supported by the finding that, as described above, the *F. fulva* genome is extensively affected by RIP. RIP is a genome defence mechanism that is typically associated with the sexual phase of filamentous fungi (reference).

Genomic characterisation has confirmed the presence of two distinct mating-type idiomorphs, designated MAT1-1 and MAT1-2, which are hallmarks of heterothallic Ascomycetes (Stergiopoulos et al., 2007). The MAT1-1 locus harbours the *MAT1-1-1* gene, encoding a protein containing an alpha-box domain, while the MAT1-2 locus

carries the *MAT1-2-1* gene, which encodes a High Mobility Group (HMG) box protein (Stergiopoulos et al., 2007; Zaccaron et al., 2022). Crucially, individual isolates of *F. fulva* carry only one of these two idiomorphs, a configuration inconsistent with homothallism and instead supporting classification of the species as potentially heterothallic (Stergiopoulos et al., 2007).

Analysis of global populations provides further insight into the pathogen's reproductive biology. In numerous local populations, MAT1-1 and MAT1-2 isolates coexist, in some cases approaching a 1:1 ratio, a distribution broadly consistent with expectations for sexually reproducing populations (Stergiopoulos et al., 2007). Although *F. fulva* appears predominantly clonal at a global scale (likely reflecting the widespread dissemination of highly successful lineages), evidence of genetic recombination has been detected in certain populations, suggesting that cryptic sexual reproduction may occur even in the absence of observed fruiting bodies such as cleistothecia or pseudothecia (Stergiopoulos et al., 2007; Mesarich et al., 2023). This inference is further supported by the significant synteny and high sequence homology observed between the mating-type loci of *F. fulva* and those of known sexual relatives within the Mycosphaerellaceae, including *D.septosporum* and the related leaf blotch fungus, *Zymoseptoria tritici* (Mesarich et al., 2023; Zaccaron et al., 2022).

Collectively, the identification of functional mating-type idiomorphs, the population-level evidence for recombination, and evidence of RIP in the genome indicate that *F. fulva* retains the molecular capacity for sexual reproduction (Stergiopoulos et al., 2007; Zaccaron et al., 2022). This heterothallic architecture may represent a critical, if infrequently realised, mechanism for generating the genetic diversity required to overcome leaf mould resistance in tomato over evolutionary time (Mesarich et al., 2023; Thomma et al., 2005).

2.6. Dissection of the *Fulvia fulva*–tomato interaction at the molecular level

2.6.1. Compatible Interactions (Disease Susceptibility)

To colonise tomato leaves and promote disease, *F. fulva* must secrete an arsenal of at least 75 small, non-enzymatic virulence factors, called effectors, into the leaf apoplast (Gül et al., 2024; Iida et al., 2010, 2015; Mesarich et al., 2018; Thomma et al., 2005). In most cases, these effectors are also rich in cysteine residues, which form disulphide bonds that contribute to their stability within the protease-rich apoplastic environment of tomato leaves (de la Rosa et al., 2024; de Wit et al., 2012; Thomma et al., 2005; van Esse et al., 2006; Wulff et al., 2009).

Among the effectors to be functionally characterised to date is Avr2, a potent cysteine protease inhibitor that targets multiple host proteases in the apoplast, including Rcr3 and Pip1 (Rooney et al., 2005). By inhibiting these enzymes, Avr2 effectively suppresses the host's basal defence mechanisms (van Esse et al., 2008).

Another functionally characterised effector is Avr4, which functions as a chitin-binding protein that protects the fungal cell wall: it contains a carbohydrate-binding module that shields fungal hyphae from host chitinases in the apoplast during infection (van Esse et al., 2007).

A third effector example is Ecp6, which is a critical stealth factor containing three LysM domains that suppresses chitin-triggered immunity in the apoplast (Bolton et al., 2008). It achieves this by sequestering chitin fragments released from the fungal cell wall, thereby preventing their detection by host cell-surface-localised chitin immune receptors (Bolton et al., 2008; van Esse et al., 2008).

Additional effectors include Ecp1 and Ecp2-1, which are established virulence factors. Disruption of the genes encoding these proteins significantly reduces fungal aggressiveness (van Esse et al., 2008). Likewise, *Avr5* has been confirmed as a virulence factor via gene complementation experiments in isolates naturally lacking

this effector gene, as its presence correlates with increased fungal biomass during colonisation (Mesarich et al., 2014).

2.6.2. Incompatible Interactions (Disease Resistance)

The genetic interaction between *F. fulva* and its host adheres to the classic gene-for-gene model (de Wit et al., 2012; Thomma et al., 2005). This means that for every tomato resistance gene, there is a corresponding effector gene in *F. fulva* (Wulff et al., 2009). If brief, when both genes are present, then disease resistance is the outcome. However, if either or both are absent, then disease susceptibility is the outcome.

In resistant tomato varieties, typically one of two resistance genes is present. These are called *Cf* genes. Each of these *Cf* resistance genes encodes a specific cell-surface-localised immune receptor, all identified to date belonging to the RLP class (Mesarich et al., 2018; de la Rosa et al., 2024; Wulff et al., 2009; see subsection [2.6.3.] for more details on RLPs). Each Cf immune receptor recognises a specific corresponding *F. fulva* effector (de la Rosa et al., 2024; Wulff et al., 2009). To date, only a small number of *F. fulva* effectors have been identified that are recognised by corresponding Cf immune receptors. These are Avr2, Avr4, Avr4E, Avr5, Avr6, Avr9 and Avr9B, which are recognised by the corresponding Cf immune receptors Cf-2, Cf-4, Cf-4E, Cf-5, Cf-6, Cf-9C and Cf-9B, respectively (de la Rosa et al., 2024; Schol et al., 2025).

Upon recognition, defence responses are initiated, including a hypersensitive response (HR), which halts pathogen growth through a localised form of programmed cell death immediately adjacent to the invading fungal hyphae. This HR restricts the fungus in a limited area of hostile, necrotic tissue that is devoid of nutrients (Lazar et al., 2022; Lucentini et al., 2021; Mesarich et al., 2018; Thomma et al., 2005). Effectors that elicit these defence responses are termed avirulence (Avr) effectors because their recognition by corresponding Cf immune receptors renders *F. fulva* avirulent, preventing disease development (de la Rosa et al., 2024; Lucentini et al., 2021; Mesarich et al., 2014). That is, their perception by the host in resistant (incompatible)

tomato lines prevents successful colonisation and sporulation (Gül et al., 2024; Lucentini et al., 2021; Mesarich et al., 2014).

To circumvent these defences, the fungus evolves rapidly by acquiring genetic changes in the genes encoding recognised effectors. These changes include gene deletions, frameshifts, premature stop codons, and transposable element insertions, which eliminate or lead to the production of a significantly altered effector, as well as point mutations that alter recognition while preserving effector function (e.g. the loss of a disulfide bond through the conversion of a cysteine residue to another amino acid type), thereby enabling the fungus to evade recognition, resulting in the emergence of new physiological races (de la Rosa et al., 2024; Iida et al., 2015; Lucentini et al., 2021; Mesarich et al., 2014, 2018; Thomma et al., 2005; Zaccaron et al., 2022; Zhang et al., 2025). Since 2007, research has mainly focused on how *F. fulva* evolves through genetic changes in effector gene sequences (Iida et al., 2015; Lucentini et al., 2021; Stergiopoulos et al., 2007).

2.6.3. Cf Immune Receptor (Resistance) Proteins

As mentioned above, the immune receptor proteins encoded by all cloned *Cf* genes belong to a distinct structural class, the RLPs (Mesarich et al., 2018). The molecular architecture of RLPs is composed of an extracellular domain composed of multiple Leucine-Rich Repeats (LRRs) (de la Rosa et al., 2024; Dixon et al., 1996; Mesarich et al., 2014), a transmembrane (TM) domain, which anchors the receptor firmly within the plasma membrane (Dixon et al., 1996; Mesarich et al., 2014, 2018), and a C-terminal cytoplasmic tail, which is notably short (Dixon et al., 1996; Mesarich et al., 2014, 2023; Zhang et al., 2025).

Different Cf immune receptors utilise distinct recognition mechanisms to detect *F. fulva* effectors. For instance, the *Cf-4* resistance gene introgressed from *Solanum habrochaites* on chromosome 1 confers resistance by encoding an RLP that recognises a fungal chitin-binding factor in the globular fold of the Avr4 effector protein (Dixon et al., 1996; Mesarich et al., 2014, 2023; Thomma et al., 2005). Pathogen evasion of this receptor typically occurs through mutations that destabilise the Avr4

protein, leading to its degradation in the plant apoplast before recognition can occur (Dixon et al., 1996; Jones et al., 1993; Mesarich et al., 2018).

In contrast, the *Cf-2* locus on chromosome 6 is associated with the Guard Model of indirect recognition. Here, the Cf-2 receptor monitors the host protease Rcr3; when the fungal effector Avr2 inhibits Rcr3 to promote colonisation, Cf-2 detects this molecular modification and triggers an HR (Gül et al., 2024; Thomma et al., 2005; Van Esse et al., 2008). Closely linked to *Cf-2* on chromosome 6 is *Cf-5*, which encodes an RLP that recognises the Avr5 effector. Despite high homology with Cf-2, its specificity for Avr5 is localised to specific LRR regions (Mesarich et al., 2014). Most fungal strains frequently overcome *Cf-5*-mediated resistance by deleting the *Avr5* gene (Iida et al., 2015; Mesarich et al., 2014; Zaccaron et al., 2022). Similarly, the recently deployed *Cf-6* gene has been mapped to the short arm of chromosome 12, likely allelic with *Cf-Ecp5.12*, and is anticipated to encode an RLP recognising Avr6 — now identified as the apoplastic protein Ecp5. *Cf-6* resistance has already been overcome in several regions through deletion or non-synonymous mutation of *Avr6* (Schol et al., 2025)..

The *Cf-9* locus on chromosome 1 represents a complex genetic region containing paralog genes: *Cf-9A*, *Cf-9B*, *Cf-9C*, *Cf-9D*, and *Cf-9E*, which provide stage-specific defence (de la Rosa et al., 2024). *Cf-9C* (commonly referred to as *Cf-9*) encodes an RLP that recognises the Avr9 effector, triggering a rapid HR that restricts the fungus to the immediate infection point and provides immune-type resistance during all growth stages (de la Rosa et al., 2024; Dixon et al., 1996). Conversely, *Cf-9B* encodes an RLP that specifically recognises the Avr9B effector, providing mature plant resistance during the flowering and fruiting stages. Unlike the *Cf-9C* HR, *Cf-9B*-mediated resistance features leaf chlorosis and a heavy accumulation of PR proteins that gradually halt fungal growth within the mesophyll (de la Rosa et al., 2024).

2.7. Resistance to *Fulvia fulva* in Commercially-Grown Tomatoes

Most leaf mould-resistant cultivars used in commercial tomato production are designated Ff:A-E, Pf:A-E or Cf:A-E (de la Rosa et al., 2024; Li et al., 2015). The letters “A” through “E” represent a classification system for the specific dominant resistance

Cf genes integrated into the tomato genome: *Cf-2*, *Cf-4*, *Cf-5*, *Cf-6,* and *Cf-9* (Jones et al., 1993; Parniske et al., 1997; van der Beek et al., 1992). However, *Cf-9C* and *Cf-9B* (*Cf-9* locus) are the only remaining genes providing resistance against *F. fulva* (de la Rosa et al., 2024).

However, uninterrupted, intensive year-round tomato cultivation has led to the development of *F. fulva* races capable of overcoming both *Cf-9C* and *Cf-9B* (Mesarich et al., 2018). For example, this has been achieved through gene deletion, or disruption through transposable element insertion, of the *Avr* effector genes *Avr9* and *Avr9B*, respectively (de la Rosa et al., 2024).

In New Zealand, a *F. fulva* strain (IPO 2679) isolated back in the 1980s already demonstrated the ability to bypass both the *Cf-9C* and *Cf-9B* resistance genes (Laugé et al., 1998).

2.8. New Resistances to Leaf Mould Identified in Wild Tomato

Current research and breeding efforts focus on expanding the repertoire of resistance genes available for crop protection by combining high-resolution genetic mapping with functional genomics approaches. One such approach, known as effectoromics, uses pathogen effectors to probe wild germplasm for novel resistance specificities, after which the corresponding resistance genes can be mapped and ultimately cloned using high-resolution genetic approaches (Du & Vleeshouwers, 2014; Mesarich et al., 2018).

Recently, effectoromics screening of 41 of 70 apoplastic effector candidates from F. fulva revealed that nine of them (Ecp8 through Ecp16) triggered an HR in specific wild tomato accessions, suggesting they function as *Avr* determinants corresponding to yet-uncharacterised *Cf* resistance genes (Mesarich et al., 2018).

Another gene of interest is *Cf-12* (first mapped in 1980 to the long arm of chromosome 8, but successfully cloned only in 2020). *Cf-12* provides a high level of resistance against multiple races of *F. fulva*, including those that have already overcome the widely utilised *Cf-5* and *Cf-9* resistance genes (Zhang et al., 2025).

Similarly, the recently cloned *Cf-19* gene encodes an immune receptor that induces a resistance response that involves differential gene expression across various defence pathways and hormone signalling (Mesarich et al., 2023; Pei et al., 2026; Zhang et al., 2025).

In contrast, the *Cf-3* and *Cf-11* loci, which correspond to pathogen effector genes that remain unidentified, *Avr3* and *Avr11*, were recently localised to a narrow region on chromosome 11, which lacks the typical sequences encoding RLPs, suggesting that *Cf-3* and *Cf-11* may represent an entirely different class of immune receptors within the tomato genome (Mesarich et al., 2023).

Together, these findings broaden the genetic resources available for tomato breeding and, by encompassing potentially novel receptor classes, offer the mechanistic diversity on which durable, pyramided resistance depends.

2.9. Emerging Challenges in New Zealand's Leaf Mould Management

The significance of the research undertaken in this thesis is underscored by a critical knowledge gap regarding the specific *F. fulva* races currently circulating within New Zealand, and their role in the widespread erosion of resistance in tomato observed over the last decade. While the domestic market offers an extensive array of tomato cultivars marketed with genetic resistance to leaf mould (Table 1), the pathogen has shown a troubling trend of increasing virulence and resistance to traditional management practices normally utilised by local growers.

Longitudinal observations documented by industry sources confirm this clear escalation in disease pressure over the last decade. In 2018, leaf mould emerged as a significant issue across multiple sites following periods of extreme heat and "weather bombs" characterised by heavy rainfall (Vogrincic, 2018). The situation worsened in 2020, with growers reporting "rampant" increases in the disease at several properties. During this period, traditional control methods yielded "less than desired results" compared to previous seasons, suggesting a shift in the efficacy of available

treatments (Vogrincic, 2020). As of April 2024, the disease remains a major threat, increasingly difficult to manage, and “never leaves the crop” (Vogrincic, 2024).

Table 1. *The 22 commercial tomato cultivars available in New Zealand that are marketed as resistant to leaf mould, showing the resistance designation and supplier for each. Designations are Ff:A-E or Pf:A-E, denoting cultivars bred to carry the* Cf-2*,* Cf-4*,* Cf-5*,* Cf-6 *and* Cf-9 *resistance genes (see Section 2.7); no cultivar in this list carries the Cf:A-E designation. Modified from Bayer Vegetables New Zealand (2026a, b, c, d, e, f), Enza Zaden New Zealand (n.d.), Terranova Seeds New Zealand (2026a, b, c, d) and Syngenta (2026).*

Cultivar Name	Type/Segment	Resistance Code	Source / Supplier
DR0603TC	Plum/Small Grape	Pf:A-E	De Ruiter / Bejo
DR0607TC	Cherry	Pf:A-E	De Ruiter / Bejo
Grandice	Extra-large Truss	Pf:A-E	De Ruiter
Marinice	Large Round (Truss)	Pf:A-E	De Ruiter
Merlice	Large Truss	Pf:A-E	De Ruiter / Bejo
Avalantino	Cluster	Pf:A-E	Enza Zaden New Zealand
Avalantino-Rei	Cluster	Pf:A-E	Enza Zaden New Zealand
Formoza	Beef, Cluster	Ff:A-E	Enza Zaden New Zealand
Maxeza	Cluster (Large Beef)	Pf:A-E	Enza Zaden New Zealand
Rhodium	Cluster	Pf:A-E	Enza Zaden New Zealand
Saint Anna	Cocktail	Pf:A-E	Enza Zaden New Zealand
Tobinaro	Loose Round	Pf:A-E	Enza Zaden New Zealand
ENDEVOUR RZ	Large truss / loose	Ff:A-E	Rijk Zwaan / Terranova Seeds
SANTIANA RZ	Large, Loose	Ff:A-E	Rijk Zwaan / Terranova Seeds
SASSARI RZ	Cherry, Loose	Ff:A-E	Rijk Zwaan / Terranova Seeds
GLORIETTE RZ	Large, Loose	Pf:A-E	Rijk Zwaan / Terranova Seeds
Romindo	Plum (Loose)	Ff:A-E	Syngenta
Romatico	Plum (Cluster/Loose)	Ff:A-E	Syngenta
Duelle	Snack (Loose)	Ff:A-E	Syngenta
Dunistar	Mini Plum	Ff:A-E	Syngenta
Climundo	Vine (Cluster/Loose)	Ff:A-E	Syngenta
Clobogo	Loose	Ff:A-E	Syngenta

3. Research Objectives and Hypotheses

3.1. Objectives

Research objectives evolved in response to biosecurity constraints and field observations that revealed industry knowledge gaps in disease identification. The final objectives were:

- Evaluate Pathogen Prevalence (Objective 1): To quantify the occurrence of tomato leaf mould on Ff:A-E resistant tomato cultivars across New Zealand commercial growing operations.

- Characterise Local Pathogen Strains (Objective 2)**:** To characterise the *Avr* and *Ecp* effector gene complement of New Zealand *F. fulva* isolates using whole-genome sequencing, identifying mutations, truncations and gene-loss events across effectors corresponding to deployed *Cf* resistance genes, and comparing these against reference alleles and previously reported international variants.

- Optimise Management Strategies (Objective 3): To provide data-driven insights that enable growers to mitigate outbreak risks and strengthen Integrated Pest Management (IPM) programs.

3.2. Research Hypotheses

- Hypothesis 1 (Objective 1):
    - *H_1: Tomato leaf mould occurs on resistant cultivars (Ff:A-E/Pf:A-E) in New Zealand commercial operations at frequencies sufficient to indicate resistance breakdown or presence of virulent pathogen races.*
    - *H_0: No significant occurrence of leaf mould will be detected on resistant tomato cultivars in commercial operations.*

- Hypothesis 2 (Objective 2):

    - *H_1: New Zealand* F. fulva *isolates possess* Avr *(and/or* Ecp*) effector genes that are absent, truncated, or carry non-synonymous mutations, enabling circumvention of one or more* Cf *resistance genes deployed in commercial cultivars.*
    - *H_0: New Zealand F. fulva isolates possess intact, reference-type* Avr *(and* Ecp*) effector genes, with no absences, truncations, or non-synonymous mutations that would enable circumvention of deployed* Cf *resistance genes.*

- Hypothesis 3 (Objective 3):
    - *Aim: To situate the genomic and field findings from Objectives 1 and 2 within the published literature on* Cf*-mediated resistance durability and protected-cropping microclimate management, generating literature-informed, qualitative recommendations for growers and IPM programmes responding to resistance breakdown in New Zealand. This aim is addressed through synthesis and interpretation of existing evidence rather than through statistical hypothesis testing.*

3.3. Thesis structure and overview

The three objectives above form a deliberately integrated sequence, moving from the scale of the industry to the scale of the genome and back to practical management. Together they address a single overarching question: whether, where, and by what molecular mechanism *Cf*-mediated resistance to leaf mould has broken down in New Zealand, and what this means for the tomato industry. Objective 1 examines the field evidence for resistance breakdown, documenting how often disease occurs on cultivars carrying *Cf* resistance among the sites and cultivars sampled, and thereby indicating whether a breakdown may have taken place. Objective 2 investigates the molecular basis of any such breakdown, using whole-genome sequencing to determine which effector genes have been lost or altered in local *F. fulva* isolates and

how these changes relate to the deployed *Cf* genes and to variants reported internationally. Objective 3 translates these findings into practical guidance, situating the results within the published literature on Integrated Pest Management to help growers interpret and respond to outbreak risk. In this way, the study connects field-level observation, molecular explanation, and applied recommendation, rather than treating any one in isolation.

The remainder of this thesis is organised to follow this progression. Chapter [1] reviews the relevant literature, covering the biology of *F. fulva*, the effector–*Cf* recognition system, and the genomic architecture that underpins the pathogen's capacity for rapid adaptation. Chapter [2] details the materials and methods used across the field survey, isolate collection and characterisation, DNA extraction, genome sequencing, and the bioinformatic pipeline developed for effector analysis. Chapter [3] presents the results of the field survey and the genomic characterisation of the sampled isolates. Chapter [4] discusses these findings in the context of the international literature — assessing which *Cf* resistances have likely been overcome, whether the New Zealand population is clonal, and what the results imply for resistance deployment — before Chapter [5] draws together the main conclusions and identifies priorities for future work.

Chapter 2

4. Materials and Methods

4.1. Stakeholder Engagement and Participant Recruitment Strategy

Growers from around the country were contacted directly by TomatoesNZ and/or the main researcher via email and/or phone. Additionally, a formal request for samples was circulated to all 140 registered New Zealand tomato growers (TomatoesNZ, 2026) via the TomatoesNZ November 2024 Newsletter, highlighting the study's significance to the national industry.

At the request of TomatoesNZ, a research call was also published in the Grower2Grower newsletter (https://www.grower2grower.co.nz/leaf-mould-cladosporium-plant-samples-required/) to engage a broader network of growers and agronomists across New Zealand.

Continuous sampling efforts were supported by professional networking with industry players (including advisors, contractors, and research collaborators) facilitated through both TomatoesNZ and the primary researcher's existing professional connections.

4.2. Sample Collection Protocol

A standardised sampling protocol was implemented to ensure the integrity and traceability of *F. fulva* specimens collected across diverse geographic locations. To maintain methodological consistency, each participating grower received an identical sampling kit via courier. These kits contained six disposable gloves, a bottle of hand sanitiser, three resealable plastic bags, three sampling forms, and a prepaid postage bag for return dispatch.

The procedural framework was supported by a comprehensive documentation suite provided within each kit that included a step-by-step procedural manual (Tomato Leaf Mould Sampling Guidelines; see Appendix I), a visual reference for field identification

(Tomato Leaf Mould Symptoms Guide; see Appendix II), a technical information detailing the disease cycle and key symptoms (Tomato Leaf Mould Factsheet; see Appendix III), and a dedicated document for recording metadata, including grower location, cultivar name, and crop age (Sampling Form; see Appendix IV).

To ensure morphological details remained clear for retrospective diagnostic verification, field symptoms were documented using a high-resolution digital photography setup (Canon EOS R7 APS-C Mirrorless Camera, Sigma 18-50 mm f/2.8 DC DN Contemporary Lens, 7Artisans 60mm F2.8 Macro 2x Canon RF Lens, Godox TT520II Speedlite Flash and a flash diffuser).

4.2.1. Operational Procedure

The protocol emphasised strict segregation of plant material, requiring that each resealable bag contain leaves from only a single cultivar or specific glasshouse area to prevent cross-contamination. Furthermore, growers were instructed to dispatch samples on the day of collection to maintain viability; if same-day postage was unavailable, samples were to be refrigerated overnight and posted the following morning.

The collection procedure began with thorough handwashing, followed by identification of glasshouse zones exhibiting clear leaf mould symptoms. Sampling was strictly limited to the lower canopy, where growers selected one to three symptomatic leaves within a 5 m radius, potentially from the same or neighbouring plants. Just before excision, the sampler donned disposable gloves and applied hand sanitiser to the gloved surface to mitigate the risk of introducing external contaminants.

4.2.2. Specimen Recovery and Biosecurity

Specimen collection involved removing the entire leaf at its junction with the main stem and placing it immediately into a resealable plastic bag. After purging excess air and sealing the bag, a completed sampling form was included to document the specific cultivar and location data. After successfully bagging the material, gloves were

discarded, and the sampler performed a final hand-sanitising or handwashing step. This sequence was repeated for each subsequent area or cultivar sampled, ensuring that every specimen was handled with the same level of biosecurity and precision.

4.3. Fungal Isolation

The collected samples were dispatched to two primary facilities: Massey University's Manawatu Campus in Palmerston North for initial isolation, and New Zealand Institute for Bioeconomy Science's (BSI) Mount Albert Research Centre in Auckland for both isolation and subsequent culturing. The established conservation protocol required leaves to be air-dried and stored individually in plastic or paper bags.

Under constant room conditions (20° at an average RH of 85%), specimens remained viable for approximately 14 days; however, logistical constraints during the peak summer window resulted in the loss of 7 of 10 samples collected between December 2024 and February 2025.

The isolation of *F. fulva* followed distinct pathways at different institutions:

At Massey University, small sections (5–10 mm) were isolated from dried samples, specifically targeting areas displaying lesions compatible with leaf mould. At the BSI, a similar isolation was performed using fresh samples, which were then subjected to a rigorous surface sterilisation process.

This involved a one-minute immersion in 70% (v/v) ethanol followed by a sterile reverse osmosis (RO) water rinse, a 1-min treatment with an approximate 10% (v/v) bleach concentration (diluted from Sodium hypochlorite 12-15%), and a final RO water rinse (Sudermann et al., 2022). Following a 5-min air-drying period on sterile filter paper, the material was plated on potato dextrose agar (PDA; Oxoid, Basingstoke, UK) amended with chloramphenicol (100 mg/L; Sigma-Aldrich, St. Louis, MO, USA) or 1% lactic acid to prevent bacterial growth and delay growth of undesired contaminants (Sudermann et al., 2022).

These cultures were maintained for several weeks at 20°C, while others were incubated at 25°C with 85% average RH, beginning with a seven-day dark cycle.

To achieve purified isolates, a single-spore isolation technique was employed: mycelium and conidia from the colony edge were suspended in 1–2 mL of sterile RO water and vortexed for 30 s. From this, 5 mL of the suspension was transferred to a new tube and diluted with 50 mL of sterile RO water (Sudermann et al., 2022). Aliquots of 50 µL were then spread on PDA following a 12-to-16-h dark incubation cycle at 20°C.

Germinating conidia were identified using a Leitz Wetzlar inverted microscope (Ernst Leitz Wetzlar GmbH, Wetzlar, Germany) equipped with Periplan 10x oculars within a biosecurity cabinet and transferred to fresh media using sterile microtools.

These samples were incubated at 20°C to 25°C for two to four weeks. Identification as *F. fulva* was verified first through visual assessment of colony morphology, colour and texture, followed by microscopic analysis of fungal structures using a Leica DM1000 LED microscope (Leica Microsystems, Wetzlar, Germany). Samples were prepared using lactophenol cotton blue stain (cotton blue 0.05% [w/v]; phenol 20% [w/v]; lactic acid 20% [v/v]; glycerol 40% [v/v]; distilled water 20% [v/v]). Images were captured and processed using the Leica Application Suite X (LAS X; version 5.3.3, Leica Microsystems, Wetzlar, Germany) software to examine conidium shape and sporulation bodies.

4.4. Cryopreservation and Long-Term Storage

Performed only for DC2, PT1 and GR1 isolates (see section [5.5.] and Table 4). Colonies for these isolates were preserved for long-term storage by culturing in Potato Dextrose Broth (PDB; Oxoid, Basingstoke, UK) until peak mycelial growth was achieved. Aliquots of the culture were combined with a sterile glycerol solution (Sigma-Aldrich, St. Louis, MO, USA) to achieve a final concentration of 20% (v/v) glycerol. The suspensions were transferred to sterile 2 mL Cryo.s™ cryovials (Greiner Bio-One, Frickenhausen, Germany), mixed thoroughly by vortexing, and equilibrated at 4°C for

30 minutes before being placed directly into a -80°C ultra-low temperature freezer for long-term storage.

4.5. Genomic DNA Extraction from Fungal Isolates

Biomass production from *F. fulva* isolates for genomic DNA extraction was initiated using conidial suspensions derived from uncontaminated single-spore PDA plates. In one method, 1 mL of suspension was used to inoculate 50 mL of PDB, which was cultured at 22°C and 150 rpm for 48 to 116 h in a MaxQ™ 4000 Benchtop Orbital Shaker (Thermo Fisher Scientific, Waltham, MA, USA; Figure 5).

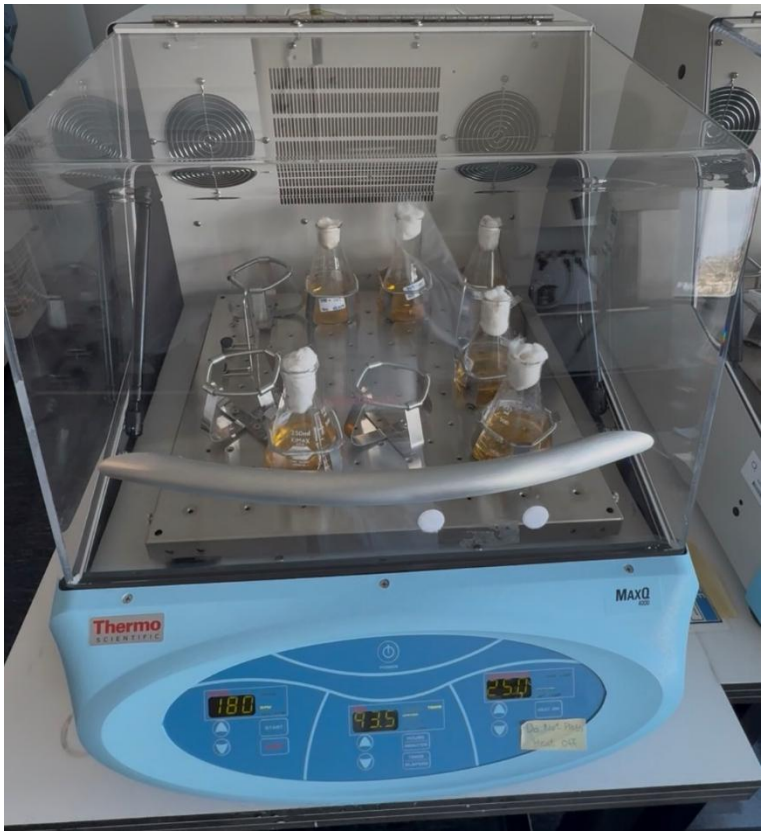

Figure 5. *MaxQ™ 4000 Benchtop Orbital Shaker (Thermo Fisher Scientific, Waltham, MA, USA) containing Potato Dextrose Broth cultures of* Fulvia fulva.

Alternatively, 2–8 mm colony edge plugs were used to inoculate 80–100 mL of PDB in 250 mL Erlenmeyer flasks, which were maintained under the same conditions for 96 h. Following incubation, the resulting biomass was strained through a funnel lined with Miracloth (Calbiochem, MilliporeSigma, Burlington, MA, USA) using sterile RO

water to clear PDB. After removing excess moisture, the biomass was wrapped in foil, compacted, snap-frozen in liquid nitrogen, and transferred to long-term storage at -80°C.

4.6. DNA Extraction Protocol

Genomic DNA from *F. fulva* was isolated using two modified extraction methods: a CTAB (cetyltrimethylammonium bromide) extraction based on the protocol described by Doyle and Doyle (1987), and a modified protocol from the high-molecular-weight DNA extraction protocol published by Möller et al. (1992).

4.6.1. CTAB DNA Extraction Method

4.6.1.1. Extraction and Phase Separation

For each sample, approximately 50 mg of mycelium, instantly frozen in liquid nitrogen and ground to a fine powder using a pre-chilled mortar and pestle, was transferred to a sterile 1.5 mL microcentrifuge tube. Each sample was treated with 600 µL of CTAB buffer (CTAB 2% [w/v]; PVP-40 1% [w/v]; Sodium chloride [NaCl] 1.4 M; EDTA 20 mM; Tris HCl ([pH 8.0] 0.1 M) buffer and 2 µL of RNase A (20 mg/mL; New England Biolabs, Ipswich, MA, USA), mixed thoroughly, and incubated at 37°C for 10 min. Following incubation, samples were heated in a water bath at 65°C for 40 min with inversion every 10 min.

Once cooled below 60°C, 600 µL of chloroform was added in a fume hood. The mixture was allowed to stand for 2 min to facilitate phase separation, then centrifuged in an Eppendorf Centrifuge 5424 R (Eppendorf, Hamburg, Germany) at 13,000 rpm for 5 min at 4°C. The resulting aqueous phase was then carefully transferred to a fresh sterile tube.

To enhance DNA purity, an organic extraction was performed by adding 100 µL of 1:1 phenol:chloroform to the aqueous phase, then centrifuging as above at 13,000 rpm for

5 min. The upper aqueous phase was further extracted with chloroform, then centrifuged in an Eppendorf Centrifuge 5424 R at 13,000 rpm for 2 min at 4°C.

4.6.1.2. Precipitation and Re-suspension

DNA precipitation was achieved by adding 600 µL of 100% isopropanol (v/v) and incubating at -20°C for 30 min, followed by a gentle pulse centrifugation in the Eppendorf Centrifuge 5424 R (7,000 rpm for 1 min).

The resulting DNA pellet was washed twice with 600 µL of ice-cold 70% (v/v) ethanol and centrifuged briefly as above to settle the material. After removing all traces of residual ethanol, the pellet was air-dried and re-suspended in 50 µL of TE buffer (10 mM Tris-HCl, pH 8.0; 1 mM EDTA, pH 8.0).

4.6.2. High Molecular Weight DNA Extraction Protocol

4.6.2.1. Day 1: Lysis and Phase Separation

Between 0.1 and 0.2 g of ground tissue was suspended in 5 mL of TES buffer (100 mM Tris, pH 8.0; 10 mM EDTA; 2% [w/v] SDS) in a 50 mL Falcon tube. Protein digestion was initiated by adding 10 µL of Proteinase K (Invitrogen, Thermo Fisher Scientific, Waltham, MA, USA). The tube contents were gently inverted three times and incubated for 60 min at 55 °C.

Post-incubation, the salt concentration was adjusted by adding 1.40 mL of 5 M NaCl. Subsequently, approximately 850 µL of 10% CTAB (1/10 volume) was added. The mixture was incubated at 60°C for 20 min until the solution cleared. To remove RNA, 50 mL of RNase A was added, and the mixture was incubated at 37°C for 10 min. Proteins and lipids were removed by adding 7 mL of chloroform:isoamyl alcohol (24:1, v/v). The phases were separated via centrifugation using an Eppendorf Centrifuge 5804 R (Eppendorf, Hamburg, Germany) at 3000 rpm for 15 min at room temperature (20°C). Up to 5 mL of the resulting supernatant was carefully transferred into a new 50 mL Falcon tube, mixed with 2.25 mL of 5 M ammonium acetate ($NH_4CH_3CO_2$), and

incubated overnight at 4°C to precipitate ontaminants (e.g. residual proteins and polysaccharides), which were subsequently removed by centrifugation.

4.6.2.2. Day 2: DNA Precipitation and Recovery

The chilled mixture was placed in a Sorvall RC6 Plus centrifuge (Thermo Fisher Scientific, Waltham, MA, USA) and centrifuged at 1542 × *g* for 15 min at room temperature (20°C). The supernatant was transferred to a new 50 mL Falcon tube, and 4 mL of 100% v/v isopropanol (0.55 volume) was added. The solution was mixed gently by inversion 50 times and placed at -20°C for 30 min. After this time, the samples were centrifuged in the Sorvall RC6 Plus at 3000 rpm for 15 min at 4°C to pellet the DNA.

The resulting pellet was washed with 5 mL of ice-cold 70% ethanol, centrifuged for 10 min at 4°C in the Eppendorf Centrifuge 5424 R, and the supernatant discarded. The pellet was air-dried for 30 min to remove residual ethanol. Finally, the DNA was re-suspended in 50 mL of UltraPure™ DNase/RNase-Free Distilled Water without pipetting to maintain polymer integrity and stored at 4°C.

4.7. Assessment of DNA Quality and Concentration

4.7.1. Fluorometric and Spectrophotometric Quantification

DNA concentration and purity were assessed using a DeNovix DS-11 FX+ Spectrophotometer/Fluorometer (DeNovix Inc., Wilmington, DE, USA).

4.7.2. Agarose Gel Electrophoresis for DNA Integrity

To evaluate structural integrity and verify the presence of high-molecular-weight genomic DNA prior to sequencing, the extracted fungal DNA samples were subjected to agarose gel electrophoresis. A 0.8% (w/v) agarose gel was prepared by melting molecular biology-grade agarose powder in 1X Tris-acetate-EDTA (TAE) buffer. The solution was heated in a microwave in 30-s intervals with intermittent swirling until the

agarose was completely melted and transparent. The mixture was allowed to cool to approximately 60°C before being supplemented with SYBR™ Safe DNA gel stain (Invitrogen, Carlsbad, CA, USA) at a 1:10,000 dilution. The liquid agarose was gently swirled to avoid bubble formation, poured into a gel casting tray fitted with an appropriate well comb, and allowed to polymerise at room temperature for 30 minutes.

Once solidified, the comb was removed, and the gel was transferred into a horizontal electrophoresis chamber submerged in 1X TAE running buffer to a depth of approximately 3 mm above the gel surface. DNA samples were thawed on ice and prepared for loading by combining 5 µL of genomic DNA with 1 µL of 6X DNA loading dye (New England Biolabs, Ipswich, MA, USA). A negative water control was prepared concurrently by mixing 5 µL of nuclease-free water with 1 µL of 6X loading dye.

Samples were loaded systematically into the wells according to a predefined layout: a premixed 1 kb Plus DNA molecular weight marker (15 µL; New England Biolabs, Ipswich, MA, USA) was introduced into Lanes 1 and 7, followed sequentially by genomic DNA of isolates ICMP 7320, CM1 and CO1 in Lanes 2, 3, and 4, respectively. The negative water control was loaded into Lane 5; Lane 6 remained empty. Electrophoresis was executed at a constant voltage of 90 V for 60 min, allowing the bromophenol blue tracking dye front to migrate across two-thirds of the gel length. Following separation, the gel was removed from the chamber, and the DNA fragments were visualised and digitally documented via a Large Blue LED Transilluminator (IO Rodeo Inc., Pasadena, CA, USA).

4.8. Bioinformatic Pipeline

4.8.1. Genome Sequencing

Sequencing libraries were prepared at the Massey Genome Service (MGS). The Illumina Nextera™ XT library preparation method was used to prepare a pooled library. The library was sent to Novogene for sequencing on the Illumina NovaSeq™ platform, yielding 21G of raw 150 bp paired-end reads.

Bioinformatic analysis was undertaken on the REANNZ cluster. Raw reads were quality-controlled and trimmed with TrimGalore v0.6.10, removing the Illumina Nextera adapters and poly (G) tails. Sequences were assembled with SPAdes v4.0.0 using the --careful flag. Contigs less than 1 kb were removed with SeqKit v2.12.0. Assemblies were quality-controlled with BUSCO v5.8.2 using the dothideomycetes_odb10 dataset (Table 2).

***Table 2**. Assembly statistics for the three sequenced* Fulvia fulva *isolates. Genome assemblies were generated with SPAdes v4.0.0 (--careful), filtered to remove contigs shorter than 1 kb (SeqKit v2.12.0), and assessed for completeness with BUSCO v5.8.2 against the dothideomycetes_odb10 lineage dataset. BUSCO (%) is the proportion of complete single-copy orthologues recovered; N50 is the contig length at which half the total assembly length is contained in contigs of that size or longer. Length is the total assembled length in base pairs. Isolates are ordered by collection date: ICMP 7320 (1980s), CM1 (2022), CO1 (2025).*

Isolate	Busco (%)	No. of Contigs	Length	N50
CM1	99.4	3305	67,565,517	68,120
CO1	99.3	10584	80,198,756	40,026
ICMP 7320	99.1	3334	65,245,698	38,864

4.8.2. Reference and Isolate gDNA Alignment and Output Overview

Reference alleles were provided by genomic DNA (gDNA) from strain 0WU for all effectors except Avr4E, for which strain R5 was used. This is because isolate 0WU carries up to two Cf-4E-breaking mutations in Avr4E, whereas isolate R5 contains a wild-type allele. Effector coding sequences from three *F. fulva* isolates — ICMP 7320 (1980s), CM1 (2022) and CO1 (2025) — were then compared against these reference alleles using a custom, modular pipeline implemented in Python (version 3.12.8) through PyCharm 2026.1.4 (Build #PY-261.26222.68), orchestrated to run end-to-end from a single command. The pipeline is fully deterministic: all integrity, variant and absence calls derive from sequence alignment and translation, with no stochastic or model-based inference. It proceeds through six stages — (1) intron excision, (2) multiple sequence alignment, (3) variant calling and integrity classification, (4) conservation/divergence profiling, (5) difference-alignment figures, and (6) generation of the effector-integrity matrix — with each stage passing structured output to the next.

4.8.3. Sequence Preparation and Intron Excision

Isolate sequences were genomic (intron-containing), whereas reference coding sequences were intron-free; introns were annotated only in the reference. To place isolate and reference on a common coding-sequence footing, a homology-based excision step was applied. For each effector, the reference intron positions (annotated in the reference gDNA) were used to construct a per-base intron mask. Each isolate genomic sequence was aligned to the reference gDNA by global pairwise alignment (Biopython PairwiseAligner; [Cock et al., 2009]; match +2, mismatch −1, gap-open −5, gap-extension −0.5), and the reference intron mask was transferred across the alignment by homology. Isolate bases aligning to reference *exon* positions were retained and concatenated to yield an intron-free isolate coding sequence; bases aligning to reference introns were discarded.

For each isolate–effector gene combination, an exon-coverage fraction was recorded (recovered exon positions ÷ total reference exon positions). Coverage ≥0.95 was taken as full coding-sequence recovery; coverage below this threshold indicated that the isolate did not span the entire gene and was flagged as a partial recovery (candidate gene deletion/disruption). Effector genes recorded as not detected in an isolate were logged as absence events and excluded from that effector's alignment rather than represented by any placeholder sequence. Reconstructed coding sequences were translated to protein using the standard genetic code (Biopython).

4.8.4. Multiple Sequence Alignment

Intron-free coding sequences for each effector were aligned in Clustal Omega (version 1.2.2; Sievers et al., 2011) under default parameters, preserving input order (--output-order=input-order) to retain the reference sequence as the first entry. Protein alignments were generated separately from the translated coding sequences. MAFFT (v7.505; Katoh & Standley, 2013) was available as an interchangeable alternative aligner; alignments produced by the two tools were compared during development and gave identical integrity classifications. Effectors with fewer than two sequences (e.g. those absent from all isolates) were not aligned and were retained only as absence records.

4.8.5. Variant Calling and Integrity Classification

Variants were called from each reference-anchored alignment. At every alignment column, isolate residues were compared to the reference; single-nucleotide substitutions, insertions and deletions were recorded in reference coordinates using an HGVS-style *c.* notation. Substitutions were classified as synonymous or missense by translating the affected reference codon with and without the change. The protein-level consequence for each isolate was determined by translating its reconstructed coding sequence from the start codon and comparing the product to the reference protein. Each effector–isolate combination was assigned an integrity class — *intact* (protein identical to reference), *missense* (full length, one or more amino-acid substitutions), *truncated* (coding sequence not spanning the full gene / premature termination), or *absent* — and its percentage protein identity to the reference was recorded. Because alignment placement of gaps at insertion and truncation boundaries is not unique, junction coordinates were treated as tool-dependent and the integrity class, rather than the exact boundary position, was used as the primary descriptor.

4.8.6. Conservation and Divergence Metrics

Two per-column quantitative metrics were computed for each alignment (nucleotide and protein). **Shannon entropy** (in bits) was calculated as $H = -\Sigma\, p_i \log_2 p_i$ over the residue frequencies in each column, with the alignment gap treated as an additional symbol state so that deletions register as variation; the gap fraction per column was recorded separately. **Percentage identity to the reference** was calculated per column as the proportion of non-reference sequences whose residue matched the reference; columns at which the reference itself was a gap (insertions relative to the reference) were flagged and excluded from reference-coordinate identity. Metrics were reported on reference-coordinate axes to align with the variant coordinates. No inferential statistical testing was applied: with three isolates, the analysis is descriptive, quantifying the location and extent of divergence rather than testing hypotheses. Summary statistics per effector (mean entropy, mean identity, number of insertion columns) were tabulated.

4.8.7. Data Outputs and Structured Validation

All quantitative outputs were written in both CSV (flat, one record per row) and JSON. The JSON files use a self-describing envelope comprising a metadata header (dataset name, record and effector counts, and pre-computed category tallies) and a records/columns array, with undefined values encoded as null. This typed, self-describing structure was designed for schema validation and downstream consumption. A typed data model layer was applied to enforce and validate this schema using Pydantic (version 2.13.4; Colvin et al., 2026), described in subsection [4.8.8].

4.8.8. Literature Metadata Extraction

A corpus of 21 primary papers reporting effector allelic variation in *F. fulva* (*P. fulva* or *C. fulvum*) was compiled into a structured, machine-readable database in two stages. This component is separate from the deterministic sequence pipeline (subsection [4.8.7.]): it produced a literature database for comparison and context only and did not contribute to sequence integrity, variant, or absence calls.

First, each paper was converted from PDF to Markdown with a custom Python script based on the PyMuPDF4LLM library (version 1.28.0), run through a purpose-built graphical batch interface. Markdown was chosen over raw text extraction because it preserves section hierarchy and tabular structure, in which effector mutation data are typically presented. Second, the Markdown files were processed using a Python pipeline that combined Pydantic schema validation with the large language model (LLM) GPT-5 (OpenAI; model identifier: gpt-5; accessed 4 June 2026) via the OpenAI API. The Pydantic model enforced strict typing on the returned data and required any field not explicitly stated in the source to be returned as null rather than inferred, to constrain the model against hallucination.

Each observation recorded the effector name, target-effector status, strain name (where reported), nucleotide and amino-acid positions, nucleotide and amino-acid change, mutation type, synonymous/non-synonymous status, reported phenotype, whether resistance was reported as broken, the type of functional evidence, and free-text notes; each paper additionally recorded bibliographic metadata, geographic

regions, strains, and paper-level notes. The output comprised 970 observations across the 21 papers. Because this stage is LLM-based, its outputs are non-deterministic and subject to model deprecation, and the extracted metadata are a record of the extraction rather than an independent reading of the sources. In particular, the field indicating whether resistance was broken combines experimentally demonstrated and deduced (not experimentally tested) claims; this distinction is retained in the functional-evidence and notes fields and is carried through the cross-reference (subsection [4.8.9.]). The prompt/instruction and the Pydantic schema are available in Supplementary Appendix VI.

4.8.9. Literature Cross-Referencing

New Zealand variant calls were compared with the extracted literature database using a deterministic Python script that performs no model-based inference, ensuring exact, reproducible comparisons. The script loads the sequence-pipeline outputs and the literature database, then joins them at the effector and amino acid position levels. Effector names were normalised through a synonym map so that research-era identifiers resolve to the canonical gene (e.g. *Ecp5→Avr6*, *Ecp2→Ecp2-1*, and the *CfCE*-series names), preventing silent non-matches. Amino-acid changes were parsed from both notations present in the data — three-letter HGVS with or without a p. prefix, “from>to” strings without a position, and the one-letter combined form produced by the variant caller — to a common (effector, position, from-residue, to-residue) key, using the explicit amino-acid-position field as a fallback. Resistance-breaking claims were classified as experimental or deduced by scanning the functional-evidence and notes fields for inference markers rather than relying on the resistance-broken flag alone. The script emitted a compact digest reporting, per effector: the novelty of each New Zealand change relative to the literature (novel position, known position, or identical change); the counts of experimental versus deduced resistance-breaking observations per cognate *Cf* gene; the distribution of reported mutation positions; and the most frequently reported changes. This digest, rather than the full literature file, served as the basis for the literature comparisons reported in the Discussion (sections [6.8]–[6.16]).

4.8.10. Visualisation

Figures were generated with matplotlib (version 3.11.0; Hunter, 2007). Difference-alignment figures show the reference sequence first, with isolate residues displayed as identity dots where they match the reference and as differing residues otherwise, coloured by change type and trimmed to variable regions. The effector-integrity matrix (See Results, Figure 21) presents effectors × isolates as a categorical heatmap coloured by integrity class and annotated with protein identity. Conservation profiles plot per-column Shannon entropy and percentage identity to the reference against reference coordinates.

4.8.11. Software and Availability

Sequence pipeline: Python (version 3.12.8), Biopython (version 1.87; Cock et al., 2009), Clustal Omega (version 1.2.2; Sievers et al., 2011), MAFFT (v7.505; Katoh & Standley, 2013), and matplotlib (version 3.11.0; Hunter, 2007), organised as modular scripts (intron excision, alignment/extraction, variant calling, conservation, difference figures, integrity matrix) coordinated by a single orchestrator script.

Literature pipeline: PyMuPDF4LLM (version 1.28.0) for PDF-to-Markdown conversion, Pydantic (version 2.13.4; Colvin et al., 2026) for schema validation, GPT-5 (OpenAI; model identifier: gpt-5; accessed 4 June 2026) for extraction, and a deterministic Python cross-reference script. Code and prompts are available upon request. The extraction prompt and Pydantic schema are included in Appendix VI.

Chapter 3

5. Results

5.1. Field Collection and Geographic Distribution

A total of 19 unique samples were successfully obtained across nine distinct geographic locations throughout New Zealand. In this study, “unique samples” are defined as specimens collected from geographically separate sites or from different tomato cultivars within a single site. The sampling effort followed a hybrid model necessitated by regional biosecurity constraints: 12 samples were collected directly by the lead researcher. At the same time, the remaining seven were provided by participating growers through the standardised participant-led protocol (see Table 3).

Despite industry-wide restrictions on ToBRV, the lead researcher was able to conduct personal site visits at six locations: Reporoa, Ohaupo, Tuakau, and Bucklands in the North Island, and Heathcote Valley and Clarkville in the South Island. These visits did not require external biosecurity clearance as the sites were either directly affiliated with or related to the researcher’s established workplace operations. Furthermore, two small-scale growers in Whanganui were personally visited, as their operations are open to the general public, allowing for direct oversight of the collection process.

The visual documentation of these sites (Figures 6 to 11) illustrates the diverse growing environments and varying levels of disease pressure encountered during the survey. Each visited location provided a unique snapshot of *F. fulva* morphology and symptom progression *in situ*, contributing to a more robust understanding of the pathogen’s current distribution across the North and South Islands.

5.2. Leaf Mould Occurrence on Resistant and Non-Resistant Cultivars

Of 22 commercially available tomato cultivars marketed as *F. fulva*-resistant under the Ff/Pf/Cf:A–E denomination (Table 1), leaf samples were received from four cultivars (Clobogo, Grandice, Duelle and Avalantino) during this study (Table 1). All four showed symptoms strongly consistent with tomato leaf mould (Figures 6–17; Table 4), confirming disease on cultivars carrying deployed *Cf* resistance genes. Surveyed growers and sample suppliers further reported that leaf mould is relatively common and has been observed on considerably more resistant cultivars than those sampled here, indicating that the samples analysed represent a subset of a more widespread occurrence.

A further ten samples were received from cultivars or varieties not marketed as leaf mould-resistant (Gardecia, Campari, Provine, Olay, Alfred, Prodelle, and four unidentified; Table 4). All showed symptoms strongly consistent with leaf mould, except Campari, which showed rather few symptoms.

Both isolate ICMP 7320 (collected in the 1980s) and CM1 were obtained from a culture collection rather than the present survey and are therefore not included in this occurrence assessment. Notably, CM1 was recovered from a Campari sample collected in 2022, demonstrating that F. fulva was present despite the absence of symptoms.



Figure 6. *Leaf mould symptoms on tomato cultivar 'Grandice' in Reporoa in November 2024. Different infection stages are seen in the abaxial (lower) side of these leaves. The central leaf shows the highest concentration of velvety sporulation bodies, covering approximately 2/3 of the area.*



Figure 7. *Leaf mould symptoms on tomato landrace (landrace locally bred by the grower) 'Oley' in Whanganui in February 2025. a) Scattered, pronounced brownish sporulation bodies are observed across the abaxial (lower) side of the leaf; b) Multiple chlorotic-diffuse spots extend across the majority of the adaxial (upper) side of the leaf.*

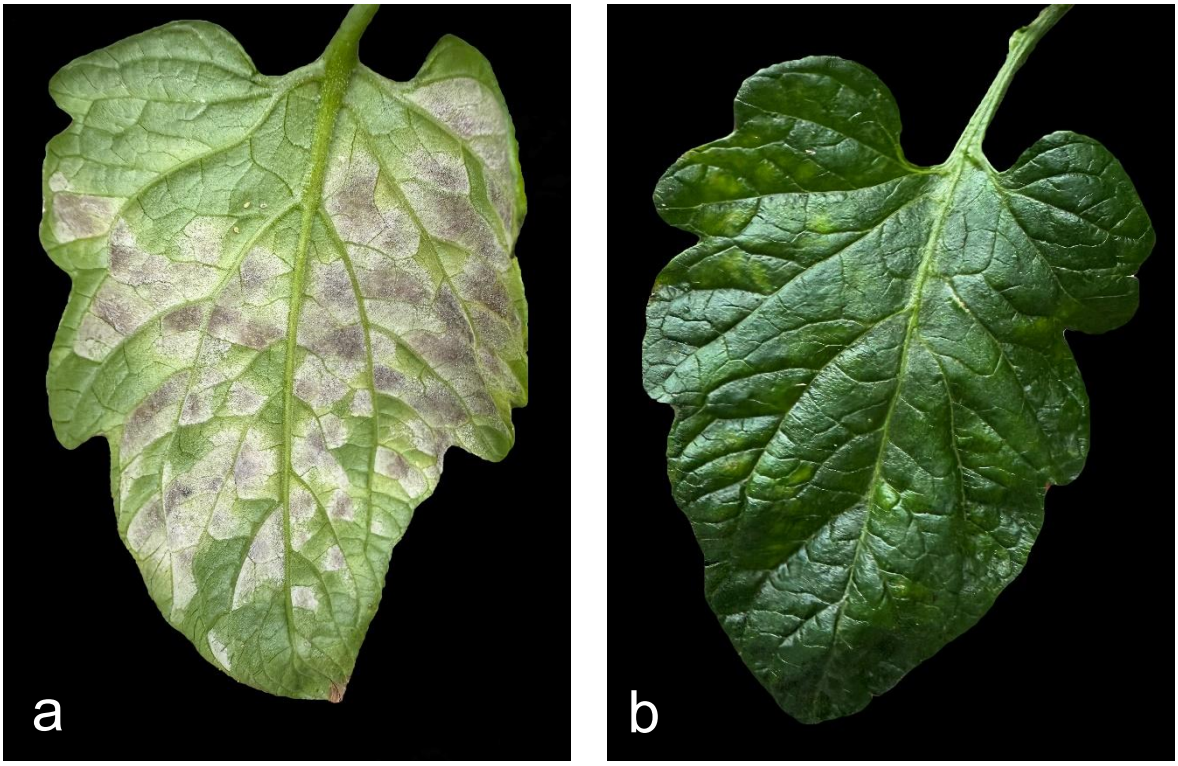

Figure 8. *Leaf mould symptoms on tomato cultivar 'Grandice' in Tuakau in February 2025. a) The majority of the abaxial (lower) side of the leaf has been overtaken by a greyish-purple clump of sporulation bodies. b) Despite advanced fungal presence in the opposite side of the leaf, the adaxial (upper) side of the leaf appears green, with mild chlorosis symptoms.*



Figure 9. *Leaf mould symptoms on tomato cultivar 'Duelle' in Heathcote Valley in February 2025. The picture shows the abaxial (lower) side of the leaf, with seven relatively scattered brown sporulation bodies across the leaf area.*

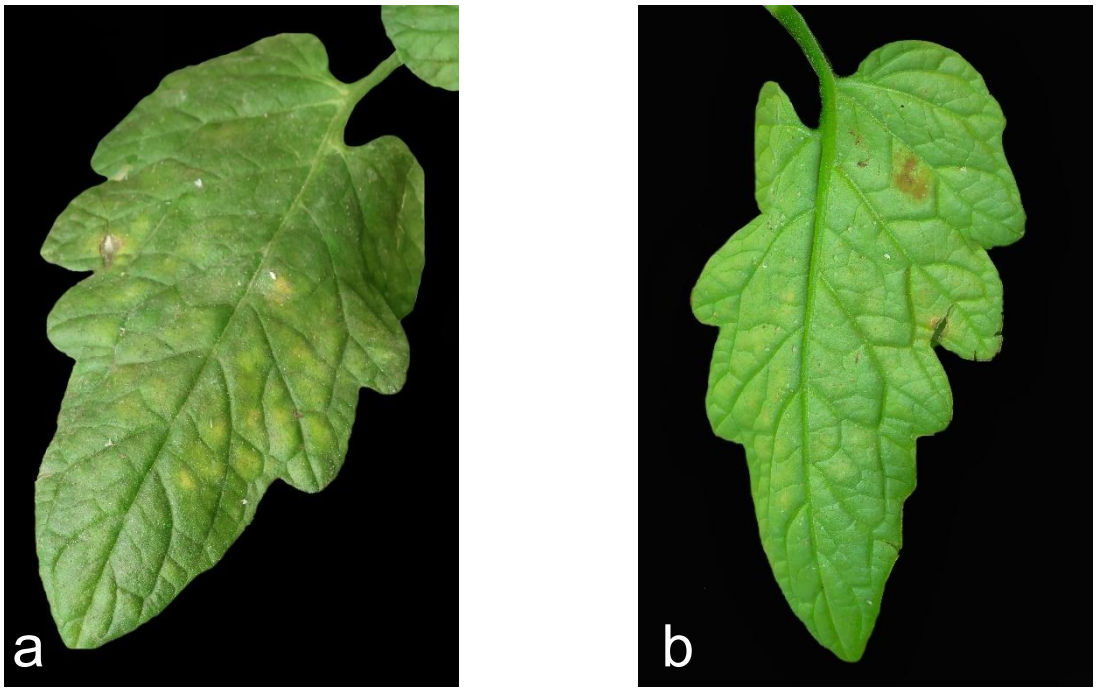

Figure 10. *Leaf mould symptoms on tomato cultivar 'Avalantino' in Clarville in February 2025. a) Mild-difusse chlorosis is present in the adaxial (upper) side of the leaf. b) A single small incipient brownish formation can be seen in the abaxial (lower) side of the leaf.*



Figure 11. *Leaf mould symptoms on tomato cultivar 'Clobogo' in Ohaupo in June 2025. In this abaxial (lower) view, a single, relatively condensed point of infection towards the tip of the leaf extends from the midrib to the margin.*

Table 3. *Field collection log outcomes for the 2024–2026 tomato leaf mould survey.*

Grower location	Grower agreed to participate	Crop displayed symptoms compatible with *Fulvia fulva*	Number of samples provided	Sample processing destination
Oamaru (Otago)	D/A	N/A	N/A	N/A
Kerikeri (Northland)	D/A	N/A	N/A	N/A
Leeston (Canterbury)	D/A	N/A	N/A	N/A
Reporoa (Waikato)	Yes	Yes	3	Massey University
Mokai (Waikato)	Yes	Yes	2	BSI / Massey University
Nelson (Nelson)	Yes	No	N/A	N/A
Wairoa (Hawke's Bay)	No	No	N/A	N/A
Buckland (Auckland)	Yes	Yes	1	BSI
Tuakau (Waikato)	Yes	Yes	3	BSI / Massey University
Whanganui (1) (Manawatū-Whanganui)	Yes	Yes	6	BSI / Massey University
Whanganui (2) (Manawatū-Whanganui)	Yes	Yes	1	BSI / Massey University
Waimauku (Auckland)	D/A	N/A	N/A	N/A
Clarkville (Canterbury)	Yes	Yes	1	BSI / Massey University
Heathcote Valley (Canterbury)	Yes	Yes	1	BSI / Massey University
West Melton (Canterbury)	Yes	Yes	1	BSI
Ohaupo (Waikato)	Yes	Yes	1	BSI
Raglan (Waikato)	Yes	Yes	0	N/A
Drury (Auckland)	Yes	Yes	1	BSI / Massey University
Clevedon (Auckland)	Yes	Yes	1	BSI / Massey University
Pokeno (Waikato)	Yes	Yes	1	BSI / Massey University[1]

D/A Did not answer
N/A Not applicable
BSI The New Zealand Institute for Bioeconomy Science

5.3. Fungal Isolation and Culture Viability

The initial phase of laboratory processing was significantly impacted by sample degradation and logistical delays. Samples from the first rounds in Clarkville, Heathcote Valley, Mokai, Drury, and Clevedon, as well as the second round from Whanganui, failed to produce viable cultures. These specimens remained in storage paper bags and partially open resealable bags for five to eight weeks (a duration that was found to exceed the viability window for *F. fulva*). Furthermore, samples from Mokai (cultivars Campari and Provine) and Whanganui (landrace Oley) suffered extensive water damage during courier transit. In the limited leaf material that survived these transit delays, morphological symptoms did not show strong compatibility with *F. fulva,* resulting in the total loss of these specimens.

Of the 22 unique samples obtained, seven were deemed viable for isolation, yielding approximately 200 initial cultures. However, only ≈20% of these cultures yielded colonies compatible with *F. fulva*.

The remaining 80% either failed to develop or were rapidly overtaken by competitive growth of bacteria and other fungal species. To augment the study's collection, the Plant Pathology Lab at Massey University provided pre-isolated colonies from the Campari (Mokai) cultivar and the reference strain ICMP 7320 (Table 4). Throughout this stage, microbial contamination remained a persistent challenge. To address this, the isolation protocol was revised to include a surface disinfection step (Sudermann et al., 2022), which markedly improved isolation success at the BSI facility. Despite these refinements, ubiquitous contaminants such as those compatible with *Penicillium* and *Cladosporium* spp. frequently appeared after sealed plates were opened for macro- and microscopic inspection and sub-culturing. Here, *Cladosporium* refers to genuine contaminant species and is not to be confused with the basionym of *F. fulva* (*C. fulvum*), as *F. fulva* is now known not to be a *Cladosporium* species and has been reclassified accordingly (Videira et al., 2017). Moreover, backup plates after extended storage (>4 weeks) began showing signs of microbial contamination (see Figure 12).

Each successfully isolated sample was assigned a unique code based on its cultivar and geographic origin to ensure traceability throughout the remainder of the study (Table 4).

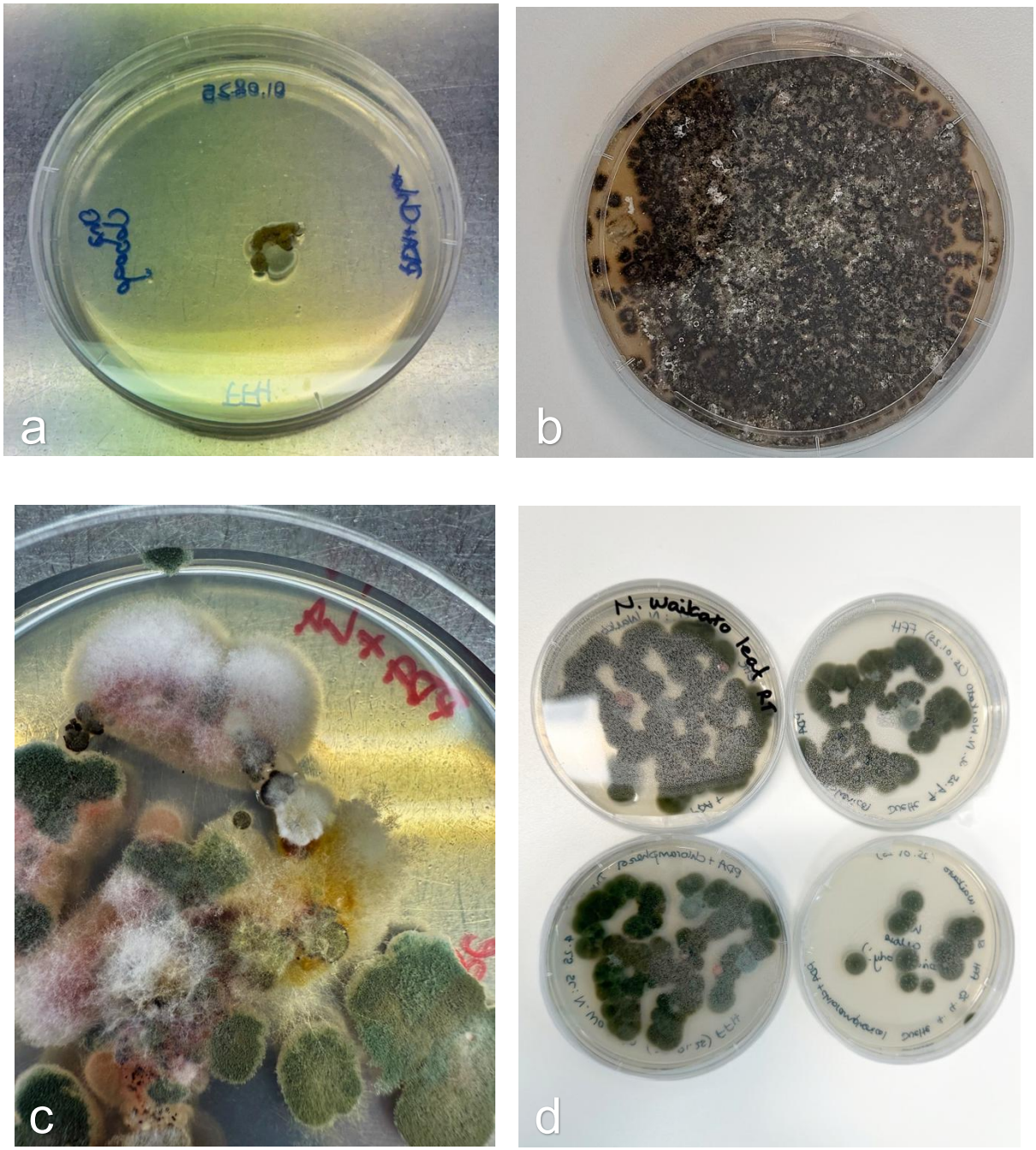

Figure 12.*Variation in culturing and isolation outcomes for* Fulvia fulva *from leaves of tomato cultivars from diverse New Zealand localities. a) Successful isolation of a compatible* F. fulva *colony from surface-disinfected 'Clobogo' leaf tissue (isolate CO1) after 15 days of incubation on Potato Dextrose Agar (PDA) + chloramphenicol (100 mg/L). b) Established* F. fulva *colonies (ICMP 7320) cultured at Massey University, approximately five weeks of age. c) Extensive microbial and fungal contamination from 'Oley' leaf tissue sample (origin: Whanganui) after three weeks of growth in PDA + Lactic Acid (LA; 1%); no* F. fulva *colonies were identified. d) Contamination, presumably by* Cladosporium *spp., from 'Duelle' leaf tissue samples (Tuakau) samples (isolate DT1) two weeks post-inoculation on PDA + chloramphenicol (100 mg/L).*

Table 4. *Summary of* Fulvia fulva *sampling efforts: temporal data, geographic distribution, and isolation success.*

Date	Sampling Round	Cultivar/Variety	Crop Age (weeks)	Sample Location	Sampled by grower?	Sample Type	Compatibility with *F. fulva*	Successfully Isolated	Code
Nov/2024	1	Clobogo	24	Reporoa	No	Leaf	++++	Yes	CR1
Nov/2024	1	Gardecia	24	Reporoa	No	Leaf	++++	No	
Nov/2024	1	Grandice	24	Reporoa	No	Leaf	++++	Yes	GR1
Jan/2025	1	Campari	26	Mokai	Yes	Leaf	+	No	
Jan/2025	1	Provine	26	Mokai	Yes	Leaf	+	No	
Jan/2025	1	Duelle	36	Tuakau	No	Leaf	++++	Yes	DT1
Jan/2025	1	Grandice	42	Tuakau	No	Leaf	++++	Yes	GT1
Jan/2025	1	Olay	28	Whanganui	Yes	Leaf	+	No	
Feb/2025	2	Olay	30	Whanganui	No	Leaf	++++	No	
Feb/2025	1	Alfred	>20	Whanganui	No	Leaf	++	No	
Feb/2025	1	Avalantino	9	Clarkville	No	Leaf	++++	No	
Feb/2025	1	Duelle	11	Heathcote Valley	No	Leaf	++++	No	
Mar/2025	1	Unknown	>12	Drury	Yes	Leaf	+++	No	
Mar/2025	1	Unknown	>12	Clevedon	Yes	Leaf	+++	No	
Mar/2025	1	Unknown	>12	Pokeno	Yes	Leaf	+++	No	
Jun/2025	3	Olay	>12	Whanganui	Yes	Leaf	+	No	
Jun/2025	1	ICMP 7320	N/A	Unknown	N/A	Culture	N/A	No	
Jun/2025	1	Campari	N/A	Mokai	N/A	Culture	N/A	No	
Jun/2025	1	Clobogo	32	Ohaupo	No	Leaf	+++	Yes	CO1
Sept/2025*	2	ICMP 7320	N/A	Unknown	N/A	Culture	N/A	No	ICMP 7320
Sept/2025*	2	Campari	N/A	Mokai	N/A	Culture	N/A	No	CM1
Mar/2026	2	Duelle	N/A	Heathcote Valley	No	Leaf	++++	Yes	DC1
Mar/2026	1	Unknown	N/A	West Melton	No	Leaf	+++	No	
Mar/2026	2	Grandice	40	Reporoa	Yes	Leaf	+++	Yes	GR2
Jul/2026	2	Prodelle	30	Tuakau	No	Leaf	++++	Yes	PT1

* Date reflects when this culture-collection stock was obtained/re-cultured for this study, not its original isolation date. Original isolation: ICMP 7320, 1980s; CM1, 2022.

Visual compatibility with *F. fulva* upon leaf examination:

\+ Low or negligible compatibility: Compatible symptoms are absent or at a very low level; typically masked by confounding biotic and/or abiotic stressors.

++ Moderate compatibility: A reasonable level of symptoms observed; characterised by one to several isolated sporulation bodies (up to 0.5 cm in diameter) scattered across the abaxial leaf surface. Other biotic or abiotic stressors may be present.

+++ High compatibility: Distinct compatible symptoms observed; characterised by multiple sporulation bodies (ranging from 0.5 cm to 1.0 cm in diameter) distributed across the abaxial leaf surface. Presence of other biotic or abiotic stressors is minimal.

++++ Very high compatibility: Profuse compatible symptoms observed; characterised by numerous sporulation bodies (0.5 cm to 1.0 cm in diameter), appearing in irregular or concentric patterns, and either scattered or clustered across the abaxial leaf surface. Other biotic or abiotic stressors are unnoticed or absent.

5.4. Morphological Characterisation and Diagnostic Identification

The fungal isolates established in axenic culture were subjected to detailed morphological assessment to confirm their compatibility with *F. fulva*. Macroscopically, the colonies exhibited a characteristic velvety mycelium, transitioning from an initial pale grey to a deep, olivaceous brown as sporulation progressed (Holliday & Mulder, 1976).

Following the guidelines described in Table 5, the microscopic examination of these cultures revealed a diagnostic suite of structures consistent with established taxonomic descriptions of the pathogen, based on in vitro observations of mycelium, hyphae, conidiophores, conidiogenous cells, and/or normally catenated conidia (Figures 13 to 17). Likewise, contamination by other fungal species (Figure 18) was commonly found at this stage.

Table 5. *Morphological Dimensions and Characteristics of* Fulvia fulva *Isolates (adapted from Videira et al., 2017).*

Feature	Description	Dimensions/Specifications
Hyphae	Hyaline to pale brown; uniform width.	2 µm diameter
Conidiophores	Pale brown; smooth to rough; simple or short branched; straight/sinuous; often curved at the tip.	20–160×2.5–10 µm
Conidiogenous Cells	Integrated, terminal, and intercalary; proliferating sympodially; polyblastic.	Rim-like loci: 1–2.5 µm
Conidia (Asexual Spores)	Catenate (forming branched chains); ovoid, obovoid, ellipsoidal, spherical, or cylindrical; straight or strongly curved.	10–30×5–10 µm
Septation	Multi-septate conidiophores; conidia are generally 1–4-septate.	1–4 septa (Conidia)
Hila	Thickened and darkened scars at the base of the conidia.	1–2.5 µm diameter

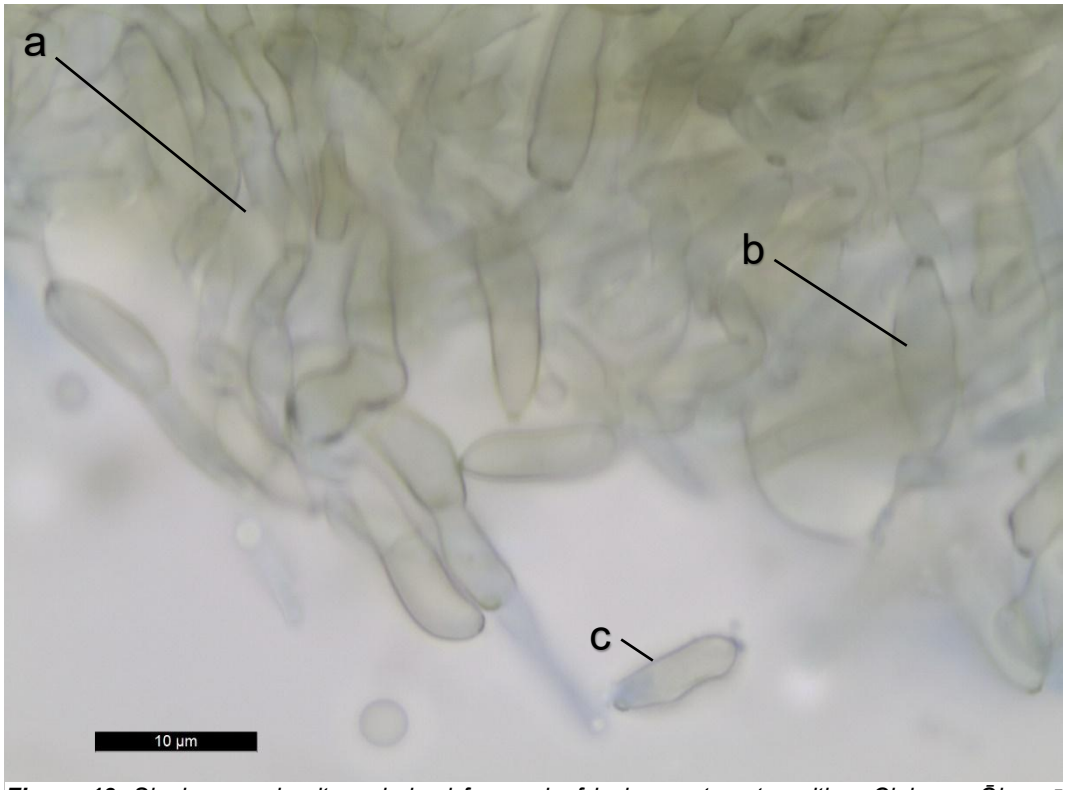

Figure 13. *Single-spored culture derived from a leaf lesion on tomato cultivar Clobogo, Ōhaupō (isolate CO1). Morphological characteristics are consistent with* Fulvia fulva*. Image shows: a) conidiophore; b) catenated conidia; and c) a conidium.*

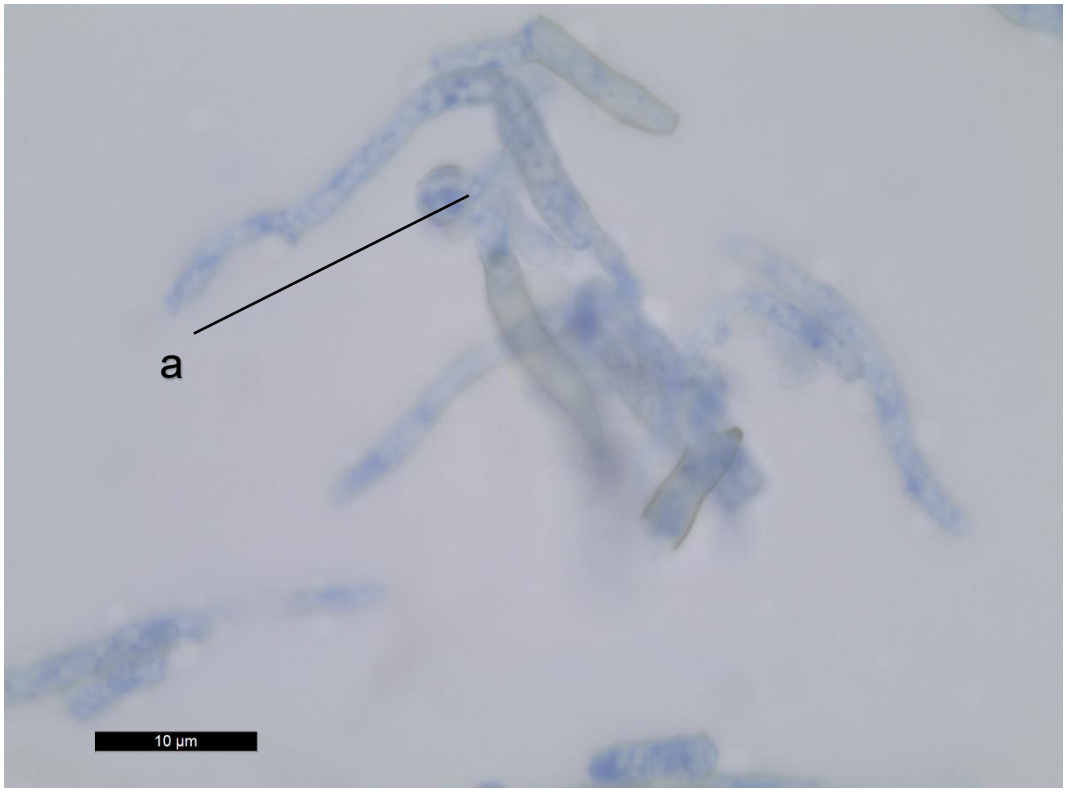

Figure 14. *Single-spored culture derived from a leaf lesion on tomato cultivar Grandice, Reporoa (isolate GR1). Morphological characteristics are consistent with* Fulvia fulva*. Image shows: a) conidiophore, stained with lactophenol blue.*

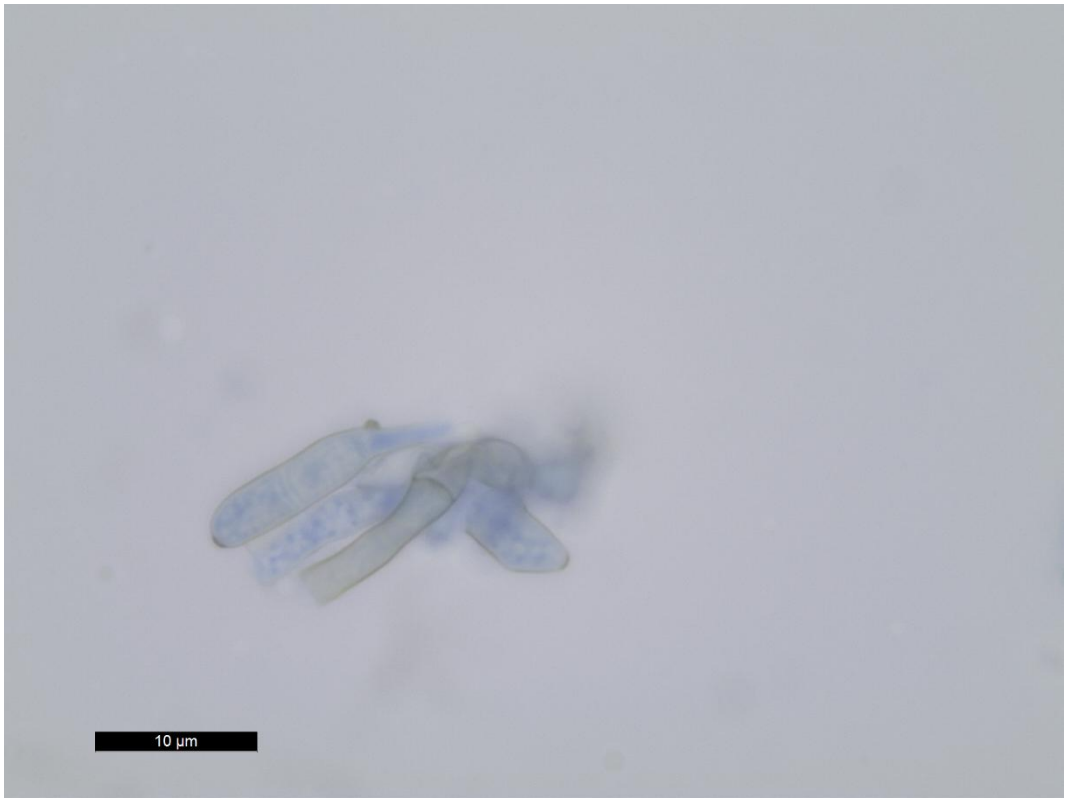

Figure 15. *Single-spored culture derived from a leaf lesion on tomato cultivar Duelle, Tuakau (isolate DT1). Morphological characteristics are consistent with* Fulvia fulva*. Image shows conidiophores, stained with lactophenol blue.*

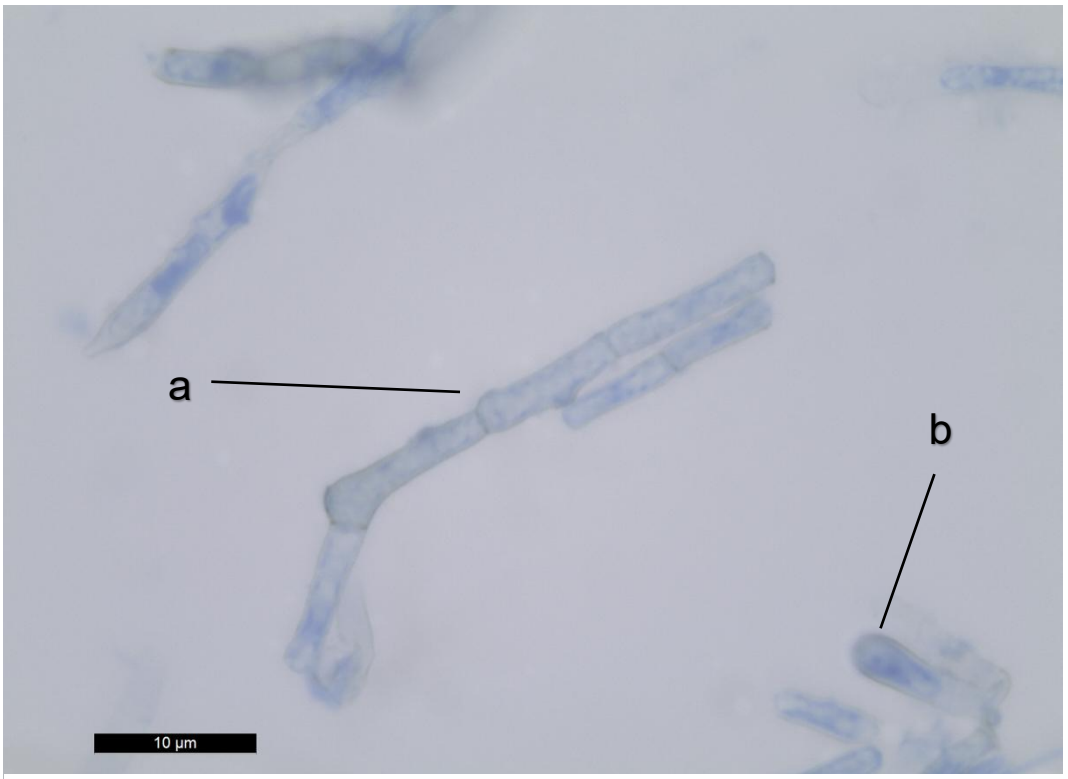

Figure 16. *Single-spored culture sourced from isolate ICMP 7320. Morphological characteristics are consistent with* Fulvia fulva*. Image shows: a) conidiophore; and b) catenate conidia, both stained with lactophenol blue.*

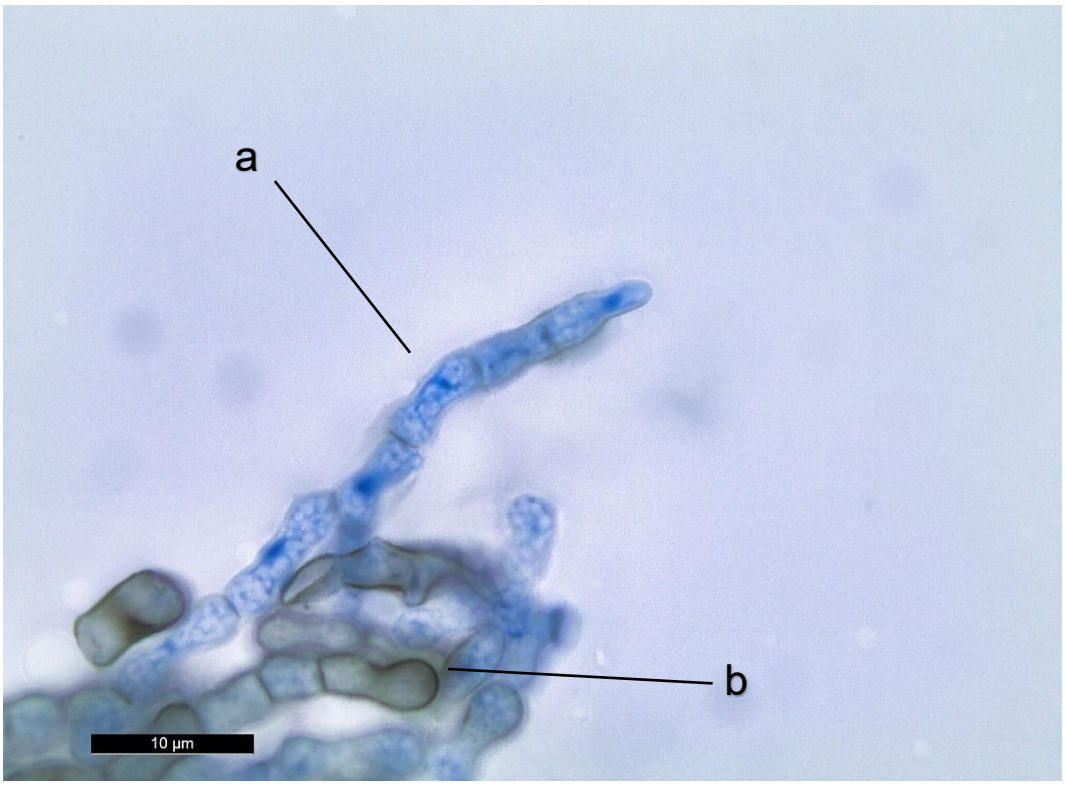

Figure 17. *Single-spored culture derived from a leaf lesion on tomato cultivar Campari, Mokai (isolate CM1). Morphological characteristics are consistent with* Fulvia fulva*. Image shows: a) conidiophore; and b) catenate conidia, both stained with lactophenol blue.*

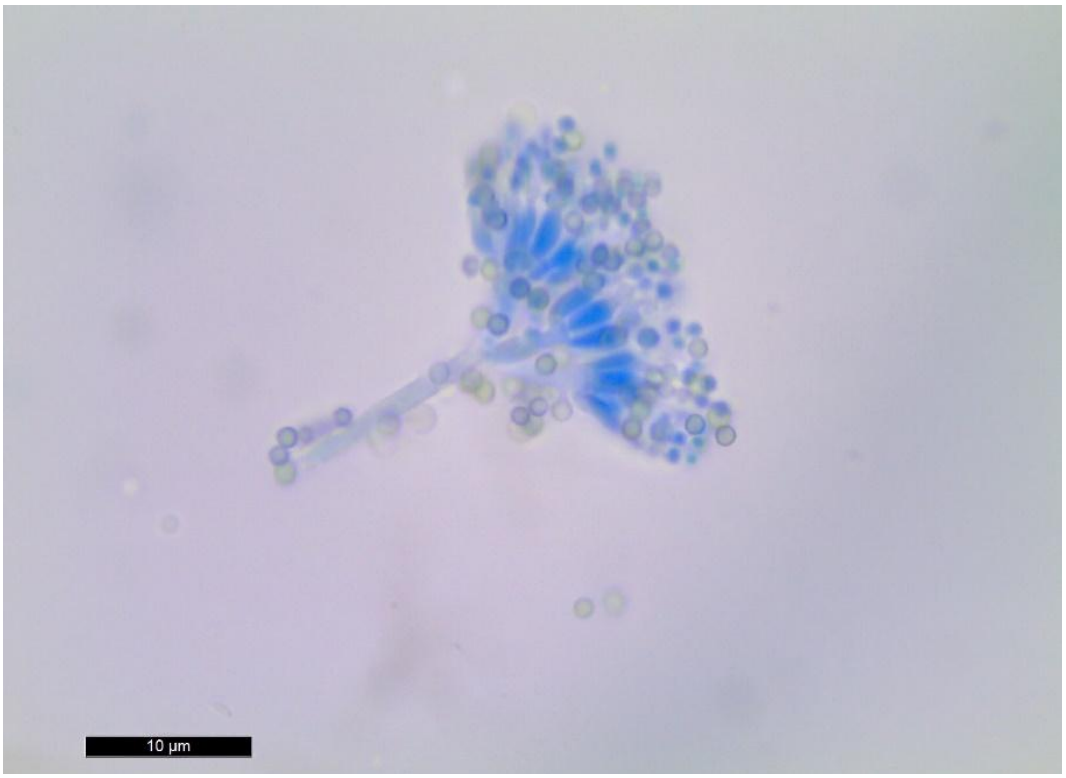

Figure 18. *Example of contaminant conidia on conidiophores found during single-sporulation culture (Lactophenol blue stain; Compatible with* Penicillium*).*

5.5. Single Spore Isolation and Purified Culture Development

Visually pristine colonies exhibiting macro- and micro-morphological features consistent with *F. fulva* were selected for single-spore (SS) purification.

From 80 SS plates derived from five unique isolates (CO1, GT1, GR1, ICMP 7320, and CM1; see Table 4 for more details), ~40% successfully developed into colonies (Figures 19 and 20). However, the remaining ~60% failed to germinate or were lost to contamination. Managing unwanted microbial growth from contaminants proved exceptionally difficult even at this stage; by the conclusion of the laboratory phase, 100% of the successfully developed SS colonies exhibited some degree of late-stage contamination by fungi compatible with *Penicillium* or *Cladosporium* spp.

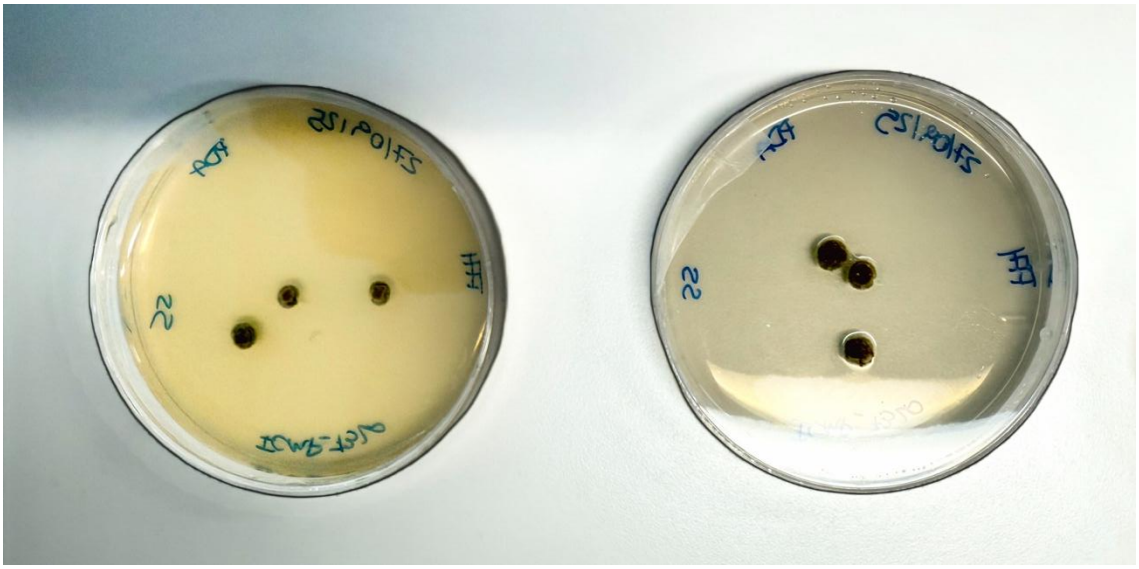

Figure 19. *Comparative biomass development of single-spore (SS) cultures for* Fulvia fulva. *Left: Isolate ICMP 7320; Right: Isolate CO1. Both isolates were photographed following 17 days of incubation on Potato Dextrose Agar (PDA). Both colonies exhibit a characteristic circumscribed, rounded morphology with typical olive-green pigmentation.*

DC2, PT1 and GR1 (Table 4) were cultured and isolated after the genome sequencing deadline established for this research expired. 18 tubes (6 for each isolate) were placed in long-term storage (-80 ºC) following the cryo-preservation method stated in subsection (4.4).

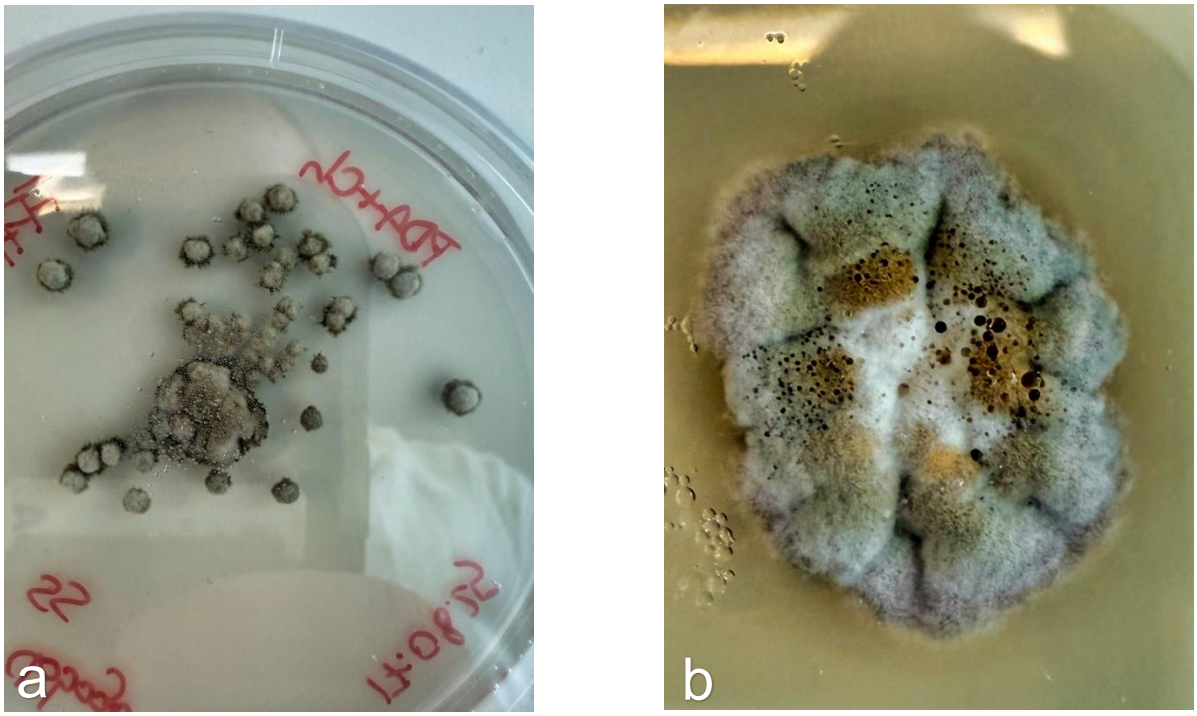

Figure 20. *Comparative biomass development in single-spore (SS) cultures of* Fulvia fulva *after 20 days of incubation on Potato Dextrose Agar (PDA) supplemented with chloramphenicol (100 mg/L). a) GR1 exhibiting multiple discrete colonies clustered around a central biomass, characterised by a pale olive-green pigmentation. b) Close-up of isolate GT1 showing a single, significantly larger colony. The morphology remains circumscribed with a complex mosaic of olive-green, grey, and brown pigmentation.*

5.6. Biomass Augmentation and DNA Extraction Outcomes

Biomass production was initiated for isolates CO1, GT1, GR1, ICMP 7320, and CM1 using conidial suspensions inoculated into PDB. Due to early interference with microbial contamination, a secondary suspension was required specifically for isolate CM1.

5.7. Pathogen Isolation and DNA Extraction Efficiency

A total of 18 unique leaf specimens were collected, representing a diverse range of tomato cultivars and geographic locations across New Zealand. From this initial sample pool, five unique *F. fulva* isolates were successfully established in axenic culture. However, the subsequent maintenance of these cultures proved challenging due to the slow growth rate of the target pathogen; two isolates were ultimately lost to persistent contamination by faster-growing fungal saprophytes. To maintain the

robustness of the study, the research supervisor provided two additional historical *F. fulva* isolates from previous seasons, bringing the final total to five unique fungal isolates available for molecular analysis.

The DNA extraction phase yielded genomic material from three of the five unique isolates. The quality and quantity of these DNA extracts were evaluated via spectrophotometry to determine their suitability for downstream applications. As detailed in Table 6, two of these isolates demonstrated high-quality profiles, characterised by adequate concentrations (ng/µL) and favourable purity indices, with A_{260}/A_{280} ratios within the target range and A_{260}/A_{230} ratios approaching optimal values. Conversely, the third isolate exhibited suboptimal purity, specifically an A_{260}/A_{230} ratio below 1.0, indicating the possible presence of residual carbohydrates or salts from the extraction process.

Table 6. *Purity and concentration of genomic DNA extracted from* Fulvia fulva *isolates. DNA concentration (ng/µL) and purity ratios were measured with a DeNovix DS-11 FX+ Spectrophotometer/Fluorometer. The A_{260}/A_{280} ratio indicates protein contamination (≈1.8 expected for pure DNA) and the A_{260}/A_{230} ratio indicates contamination by salts, phenol or carbohydrates (≈2.0–2.2 expected). Values within these ranges indicate DNA of suitable purity for library preparation and downstream whole-genome sequencing.*

Sample (isolate)	Concentration (ng/µL)	A_{260}/A_{230}	A_{260}/A_{280}
ICMP 7320	391.3	1.27	1.82
CM1	91	0.94	1.68
CO1	149	1.28	1.82

5.8. An Overview on Effector Integrity Across the *F. fulva* Isolate Panel

Twenty candidate effector coding sequences were compared across the three isolates against the reference allele for each effector, and every effector–isolate combination was classified as *intact*, *missense*, *truncated*, or *absent* (Table 7; Figure 21). Across the 60 effector–isolate combinations, 46 were intact and identical to the reference protein, six carried a single missense substitution, two were truncated, and six were recorded as absent. Sequence change was therefore the exception rather than the rule: the effector repertoire was largely conserved across the three isolates, with only a small number of discrete events, most in the *Avr* genes.

Table 7. *Effector integrity per* Fulvia fulva *isolate (protein identity to reference in parentheses; "absent" = effector not detected in that isolate).*

Effector	ICMP 7320 (1980s)	CM1 (2022)	CO1 (2025)
Avr2	missense (98.7%)	**truncated** (67.9%)	**truncated** (67.9%)
Avr4	missense (99.3%)	intact	intact
Avr4E	**absent**	intact	intact
Avr5	intact	intact	intact
Avr6	intact	missense (99.1%)	missense (99.1%)
Avr9	**absent**	**absent**	**absent**
Avr9B	intact	**absent**	**absent**
Ecp1	intact	intact	intact
Ecp2-1	intact	intact	intact*
Ecp4	missense (99.3%)	intact	intact
Ecp8	intact*	intact	intact
Ecp9-1	intact	intact	intact
Ecp10-1	intact	intact	intact
Ecp11-1	intact	intact	intact
Ecp12	missense (99.2%)	intact	intact
Ecp13	intact	intact	intact
Ecp14-1	intact	intact	intact
Ecp15	intact	intact	intact
Ecp16	intact	intact	intact
Ecp17	intact	intact	intact

* Carries a synonymous nucleotide substitution (protein unchanged).

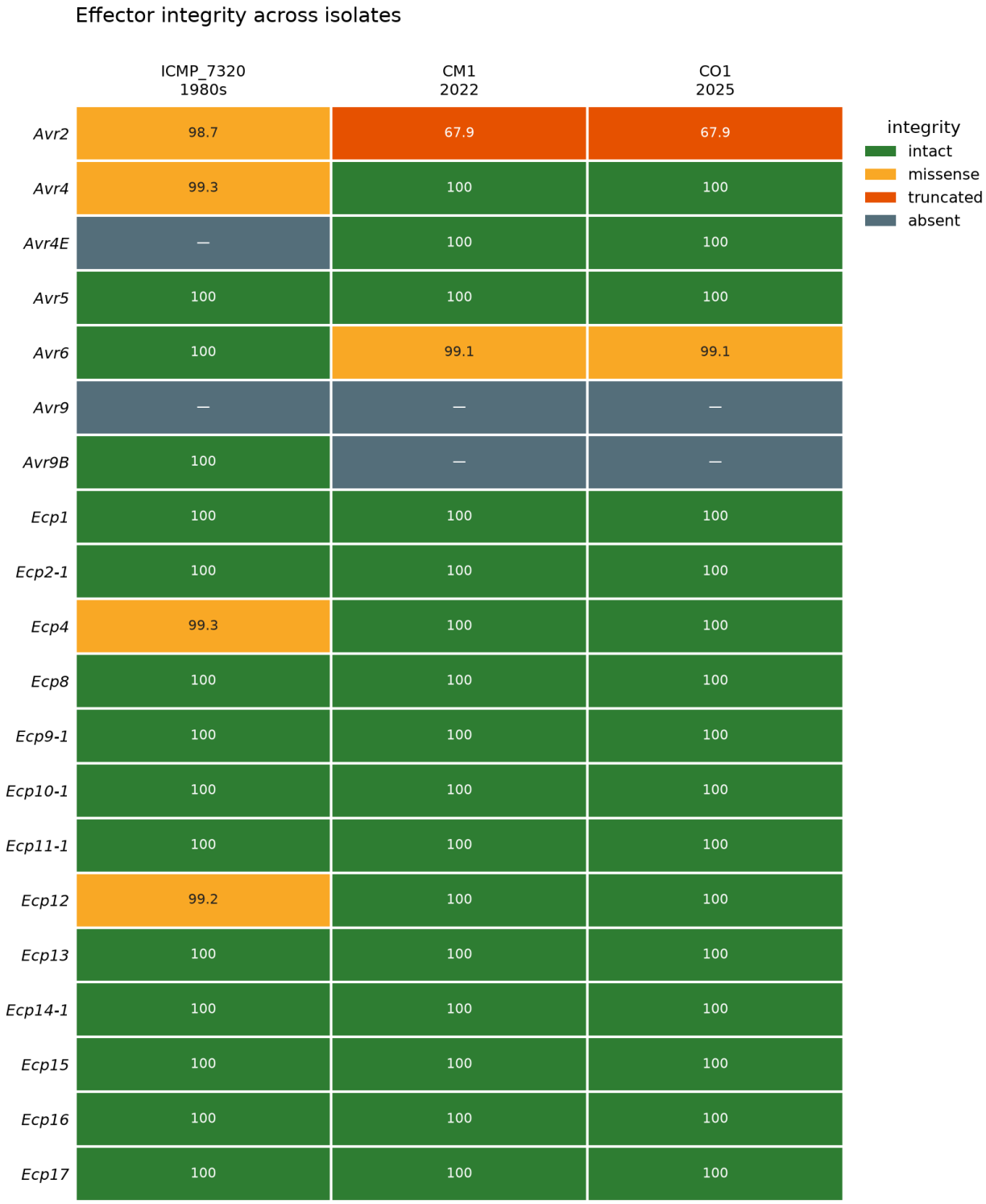

Figure 21. *Effector gene integrity across the three New Zealand* Fulvia fulva *isolates. Each cell shows the integrity status of one effector gene (rows) in one isolate (columns). Integrity was determined by whole-genome sequencing, reconstructing each coding sequence and comparing it against the reference allele (strain 0WU, except* Avr4E*, strain R5). Isolates are ordered left to right by collection date: ICMP 7320 (1980s), CM1 (2022) and CO1 (2025). Cells are coloured by integrity class: intact (green, protein identical to the reference), missense (amber, full-length with one or more amino-acid substitutions), truncated (orange, coding sequence not spanning the full gene), and absent (grey, effector not detected). Each cell is annotated with percentage protein identity to the reference (100% for intact; — for absent). Of the 60 effector–isolate combinations, 46 were intact, 6 missense, 2 truncated and 6 absent.*

5.9. Summary of Sequence Variation

Ten variants were called across seven effectors: eight single-nucleotide substitutions and two deletions. Of the substitutions, six were missense, and two were synonymous. The changes were distributed unevenly across the panel — confined to *Avr2*, *Avr4*, *Avr6*, *Ecp2-1*, *Ecp4*, *Ecp8* and *Ecp12* — while the remaining thirteen effectors were invariant across all three isolates. The two deletions constitute the *Avr2* truncation (section [5.10.]). The substitutions are described by effector in sections [5.11.] and [5.12.] Six effector–isolate combinations, involving *Avr4E*, *Avr9* and *Avr9B*, were recorded as absent (section [5.13.]).

5.10. Truncation of *Avr2* in CM1 and CO1 Isolates

In isolates CM1 and CO1, *Avr2* was truncated: only the first exon was present, while the second exon – encoding the C-terminal half of the protein – was absent. The recovered coding sequence (159 of the 237 reference coding nucleotides; positions c.160-237 absent) was identical to the reference across its length but terminated after 53 codons, yielding a predicted product of 53 residues, compared with 78 in the reference (Figure 22a and b). CM1 and CO1 carried an identical form of this truncation (Figure 22c and d). In contrast, the ICMP 7320 isolate retained a full-length *Avr2* coding sequence differing from the reference by a single missense substitution in c.127T>G, L43V (Figure 22a). *Avr2* was thus the only effector in which a structural (length) change was observed, rather than a point substitution alone.

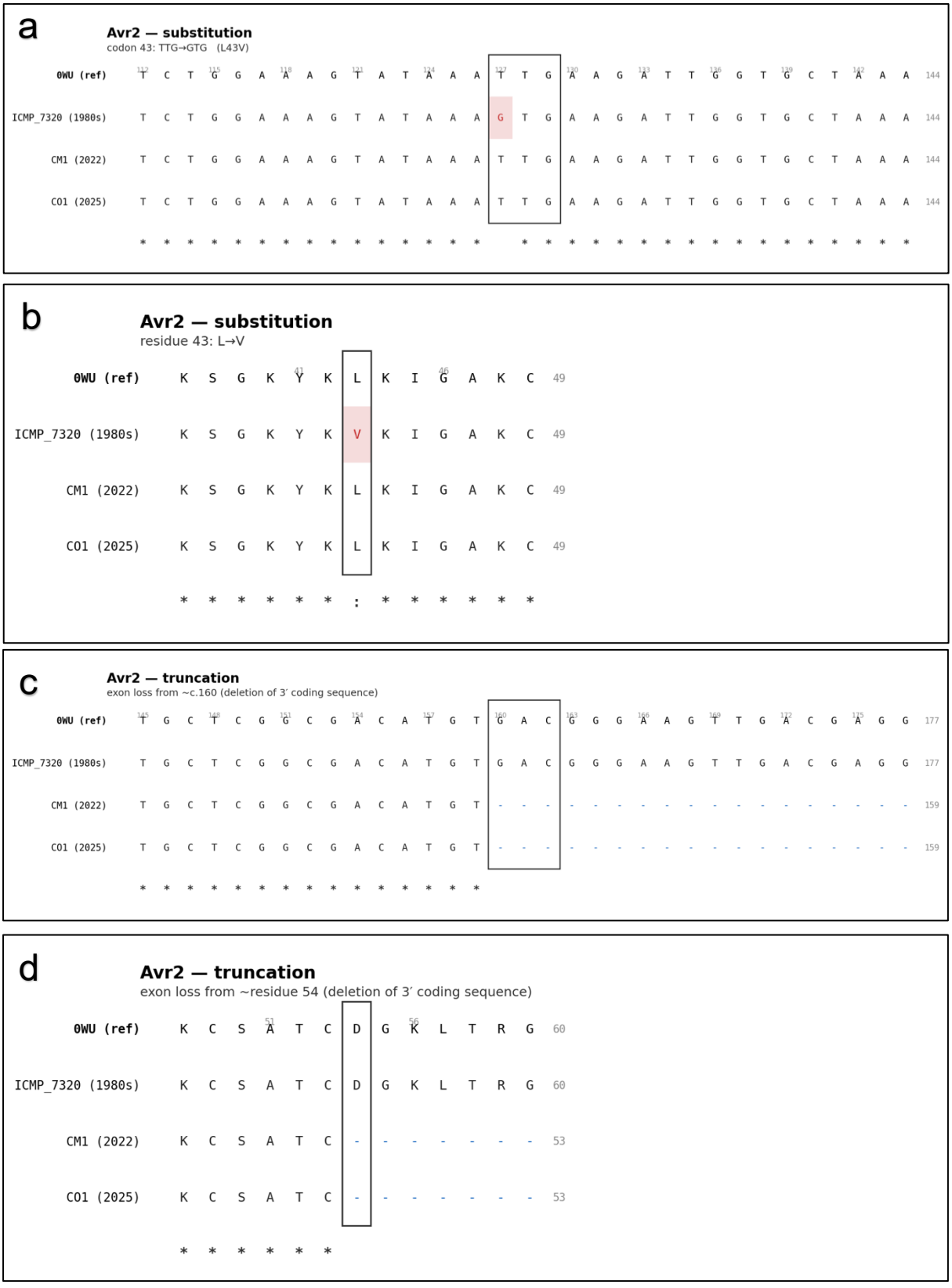

Figure 22. *a)* Avr2 *substitution (ICMP 7320). Cropped CDS alignment centred on codon 43 of* Avr2*. The reference allele (0WU) is shown at the top, with isolates ICMP 7320 (1980s), CM1 (2022), and CO1 (2025) below; the Clustal conservation line marks fully conserved columns (*). ICMP 7320 carries a single substitution (c.127T>G) altering codon 43 from TTG to GTG (L43V, boxed); CM1 and CO1 match the reference at this position. Numbers at right indicate cumulative coding nucleotides; b) Avr2 protein, substitution (ICMP 7320). Cropped protein alignment centred on residue 43 of Avr2. Reference (0WU) on top; isolates ICMP 7320 (1980s), CM1 (2022), CO1 (2025) below. ICMP 7320 carries a Leu→Val substitution (L43V, boxed); the conservation line marks this as a strong-*

group (conservative) change (:). CM1 and CO1 match the reference at this residue. ; c) Avr2 *truncation (CM1, CO1). Cropped CDS alignment at the exon 1–exon 2 junction of* Avr2*. CM1 and CO1 are identical to the reference through exon 1 but lack the second exon (deletion from c.160, shown as dashes), predicting a 53-residue product; ICMP 7320 and the reference retain the full coding sequence; d) Avr2 protein, truncation (CM1, CO1). Cropped protein alignment at the truncation boundary of Avr2. CM1 and CO1 terminate after 53 residues, lacking the C-terminal region present in the reference and ICMP 7320 (missing residues shown as dashes).*

5.11. Amino-acid Substitutions in Avr4 and Avr6

Two further *Avr* genes carried single missense substitutions, each without altering coding-sequence length.

As depicted in Figure 23a, *Avr4* in the ICMP 7320 isolate carried a single substitution (c.257G>T) in an otherwise full-length coding sequence (408 nt). At the protein level, this substitution was non-synonymous, giving a C86F change and a 135-residue protein with 99.3% sequence identity to the reference (Figure 23b). Both CM1 and CO1 isolates were intact and identical to the reference (Figure 23a and b).

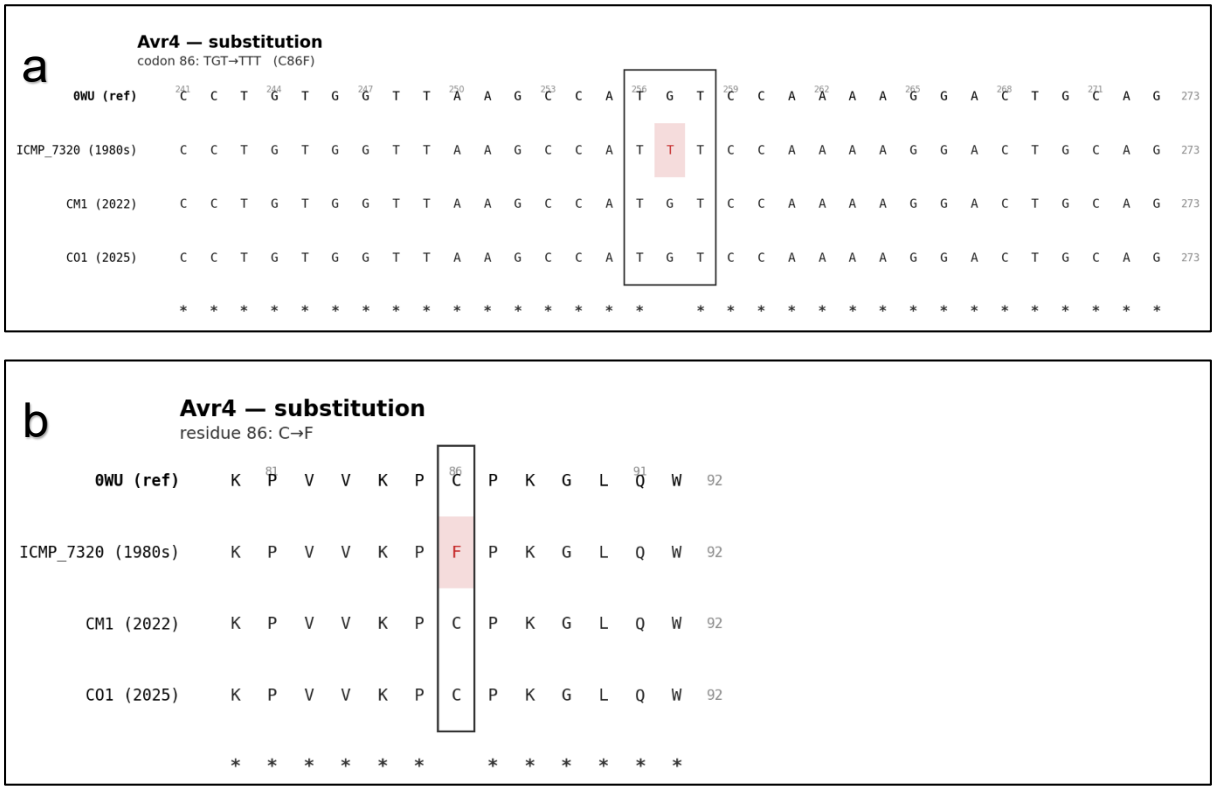

Figure 23. *a)* Avr4 *substitution (ICMP 7320). Cropped CDS alignment centred on codon 86 of* Avr4*. ICMP 7320 carries a single substitution (c.257G>T) altering codon 86 from TGT to TTT (C86F, boxed); CM1 and CO1 are identical to the reference; b) Avr4 protein, substitution (ICMP 7320). Cropped protein alignment centred on residue 86 of Avr4. ICMP 7320 carries a Cys→Phe substitution (C86F, boxed), a non-conservative change (blank conservation); CM1 and CO1 are identical to the reference.*

In *Avr6*, isolates CM1 and CO1 carried a single nucleotide substitution (c.89G>A) in a full-length coding sequence (348 nt); the isolate ICMP 7320 was intact at this position (Figure 24a). This substitution alters codon 30 from TGC to TAC, a non-synonymous change that replaces the encoded cysteine with tyrosine (C30Y), giving a 115-residue protein with 99.1% identity to the reference (Figure 24b). It was the only substitution shared by CM1 and CO1 isolates.

Thus, the ICMP 7320 carried two amino-acid substitutions (Avr2 L43V and Avr4 C86F), whereas the CM1 and CO1 isolates shared one substitution (Avr6 C30Y) and one structural change (truncation of Avr2).

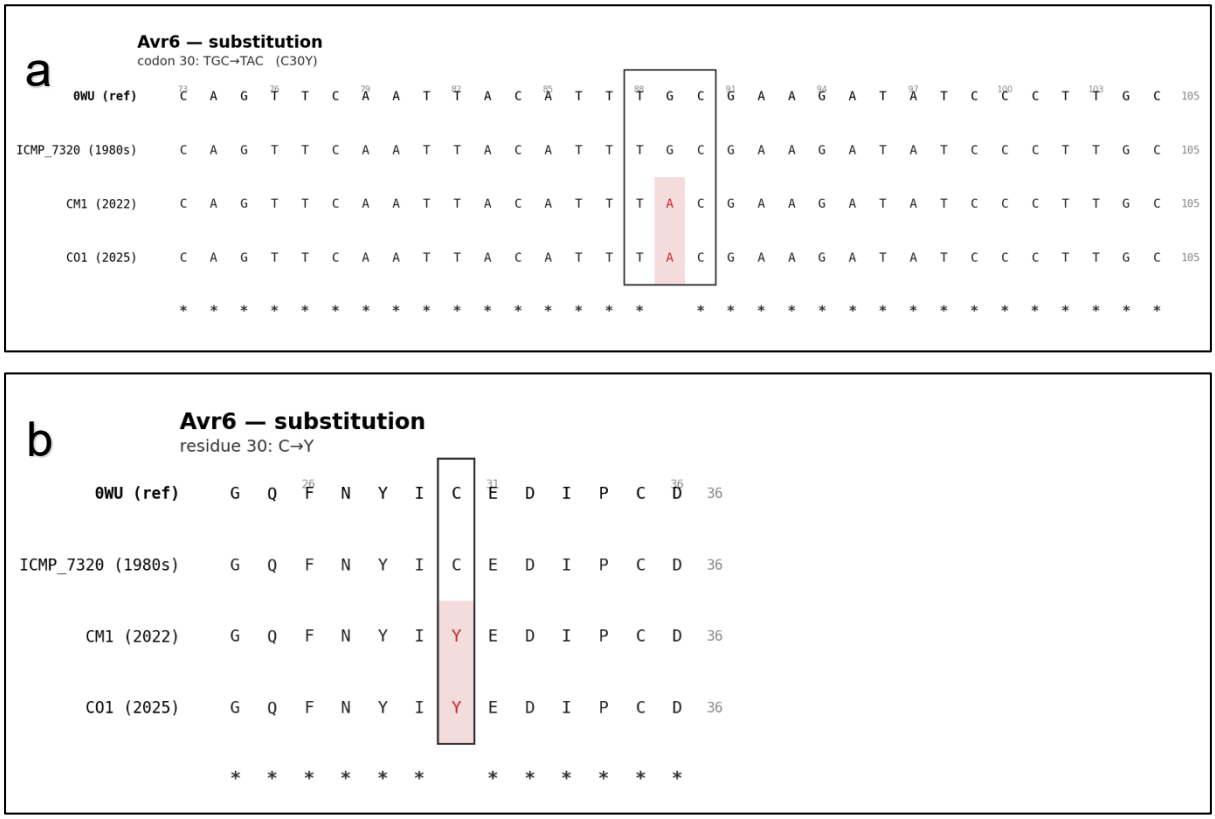

Figure 24. *a)* Avr6 *substitution (CM1, CO1). Cropped CDS alignment centred on codon 30 of* Avr6. *Both recent isolates, CM1 (2022) and CO1 (2025), carry a single substitution (c.89G>A) altering codon 30 from TGC to TAC (C30Y, boxed); ICMP 7320 is identical to the reference; b) Avr6 protein, substitution (CM1, CO1). Cropped protein alignment centred on residue 30 of Avr6. CM1 (2022) and CO1 (2025) carry a Cys→Tyr substitution (C30Y, boxed), a non-conservative change; ICMP 7320 is identical to the reference.*

5.12. Substitutions in *Ecp* Effectors

Four *Ecp* effectors carried a single nucleotide substitution each, while the remaining *Ecp* effectors were invariant.

Two of the substitutions were missense and confined to the ICMP 7320 isolate. In *Ecp4*, a single nucleotide substitution (c.380T>G) in a full-length coding sequence (414 nt) alters codon 127 (Figure 25a), a non-synonymous change giving a V127G substitution (Figure 25b); the encoded 138-residue protein shares 99.3% identity with the reference. In *Ecp12*, a single nucleotide substitution (c.370G>A) in a full-length coding sequence (399 nt) alters codon 124 (Figure 26a), giving a G124R substitution (Figure 26b); the encoded 133-residue protein shares 99.2% identity with the reference.

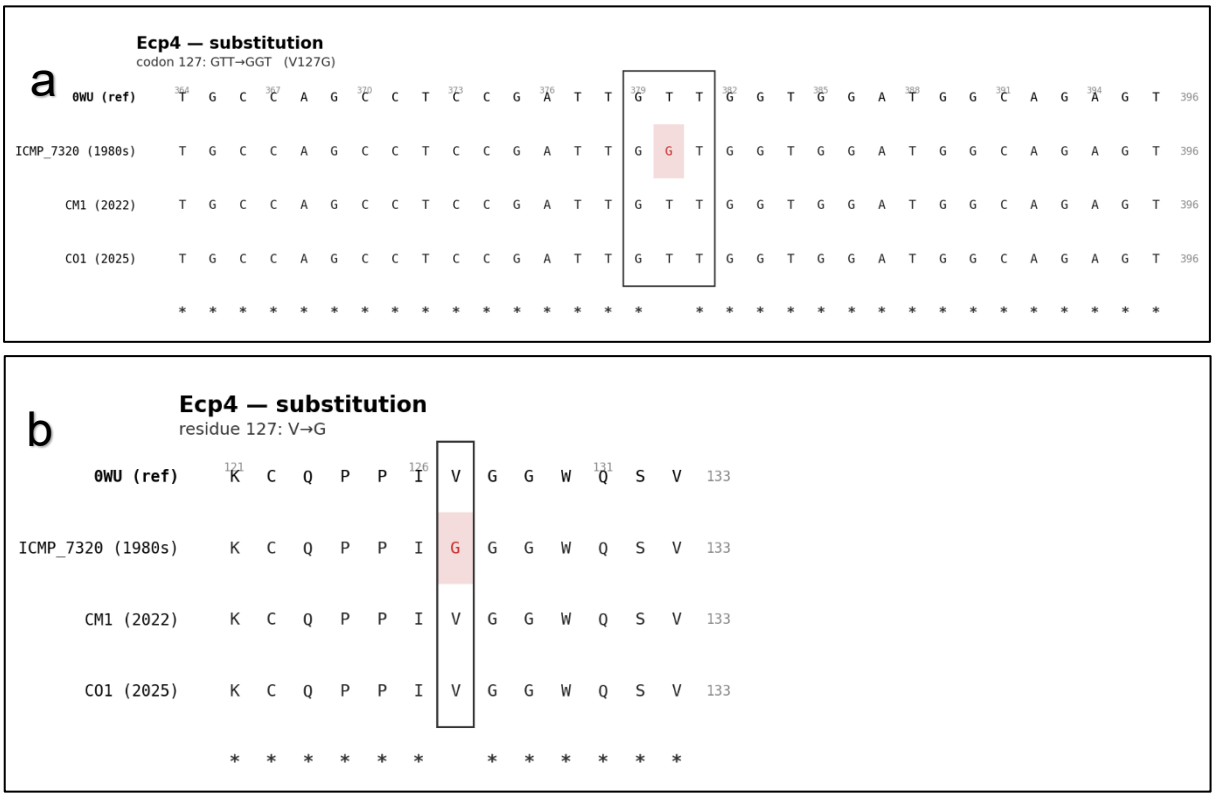

Figure 25. *a)* Ecp4 *substitution (ICMP 7320). Cropped CDS alignment centred on codon 127 of* Ecp4*. ICMP 7320 carries a single substitution (c.380T>G) altering codon 127 from GTT to GGT (V127G, boxed); CM1 and CO1 are identical to the reference; b) Ecp4 protein, substitution (ICMP 7320). Cropped protein alignment centred on residue 127 of Ecp4. ICMP 7320 carries a Val→Gly substitution (V127G, boxed), a non-conservative change; CM1 and CO1 are identical to the reference.*

The remaining two substitutions were synonymous, leaving the protein sequence unchanged: Ecp2-1 in CO1 (c.87C>A, codon 29) and Ecp8 in ICMP 7320 (c.153T>C, codon 51), both Pro→Pro. For these, the nucleotide change is visible in the CDS alignment, but the protein alignments are identical to the reference.

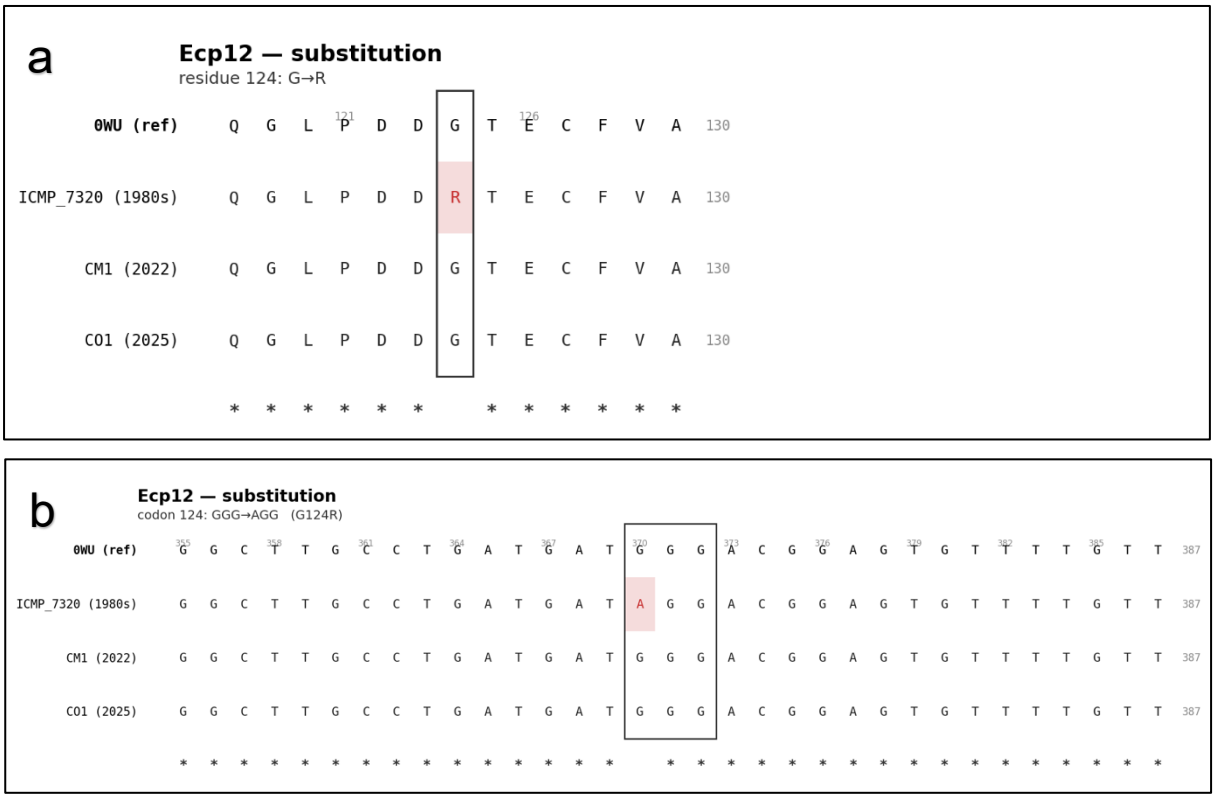

Figure 26. *a)* Ecp12 *substitution (ICMP 7320). Cropped CDS alignment centred on codon 124 of* Ecp12*. ICMP 7320 carries a single substitution (c.370G>A) altering codon 124 from GGG to AGG (G124R, boxed); CM1 and CO1 are identical to the reference; b) Ecp12 protein, substitution (ICMP 7320). Cropped protein alignment centred on residue 124 of Ecp12. ICMP 7320 carries a Gly→Arg substitution (G124R, boxed), a non-conservative change; CM1 and CO1 are identical to the reference.*

5.13. Effector Absence

Six effector–isolate combinations were recorded as absent, involving three effectors. *Avr9* was not detected in any of the three isolates. *Avr9B* was absent from both CM1 and CO1 isolates, while present and intact in the 1980s isolate, ICMP 7320. *Avr4E* was absent only in the ICMP 7320 isolate, being intact in both CM1 and CO1 isolates. These absences are shown as the “absent” category in the integrity matrix (Figure 21); because absent isolates were excluded from the corresponding alignments, absence is not represented in the per-effector alignments.

5.14. Conservation and Divergence Profiles

Per-column Shannon entropy and percentage identity to the reference were computed for each effector alignment. For every effector other than *Avr2*, mean identity to the reference was ≥99.4% at both the nucleotide and protein level, with mean per-column entropy ≤0.009 bits, consistent with at most a single variable position per effector. *Avr2* was the only substantially variable effector, with mean identity to the reference of 77.9% (CDS) and 78.2% (protein) and mean entropy of 0.333 bits (CDS); its divergence was concentrated in the 3′/C-terminal region absent from CM1 and CO1 isolates (Figure 27a and b).

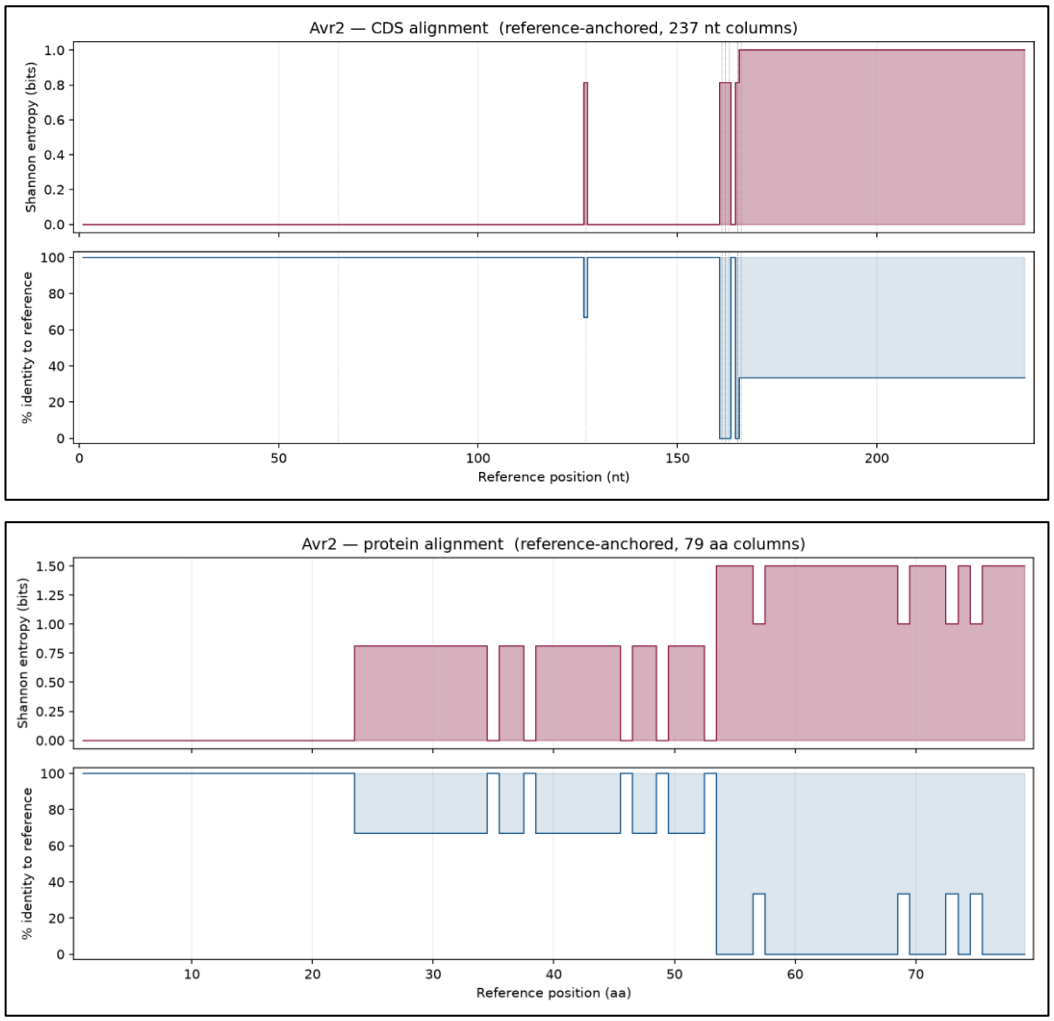

Figure 27. *Sequence conservation and divergence across* Avr2 *in three New Zealand* Fulvia fulva *isolates. Per-column Shannon entropy (bits) and percentage identity to the reference allele (0WU) are plotted against reference coordinate position for the Avr2 [coding sequence / protein] alignment of isolates ICMP 7320 (1980s), CM1 (2022) and CO1 (2025). Shannon entropy quantifies variability at each position ($H = -\Sigma\, p_i \log_2 p_i$, with the alignment gap treated as an additional character state), such that invariant positions score zero and higher values indicate greater divergence; percentage identity gives the proportion of isolate sequences matching the reference at each position. Divergence is concentrated in the 3′/C-terminal region corresponding to the second exon, which is absent in CM1 and CO1 (see Figure 22); the remainder of the gene is highly conserved. Avr2 was the only effector showing substantial divergence (mean identity 77.9% nucleotide / 78.2% protein; mean entropy 0.333 bits nucleotide).*

Chapter 4

6. Discussion

6.1. Logistical Constraints and Methodological Challenges in *F. fulva* Sampling

A complex interplay of strict biosecurity protocols and unfavourable seasonal timing significantly hampered the *F. fulva* sampling process. Following the detection of Tomato ToBRV in Australia in June 2024, TomatoesNZ implemented a restrictive policy (which remains in effect at the conclusion of this thesis) discouraging external visitors from entering glasshouses to prevent a similar incursion in New Zealand (Cohen, 2024). Consequently, the entire burden of sample collection was shifted onto the growers themselves, thereby removing the possibility of expert-led fieldwork. This logistical shift was further complicated by a seasonal conflict: the prevalence of *F. fulva* peaks during the warmest months, which directly coincide with the industry's most intensive production cycle. The overlap created a significant operational bottleneck, as growers lacked the necessary bandwidth to prioritise scientific collection during their peak commercial season.

Beyond seasonal constraints, the project encountered a critical methodological flaw regarding the intersection of sample longevity and laboratory accessibility. The initial isolation protocol established a viability window of only a few weeks; as a result, many specimens underwent irreversible degradation when their collection coincided with the university's summer closure. This loss was exacerbated by the absence of alternative facilities, as access to BSI laboratories was not secured until April 2025. To prevent such losses in the future, subsequent iterations of this protocol must incorporate more robust preservation techniques or align sampling schedules with institutional calendars to ensure that peak-season material is processed before it degrades.

6.2. Participant-Led Sampling Limitations

The forced reliance on participant-led sampling introduced several difficulties that impacted the volume and quality of the viable material collected. Of the nine samples submitted by growers/third parties, only three displayed high compatibility with *F. fulva* symptoms (Drury, Clevendon and Pokeno; all round 1); four did not show significant symptom compatibility (Whanganui and Mokai, both round 1), and the remaining two were damaged during transport due to excessive moisture (Whanganui, round 3).

Despite guidance on identifying leaf mould in crops, at least two growers struggled to accurately identify visual symptoms consistent with *F. fulva* infection, resulting in missed collection opportunities.

Throughout the research, several growers and tomato producers approached TomatoesNZ with concerns about *F. fulva*. In response to this industry interest, sampling kits were dispatched directly to at least three of these growers, with additional kits provided to TomatoesNZ for secondary distribution. Despite this initial engagement and the provision of all necessary materials for specimen collection, no further communication or samples were received from these participants. This lack of follow-up reflects the broader logistical challenges discussed previously, in which the high labour demands of peak production likely superseded growers' ability to perform non-essential research tasks.

6.3. Procedural Fidelity Audit

While the standardised sampling protocol was designed to minimise contamination and ensure specimen integrity, the researcher's inability to supervise the process in person (due to the aforementioned ToBRV biosecurity restrictions) remained a primary limitation of this study. Consequently, although all participating growers were provided with identical kits and comprehensive guidelines, the degree of procedural fidelity could not be independently verified.

Variations in the timing of leaf excision, the thoroughness of hand sanitisation, or adherence to strict refrigeration protocols may have influenced the initial viability of some specimens or created niches for enhanced sample contamination, potentially leading to variability in sample quality and consistency.

6.4. Operational and Biological Constraints on Genome Sequencing

While a primary objective of this research was to sequence the genomes of isolated *F. fulva* races, several multifaceted challenges ultimately precluded this analysis. The primary constraint was the pathogen's inherent biology; *F. fulva* exhibits exceptionally slow radial growth compared to common fungal contaminants (Holliday & Mulder, 1976), making the establishment of axenic cultures a protracted process (Feix et al., 2023). In this study, the timeline from initial leaf inoculation to the production of sufficient biomass for high-quality DNA extraction often spanned several months. Consequently, any disruption in the culturing pipeline (such as repeated contamination of plates by faster-growing species, including *Penicillium* and other *Cladosporium* spp.) resulted in significant cumulative delays, often setting the research back by several weeks per incident.

External logistical pressures and institutional timelines compounded these biological obstacles. Periods of funding uncertainty and scheduled university closures often coincided with critical stages of sample preparation, leading to unavoidable loss of viable material during extended storage. Furthermore, the technical complexity of isolating high-molecular-weight DNA from recalcitrant fungal tissue was further affected by minor procedural inconsistencies and occasional handling errors typical of complex laboratory workflows. When combined with the limited availability of specialised laboratory facilities during the project's initial phases, these factors created operational bottlenecks. Ultimately, the cumulative effect of these pushbacks delayed the isolation process beyond the viable window required for successful genomic sequencing within the current project scope.

6.5. Understanding how Protected Crop Conditions Influence Pathogenesis

Development of leaf mould disease requires high RH and warm temperatures (Gül et al., 2024; Sudermann et al., 2022). In a Controlled Environment Agriculture (CEA) setting, such as a high-tech glasshouse, RH and temperature (T°) are useful indicators offering an overview of climate conditions within the growing environment. However, from a technical perspective, vapour pressure deficit (VPD) is a superior metric for anticipating fungal pathogenesis, as RH is inherently temperature-dependent (Stanghellini et al., 2019).

While RH indicates the percentage of moisture that air can hold at a given T° (Paull, 1999), it fails to account for the absolute moisture-carrying capacity of the air. Thus, growers consider VPD, which essentially reflects the difference between the vapour pressure within the leaf and the water vapour pressure in the surrounding air (Amitrano et al., 2019).

Despite the implementation of advanced heating and screen systems, microclimate phenomena often create localised variances in VPD that facilitate fungal establishment (Stanghellini et al., 2019; Sudermann et al., 2022). While these technologies effectively manage the standard greenhouse environment, they frequently fail to mitigate specific physical triggers for infection, most notably localised condensation and thermal lag (Stanghellini et al., 2019).

Manual or automated sanitisation systems and optimised airflow are examples of strategies used to minimise the development of crop diseases. Nevertheless, pathogens are frequently introduced via irrigation, seeds, or personnel (particularly in CEAs), where the open-flow design complicates biosecurity efforts (Cotter et al., 2024).

6.5.1. Temperature and Humidity Gradients

Even within highly regulated climate-controlled glasshouses, environmental conditions are rather heterogeneous, creating microclimate pockets within the glasshouse (Li et al., 2018). In tall tomato crops, net radiation varies significantly with canopy depth, often leaving the lower foliage colder than the upper levels, creating a particular risk of “cold spots” (De Boeck et al., 2012; Stanghellini et al., 2019). Even when mean crop temperatures (as calculated by centralised climate sensors) appear to remain safely above the dew point, horizontal variations in insulation or airtightness can cause temperatures in specific zones to drop below the grower's safety threshold. In these localised areas, condensation occurs, creating the conditions for fungal germination (Stanghellini et al., 2019).

According to Stanghellini et al. (2019), a critical vulnerability occurs during the “morning transition” at sunrise, when rapidly increasing transpiration raises the dew point before the high thermal mass of stems and fruit can sufficiently warm. As solar radiation increases, plants experience a transpiration surge, rapidly elevating the internal dew point by pushing moisture into the greenhouse atmosphere. However, while leaves adjust to temperature changes within one to two minutes, stems and fruit possess significant thermal mass and warm at a much slower rate; thus, the rising dew point inevitably surpasses the temperature of these slowly warming organs. The resulting condensation on stems and fruit provides the free water required for *F. fulva* conidia to settle and enter the plant via open stomata (Sudermann et al., 2022).

Furthermore, nighttime disease pressure is exacerbated by radiative cooling, which lowers crop temperatures below the surrounding air temperature. On clear nights, radiative losses through the greenhouse cover to the sky can reach 150 W/m²; without effective screen positioning or a heating system, the crop temperature inevitably falls below the air temperature (Stanghellini et al., 2019).

6.5.2. Hydraulic Feedback and Stomatal Dynamics

Grower interventions can occasionally create unintended VPD variances through a process known as hydraulic feedback (Stanghellini et al., 2019). Heating strategies that aim to dry the air by increasing the moisture deficit (VPD) prompt the plant to increase transpiration, which subsequently cools the leaf surface, leaving the plant only slightly farther from the dew point than before the adjustment (Stanghellini et al., 2019; Amitrano et al., 2019). Consequently, the safety margin against condensation remains dangerously slim despite active intervention (Stanghellini et al., 2019).

Furthermore, the stomatal dynamics required for crop productivity inadvertently facilitate infection. As an apoplastic pathogen, *F. fulva* enters the leaf exclusively through open stomata (Stanghellini et al., 2019; de la Rosa et al., 2024). Environmental control systems designed to optimise photosynthesis by effectively regulating light and CO_2 keep stomata open, facilitating fungal entry (Stanghellini et al., 2019; Neo et al., 2022; Merilo et al., 2018). If high-humidity microclimates persist even briefly while stomata are open for gas exchange, the pathogen can successfully colonise the intercellular spaces between mesophyll cells (Sudermann et al., 2022; de la Rosa et al., 2024).

6.5.3. Strategic Management Dilemmas and the New Zealand Context

The management of these environmental parameters highlights the pervasive complexity of protected cropping: addressing a specific climatic deficit often creates unintended secondary vulnerabilities. In New Zealand, commercial growers manage environmental variables using automated climate management systems, such as PRIVA (De Lier, The Netherlands), to execute complex growing strategies. Yet, the precision required to balance irrigation, ventilation, and heating cycles demands a high degree of technical expertise (Stanghellini et al., 2019). A failure to accurately analyse the interplay between these variables can inadvertently promote fungal infection rather than suppressing it.

The challenge for the New Zealand tomato industry is further aggravated by significant economic and logistical disparities compared to global leaders like the Netherlands. According to TomatoesNZ (2023), while New Zealand adopts many facets of the Dutch glasshouse method, the operational scale is vastly different. The Netherlands maintains approximately 10,000 ha of greenhouses and benefits from a government-led transition toward sustainable energy and from its proximity to European markets, which facilitate substantial economies of scale. In contrast, the New Zealand market is characterised by geographic isolation and a significantly smaller footprint, making the high capital investment required for high-tech glasshouse upgrades unviable for many.

These constraints are particularly acute for small-scale New Zealand growers. Unlike large corporate entities, these growers often lack the advanced screen systems or supplemental heating capacity needed to execute the precise VPD interventions described earlier. Consequently, these operations have very little margin for error; their limited environmental control options often leave them unable to prevent humidity spikes and thermal lag, which act as primary triggers of *F. fulva* pathogenesis. This socio-economic bottleneck suggests that genetic resistance and biosecurity must remain the primary lines of defence for the New Zealand industry, as technical climate-shielding remains out of reach for a significant portion of the sector.

6.6. Host Resistance Erosion and Claims of the Breakdown of Commercial "Ff: A-E" Cultivars

The research findings reveal a stark discrepancy between the theoretical resistance of commercial tomato cultivars and the actual pathological outcomes in New Zealand glasshouses. As established in Objective 1, this study sought to quantify the prevalence of leaf mould within "Ff: A-E" resistant varieties. Field observations and grower consultations indicated that the disease affected a substantial proportion of the crops sampled, regardless of their resistance labelling, though the non-random, participant-led design of this survey means the finding cannot be taken as a representative national estimate. This is consistent with anecdotal evidence from the industry:

> Historically, most New Zealand growers didn't see *Fulvia fulva* as a major commercial threat. Up until the last decade, infection levels were usually mild and could be managed with normal crop practices. Localised symptoms in specific growing areas within a glasshouse were generally dealt with through routine de-leafing, and the broader spray programmes used for key pests and diseases seemed to provide enough knockdown of leaf mould as a side benefit (A. Hutchinson, personal communication, February 02, 2026).

However, the "side benefit" of historical management has clearly diminished. The strong, compatible symptoms observed in all leaf samples from cultivars labelled as resistant suggests that the breakdown of the *Cf* genes deployed in these cultivars may be more widespread than previously recognised. However, systematic surveillance across New Zealand is required to confirm the extent of this phenomenon. This observation aligns with the global scenario where *F. fulva* populations have evolved to overcome the *Cf-2, Cf-4, Cf-4E, Cf-5, Cf-6, Cf-9B* and *Cf-9C* genes through effector mutation or deletion (de la Rosa et al., 2024; Iida et al., 2015; Lucentini et al., 2021; Mesarich et al., 2014, 2023; Novak et al., 2021; Schol et al., 2025; Stergiopoulos et al., 2007; Sudermann et al., 2022; Yoshida et al., 2021). Industry leaders echo this transition from a "minor nuisance" to a primary threat:

> Over the last five to ten years, we've seen a steady rise in leaf mould cases reported by growers. It's becoming a major concern for the industry because the disease seems more aggressive now, and we're honestly running out of effective ways to treat or eliminate it (D. Cohen, personal communication, February 23, 2026).

6.7. The Chemical Deficit and the Necessity of Polygenic Breeding Strategies

A clear regulatory bottleneck compounds this management crisis, as only a single fungicide — Thiram 40F (Nufarm Ltd, New Zealand) — was identified during this research as currently registered for controlling leaf mould in tomato crops under New Zealand label specifications. While acquiring a registered arsenal of fungicides might

appear to offer a short-term solution, global precedents suggest that reliance on chemicals is a precarious strategy. Due to the high mutation rate and inherent plasticity of *F. fulva* (Thomma et al., 2005), populations of this fungus in regions such as Japan and Europe have developed resistance to common fungicides in as little as three years (Asano et al., 2024; Watanabe et al., 2017).

This rapid adaptation underscores the limitations of the “side benefit” management approach previously utilised by the New Zealand tomato industry. Consequently, the transition toward more robust breeding strategies is no longer optional but essential for long-term crop security. Moving beyond single-gene (*Cf*) resistance, which the pathogen has proven capable of overcoming through simple effector mutation or deletion, the industry must prioritise gene stacking and pyramiding strategies (Richard et al., 2022).

According to de la Rosa et al. (2024), the *Cf-9* locus already combined two resistance genes — *Cf-9C* and *Cf-9B*, recognising *Avr9* and *Avr9B*, respectively — yet was still overcome through the sequential loss of *Avr9*, followed by the loss or mutation of *Avr9B*. Critically, these two genes were not functionally equivalent: *Cf-9C* conferred resistance throughout development, whereas *Cf-9B* was effective only at mature plant stages. The durability of a stack therefore depends not only on the number of genes it contains, but on the strength, expression, and developmental breadth of each component, and on deploying genes whose corresponding effectors are least dispensable to the pathogen.

Ideally, a well-designed stack raises the evolutionary barrier such that virulence would require several independent changes to arise together rather than accumulate sequentially — the failure mode seen at the *Milky Way* locus (Soumpourou et al., 2007). Achieving this depends on combining genes whose corresponding effectors cannot be lost or mutated individually without imposing a fitness cost on the pathogen. By incorporating multiple *Cf* resistance genes into a single cultivar, the evolutionary barrier for the pathogen is significantly increased, as *F. fulva* would be required to undergo multiple simultaneous mutations to establish infection. Such polygenic strategies, informed by the genomic characterisation currently underway in this

project, represent the most viable pathway for strengthening New Zealand's Integrated Pest Management (IPM) programs against an increasingly plastic pathogen.

6.8. Predicted Breakdown of *Cf*-Mediated Resistance in New Zealand Isolates

The central question is whether the *Avr* gene mutations and absences identified in the three New Zealand isolates are consistent with breakdown of the corresponding *Cf* resistance genes. For five of the seven *Cf* genes examined — *Cf-2*, *Cf-4E*, *Cf-9*, *Cf-9B*, and *Cf-6* — the molecular evidence is consistent with resistance breakdown in at least one isolate. For *Cf-4* and *Cf-5*, the picture is more nuanced: the *Avr4* change in the ICMP 7320 isolate remains functionally unresolved, and *Avr5* was intact in all three isolates.

An important qualification applies throughout: sequence-level changes are necessary but not sufficient evidence for resistance breakdown. Definitive confirmation requires a functional assay — a differential line inoculation test — that was not performed in this research. All the statements below are therefore predictions supported by coding and protein sequence evidence and, where available, published functional data, rather than independently demonstrated statements.

6.8.1. Cf-2 / Avr2

Avr2 was disrupted in CM1 and CO1 isolates: the second exon of *Avr2* was absent, producing a 53-amino acid residue product that retains only the N-terminal half of the protein since the C-terminal portion of the coding sequence is missing. Protein truncations of Avr2 are extensively documented as resistance-breaking: Stergiopoulos et al. (2007) catalogued multiple frameshift and deletion alleles (p.Lys22AsnfsX11, p.Leu24ThrfsX18, p.Leu24TyrfsX10, p.Tyr41ValfsX1 and others) from a worldwide collection of 81 strains, all experimentally confirmed to overcome *Cf-2*-mediated resistance. The class of change — the removal of the C-terminal portion of the effector — is the same in CM1 and CO1 New Zealand isolates, although the precise

mechanism (exon-2 loss by deletion or transposon insertion, as identified in the genome assembly) differs from the frameshifts catalogued in the literature.

In ICMP 7320, *Avr2* was full length with a single missense change (leading to an L43V amino acid substitution). This position was identified by Stergiopoulos et al. (2007), although whether it leads to the breakdown of *Cf-2*-mediated resistance was not determined. The *Cf-2*-breaking status of the ICMP 7320 isolate therefore cannot be inferred solely from sequence; L43V is not among the changes known to break *Cf-2* resistance. The Avr2 protein of the ICMP 7320 isolate may therefore still be recognised by the Cf-2 receptor, rendering the isolate avirulent on *Cf-2*-carrying plants.

6.8.2. Cf-4 / Avr4

A single missense change (leading to a C86F amino acid substitution) was present in *Avr4* of isolate ICMP 7320, while this gene in isolates CM1 and CO1 was identical to the reference sequence (in isolate 0WU). Although Stergiopoulos et al. (2007) reported a C86F (p.Cys86Phe) substitution in other isolates of *F. fulva*, their accompanying annotation explicitly notes that any functional impact was deduced rather than experimentally validated (Table 2). The authors inferred that this specific cysteine substitution destabilises the protein by disrupting a critical disulphide bond. Consequently, the *Avr4* mutation observed in the ICMP 7320 isolate represents a predicted, rather than an experimentally confirmed, resistance-breaking mechanism. Because CM1 and CO1 isolates harbour an intact *Avr4* gene, they are predicted to lack the capacity to overcome *Cf-4*-mediated resistance via this specific pathway.

6.8.3. Cf-4E / Avr4E

Avr4E was not detected in ICMP 7320, whereas it was intact in both CM1 and CO1 isolates. Gene deletion of *Avr4E* is the best-documented mechanism of *Cf-4E* evasion (Mesarich et al., 2023; Stergiopoulos et al., 2007). The absence in ICMP 7320 is therefore consistent with loss of *Cf-4E*-mediated recognition in that isolate. CM1 and CO1 isolates retain *Avr4E* and are not predicted to have overcome *Cf-4E*. This pattern

is the reverse of the *Avr9B* pattern (see subsection [6.8.6.]), and CM1 and CO1 isolates with intact *Avr4E* would be expected to remain avirulent on *Cf-4E* plants.

6.8.4. Cf-5 / Avr5

Avr5 was intact and identical to the reference in all three isolates. *Avr5* was characterised in a race 5 strain by deletion and frameshift (Mesarich et al., 2014); frameshift and gene-deletion mechanisms are also the predominant resistance-breaking route recorded in the broader literature (Iida et al., 2015; Kubota et al., 2015; Mesarich et al., 2014; Mesarich et al., 2023). The complete conservation of *Avr5* in the three New Zealand isolates indicates that *Cf-5* resistance is not predicted to be overcome by any of the isolates examined here.

6.8.5. Cf-9 / Avr9

Gene deletion of *Avr9* has been consistently reported for over three decades (Mesarich et al., 2023; Stergiopoulos et al., 2007; van Kan et al., 1991). The universal absence of *Avr9* across all three isolates — ICMP 7320, CO1 and CM1 — indicates that *Cf-9*-mediated resistance has not been effective against any of the New Zealand isolates examined in this research, including ICMP 7320.

Avr9 loss is the most consistently documented route to overcoming Cf-9-mediated resistance in the surveyed literature, with gene deletion reported from the earliest studies through to the most recent (Mesarich et al., 2023; Stergiopoulos et al., 2007). In the present study, *Avr9* was absent from all three isolates, including ICMP 7320. If *Cf-9* had been deployed in New Zealand, this would imply that *Cf-9*-mediated resistance had already been circumvented at or before the time this strain was collected in the 1980s.

It is not currently possible, however, to determine how many independent *Avr9* deletion events underlie the global distribution of race 9 strains, or whether the New Zealand deletion is shared with, or independent of, those reported overseas. The

short-read data used here establish the absence of *Avr9* but do not resolve the boundaries or structure of the deleted region. Long-read sequencing (e.g. PacBio or Oxford Nanopore) would allow the full extent of the deletion to be characterised and compared directly with deletions in international isolates — including the PacBio-assembled race 9 strain of Zaccaron et al., 2022 — to test whether the New Zealand loss represents the same ancestral event or an independent, convergent deletion. Resolving this would clarify whether *Avr9* loss in New Zealand reflects a single introduced lineage or local adaptation and would place the New Zealand population within the global phylogeography of *Cf-9* breakdown.

6.8.6. Cf-9B / Avr9B

Avr9B (de la Rosa et al., 2024) was present and intact in ICMP 7320 but absent from both CM1 and CO1 isolates. In the literature, *Avr9B* loss is associated with resistance breakdown: this has been demonstrated by Polymerase Chain Reaction (PCR), which showed that *Avr9B* deletion accompanied *Avr9* deletion in race 2.9 strains of *F. fulva*, and that complementation with 0WU *Avr9B* restored avirulence on *Cf-9* plants (de la Rosa et al., 2024). In addition to gene deletion, *Cf-9B*-breaking strains from Europe carry loss-of-function mutations within *Avr9B*, including a premature stop codon (Cys107*) and a combined deletion-and-missense allele (del129–133 with L135V) (Schol et al., 2025). In CM1 and CO1 isolates, *Cf-9B* evasion is instead associated with complete absence of *Avr9B*; while the mutational route differs, the outcome — loss of a functional Avr9B effector — is consistent with these European reports. The pattern across the New Zealand isolates is sequential: the ICMP 7320 isolate lacks *Avr9* but retains *Avr9B*, whereas CM1 and CO isolates lack both. This mirrors the stepwise progression described in European populations, in which *Avr9* loss produces race 9 and subsequent loss or mutation of *Avr9B* produces race 2.9 (de la Rosa et al., 2024). The New Zealand isolates are consistent with a similar trajectory. However, this ordering cannot be established as a true temporal sequence from the present data, because the three isolates represent single time points from possibly unrelated lineages rather than a sampled progression within one lineage; the apparent stepwise pattern may instead reflect two independent genotypes.

6.8.7. Cf-6 / Avr6

Avr6 (*Ecp5*) in isolates CM1 and CO1 encoded a protein that carried C30Y, a missense change at cysteine 30. Although this change was initially flagged as a candidate novel variant in this study, cross-referencing with the literature confirmed it is documented: Schol et al. (2025) report Cys30Tyr in their dataset and provide complementation evidence that restoring wild-type *Avr6* abolishes virulence on *Cf-6* plants, explicitly confirming that C30Y breaks *Cf-6*-mediated resistance. C30Y is therefore an experimentally validated resistance-breaking change, and its presence in both CM1 and CO1 isolates is consistent with the loss of *Cf-6*-mediated resistance. *Avr6* in ICMP 7320 was intact at the codon encoding this amino acid position, suggesting that the ICMP 7320 isolate retained *Cf-6* avirulence. Of the four Avr6 cysteine mutations described to date (C30Y, C30fs, C48Y) (Schol et al., 2025), C30Y is the only missense change for which complementation data confirm loss of recognition.

Notably, a second New Zealand strain (NZ_269_1) reported by Schol et al. (2025) carries a distinct *Cf-6*-breaking substitution, Avr6 Y88H, rather than the C30Y found here and in the IPO 2679 isolate. The presence of at least two independent *Cf-6*-breaking *Avr6* alleles in New Zealand indicates that selection against *Cf-6* is not restricted to the clonal lineage sampled in this study, and mirrors the multiple independent routes to *Avr6* loss documented internationally (Schol et al., 2025).

6.9. Novel Mutations Not Previously Described in the Literature

Systematic cross-referencing of the New Zealand variant calls against the 970 literature observations (see Appendix VI) identified one genuinely novel mutation and three changes at previously reported positions with undetermined or deduced (not experimentally confirmed) significance.

Genuinely novel: *Ecp4* V127G (ICMP 7320). No literature observation at amino- acid position 127 of Ecp4 was identified in any of the consulted sources. The predominant change at *Ecp4* in the literature is C108W (Cys>Trp), reported across multiple

Argentinian isolates (Lucentini et al., 2021); no variant at position 127 was identified in any consulted sources, making the V127G change reported as novel. *Ecp4* is also noted to be under positive selection in an Argentinian population (Schol et al., 2025). V127G is positionally distinct from the reported changes at residues 108 and 90, and no phenotypic data were found for residue 127, and no phenotypic data were found for this position; whether V127G represents a fitness-neutral variant or a change under selection cannot be determined from the current data.

6.9.1. Changes at Previously-Reported Positions

The Avr2 L43V substitution (ICMP 7320) occurs at a position (residue 43) also identified by Stergiopoulos et al. (2007), who recorded no effect on Cf-2 recognition; it was not listed among the resistance-breaking variants in that study.

The Avr4 C86F substitution (ICMP 7320) occurs at residue 86 and was reported by Stergiopoulos et al. (2007) as a deduced — not experimentally tested — resistance-breaking change, attributed to disruption of a disulphide bond.

The Ecp12 G124R substitution (ICMP 7320) occurs at residue 124, recorded by Mesarich et al. (2018) as a Gly→Arg change at the same position, with no associated change in resistance phenotype.

6.10. Incursion Events and Mutation Origins in New Zealand: Are mutations or mutation profiles unique to New Zealand?

Among the sequence changes identified in the three New Zealand isolates, no change is molecularly unique in the broad sense of being absent from all surveyed sources: the *Avr2* exon-2 truncation, *Avr6* C30Y, and the absences of *Avr9* and *Avr9B* each have precedent internationally (Luderer et al., 2002; Iida et al., 2015; de la Rosa et al., 2024; Schol et al., 2025). The *manner* of *Avr9B* loss, however, appears distinctive. Internationally, *Cf-9B* has been overcome by several independent mechanisms — point mutation (W97C, Cys107*), a small deletion-plus-missense allele (del129–133/L135V), and transposon (MITE) insertion in a Japanese strain — whereas

complete deletion of the *Avr9B* locus has, to date, been reported only in New Zealand strains (de la Rosa et al., 2024; Schol et al., 2025). Moreover, de la Rosa et al. (2024) report that the New Zealand deletion strains (IPO 2679, and additional isolates) share the same ~5.4 kb deletion profile. The absence of *Avr9B* in the two recent isolates characterised here is consistent with the same New Zealand-specific deletion.

If the *Avr9B* deletion reflects a single ancestral event, its apparent restriction to New Zealand strains would suggest that the New Zealand population — or at least the lineage currently circulating — shares a common origin. This remains a hypothesis rather than a conclusion: it rests on limited international sampling from *Cf-9*/*Cf-9B* backgrounds, and confirming both the exclusivity of the deletion and its identity across New Zealand isolates would require broader worldwide sampling and long-read characterisation of the deletion boundaries.

A distinctive pattern among CM1 and CO1 isolates is the combination of changes: *Avr2* Truncated, *Avr6* C30Y, *Avr9* absent, *Avr9B* absent, with *Avr4* and *Avr5* intact. Whether this combination arose in New Zealand or was introduced as an already-assembled virulence profile cannot be determined from three isolates and requires broader population sampling.

6.11. Mutations Profile: Did These Mutations Arise After the Incursion, or Were They Present in the Founding Population?

The absence of *Avr9* in ICMP 7320 and in both CM1 and CO1 isolates indicates that at least the *Avr9* deletion predates the earliest sequenced isolate in this study — it is not a change that accumulated after incursion but was already present in the New Zealand population at the time the oldest isolate was collected. By contrast, the *Avr2* exon-2 truncation, *Avr6* C30Y, and *Avr9B* absence are present in CM1 and CO1 isolates but not ICMP 7320, which raises two non-exclusive possibilities: (1) these changes arose or spread within the New Zealand population after ICMP 7320 collection; (2) the New Zealand population experienced a re-introduction of a different lineage between the 1980s and recent sampling events. Neither possibility can be distinguished with n=3 and no intermediate time points.

6.12. Mating Types: Are Both Mating Types Present — and is Sexual Reproduction Occurring?

Stergiopoulos et al. (2007) surveyed variation in the *MAT1-1-1* and *MAT1-2-1* genes across 81 *F. fulva* strains from a worldwide collection (including New Zealand) and reported both mating types at the global population level. Whether both types are present in the specific New Zealand commercial population sampled here cannot be determined from the current dataset, because no *MAT* locus data were generated for the three isolates. In European populations, the co-occurrence of specific *Avr2* variants (Tyr41fs*42) across both mating types has been interpreted as evidence of recombination (Schol et al., 2025); however, this inference is specific to those strains and cannot be extended to the New Zealand isolates while their *MAT* status remains unknown.

This is, nonetheless, the most tractable of the outstanding questions, because it can be addressed with existing materials: the *MAT1-1-1* and *MAT1-2-1* sequences can be extracted directly from the genome assemblies generated in this study. Determining the mating-type identity of the sampled isolates in future work would establish whether both types are present in the New Zealand population and, in turn, whether sexual recombination is plausible — a question of practical relevance given that recombination could accelerate the assembly of new virulence combinations.

6.13. Clonal Profile: Is the New Zealand Population Clonal?

Isolates CM1 and CO1 sampled from unrelated companies, in different commercial greenhouses geographically apart by hundreds of km and collected approximately three years apart, were identical across all 20 effector genes examined: the same *Avr2* truncation form, the same *Avr6* C30Y, the same *Avr9* and *Avr9B* absences, and the same intact status for the remaining 16 effectors. No sequence difference was detected between them at the protein level. This level of identity across 20 loci in isolates from physically separate locations is consistent with a clonal relationship — i.e. a single lineage spreading vegetatively across glasshouses — rather than independent mutation events converging on the same profile.

Clonal spread by conidia in glasshouse environments is the expected default for *F. fulva*, given that sexual reproduction is rare in the species, has not been documented under commercial glasshouse conditions, and requires the co-occurrence of compatible mating types (Gül et al., 2024; Stergiopoulos et al., 2007) — a condition that cannot presently be evaluated for the sampled isolates, as their *MAT* status was not determined (section [6.12.]). The clonal identity observed here is therefore consistent with, but does not by itself establish, an exclusively asexual local population; resolving whether both mating types are present would clarify whether sexual recombination is even possible among these isolates.

The ICMP 7320 isolate has a substantially different profile — *Avr2* L43V, Avr4 C86F, *Avr4E* absent, *Avr9* absent, *Avr9B* intact — suggesting it belongs to a different lineage from the CM1 and CO1 isolate pair. Whether the recent lineage displaced the ICMP 7320, co-exists with it, or represents a separate introduction is unknown.

6.14. Concordance with Previous PCR-based Genotyping

The only isolate examined here that has been genotyped previously at the effector loci is ICMP 7320 by Mesarich et al. 2018, since nine HR-eliciting apoplastic effector (*Ecp*) genes — *Ecp8*, *Ecp9-1*, *Ecp10-1*, *Ecp11-1*, *Ecp12*, *Ecp13*, *Ecp14-1*, *Ecp15* and *Ecp16* — were amplified by PCR from ten *F. fulva* strains, including ICMP 7320, and compared following PCR amplicon sequencing to those from strain 0WU (Mesarich et al., 2018). That panel did not include any *Avr* gene or *Ecp1*, *Ecp2-1*, *Ecp4* or *Ecp5*. The genome-sequencing results reported here reproduce the ICMP 7320 genotype of Mesarich et al. (2018) across all nine panel genes and extend the characterisation of this strain to the Avr genes and to *Ecp1*, *Ecp2-1*, *Ecp4* or *Ecp5* for the first time.

Of the nine panel genes, Mesarich et al. (2018) reported two changes in ICMP 7320: a non-synonymous substitution in *Ecp12*, resulting in a Gly124Arg change at the protein level, and a synonymous substitution in *Ecp8* at codon 51 (nucleotide 153); the remaining seven genes showed no allelic variation in this strain. Genome sequencing confirms all three outcomes. The Ecp12 Gly124Arg change is predicted to be identical at the amino-acid level in both data sets (c.370G>A, G124R); the difference in

nucleotide numbering (reported here as c.370, versus position 484 in Mesarich et al., 2018) reflects CDS versus genomic coordinates and corresponds exactly to the 114 bp of intron sequence preceding this codon. The *Ecp8* synonymous change is located at the same codon position (codon 51, Pro→Pro). The seven genes reported as invariant in ICMP 7320 (*Ecp9-1*, *Ecp10-1*, *Ecp11-1*, *Ecp13*, *Ecp14-1*, *Ecp15*, *Ecp16*) are all intact in the genome-sequencing data, and this result independently corroborates the PCR-based finding.

In addition to the results of Mesarich et al. (2018), genome sequencing undertaken in this study reports three categories of change in ICMP 7320 for the first time: the Ecp4 V127G substitution (see sections [6.8.] and [6.15.8]); the changes affecting the *Avr* genes — two amino-acid substitutions (Avr2 L43V, Avr4 C86F) and two gene absences (*Avr4E*, *Avr9*), none of which were examined by Mesarich et al. (2018); and the intact status of *Ecp1*, *Ecp2-1* and *Ecp17*, which also lay outside that panel examined in 2018. The concordance between independent methods (PCR amplicon sequencing and whole-genome sequencing) supports the reliability of the effector genotypes reported in this study.

One apparent discrepancy was reconciled. Both studies identify a synonymous variant at *Ecp8* codon 51, but Mesarich et al. (2018) record 0WU as CCC and ICMP 7320 as CCT, the reverse of the polarity found here. Comparison with the deposited 0WU *Ecp8* reference sequence GenBank KX943038.1 (National Center for Biotechnology Information, 2016), which carries CCT at codon 51, confirms that the reference allele used in this study is correct and that the direction of the change is 0WU (CCT) to ICMP 7320 (CCC), i.e. c.153T>C. The apparent reversal in Mesarich et al. (2018) therefore reflects a difference in how the reference allele was reported rather than a genuine disagreement in the variant; the change is synonymous (Pro→Pro) and has no functional consequence.

6.15. Genomic Location and Structural Context of Effector Mutations

6.15.1. Avr2

Mutations are distributed across the mature Avr2 protein in the global literature, with position 41 the most frequently mutated (8 observations; Stergiopoulos et al., 2007, and others), followed by positions 22 and 41 (Luderer et al., 2002). The New Zealand exon-2 truncation removes the C-terminal region (residues 54–78 of the 78-residue mature protein), which contains several cysteine residues, including one (Cys63) shown experimentally to form a disulphide bond required for Cf-2-mediated recognition (Iida et al., 2015). The L43V substitution in ICMP 7320 lies in the N-terminal half of the mature protein and, being conservative, may leave the effector structurally intact. The concentration of resistance-breaking mutations at or after residue 22 in the global dataset suggests that residues in the C-terminal half of the mature protein are critical for recognition of Avr2 by Cf-2.

6.15.2. Avr4

In the wider international literature, Avr4 mutations cluster around amino acid position 64 (four observations) and also span amino acid positions 42, 66, 67, 70, 86, 89, and 109 (Mesarich et al., 2023; Stergiopoulos et al., 2007). Avr4 is a chitin-binding effector, and several resistance-breaking changes disrupt cysteine residues involved in disulphide bonds (van den Burg et al., 2006). The C86F substitution identified here in Avr4 (ICMP 7320 isolate) is reported only once in the literature; no independent experimental confirmation of its effect on recognition by Cf-4 has been identified.

6.15.3. Avr4E

Two amino acid positions dominate the literature: 82 (22 observations) and 93 (22 observations), with substitutions p.Phe82Leu and p.Met93Tyr documented in multiple studies and confirmed as enabling resistance conferred by Cf-4E to be broken (Westerink et al., 2004). *Avr4E* gene deletion — as found in ICMP 7320 — is also a

common resistance breakdown mechanism. The CM1 and CO1 isolates carry intact *Avr4E* and are not among the strains expected to overcome *Cf-4E*.

6.15.4. Avr5

Mutations in the literature are sparse: amino acid positions 5 and 90 each have a single observation in the position-resolved data, with Gly90Arg confirmed experimentally to confer breakdown of Cf-5-mediated resistance (Iida et al., 2015). Most resistance-breaking changes in *Avr5* are deletions or frameshifts, particularly gene-level deletions, which is the dominant mode in the race 5 literature (Mesarich et al., 2014). All three New Zealand isolates carry intact *Avr5*.

6.15.5. Avr6

Schol et al. (2025) provide the most comprehensive catalogue of *Avr6* variation: resistance-breaking changes span deletion of the ~18 kb *Avr6* locus, nonsense mutations (e.g. Lys22*), frameshifts (at residues Val40, Cys30 and Val98), and missense substitutions, including changes at cysteine residues (C30Y, C48Y) and Tyr88His. The C30Y substitution identified here (in CM1 and CO1 isolates) affects cysteine 30, one of the residues experimentally shown to be critical for Cf-6 recognition. Reported missense changes cluster at these cysteine positions (residues 30 and 48), with no missense substitutions currently reported between residues 53 and 88, consistent with a structural role for the cysteines in the mature effector.

6.15.6. Avr9

With 60 experimentally confirmed resistance-breaking observations (all by gene deletion), *Avr9* loss by gene deletion is the most consistently reported mechanism of Cf-9 evasion in the surveyed literature (Stergiopoulos et al., 2007; Mesarich et al., 2023). The only recurrent point change, a Val8Ala (V8A) substitution at residue 8, has been reported across multiple studies but has not been shown to affect Cf-9-mediated recognition (Stergiopoulos et al., 2007; Iida et al., 2015). The universal absence of

Avr9 across all three New Zealand isolates places the New Zealand population within the well-documented race 9 lineage.

6.15.7. Avr9B

Avr9B is relatively underrepresented in the literature, with most records deriving from de la Rosa et al. (2024) and Schol et al. (2025). Reported routes by which *Avr9B* escapes Cf-9B-mediated recognition include a nonsense mutation (Cys107*), a combined deletion-and-missense allele (del129–133 with L135V), and complete deletion of the *Avr9B* locus. In the two recent New Zealand isolates characterised here, *Avr9B* was lost due to the absence of the entire locus. This is consistent with the deletion route reported by de la Rosa et al. (2024), which — in contrast to the point and indel alleles described in European strains — has to date been observed only in New Zealand isolates, all of which share the same deletion profile. Because short-read sequencing establishes the absence of *Avr9B* but does not define the boundaries of the deletion, whether the deletion in these isolates is identical to that in the earlier New Zealand strains cannot yet be confirmed. Long-read sequencing (e.g., PacBio, as used for the race 9 assembly in Zaccaron et al., 2022) would allow deletion boundaries to be characterised and directly compared.

6.15.8. Ecp genes: Ecp Effectors with New Zealand Changes

Ecp4: Amino acid position 108 (C108W) is the dominant change in the literature (19 observations, all from Lucentini et al., 2021). Amino acid position 90 carries one observation (G90V; Stergiopoulos et al., 2007). The V127G substitution observed in New Zealand isolates at amino acid position 127 lies outside both documented hotspots. No cognate *Cf* gene for *Ecp4* has been identified.

Ecp12: Amino acid position 124 carries two observations in Mesarich et al. (2018), both the same Gly>Arg change, with no phenotypic consequence recorded. The G124R substitution observed in New Zealand isolates is the same change at the same

position, confirming that this is a recurrent variant rather than a New Zealand-specific mutation. No cognate *Cf* gene has been identified for *Ecp12*.

Two further changes were synonymous and are therefore not considered further with respect to effector function: a c.87C>A substitution in *Ecp2-1* (CO1 isolate) and a c.153T>C substitution in *Ecp8* (ICMP 7320 isolate). Both alter the third position of a codon without changing the encoded amino acid, so the Ecp2-1 and Ecp8 protein sequences remain identical to the reference.

6.16. Ongoing Genomic Characterisation and Future Directions

The three high-quality genome sequences obtained (CO1, CM1, and ICMP 7320) represent the first critical step in identifying New Zealand's specific *F. fulva* races. The theoretical and practical groundwork has been successfully established for further expansion.

As work on this project extends beyond the submission of this thesis, isolation of strain PT1 is currently underway, with GR2 and DC1 scheduled for the same process (Table 4). These isolates will undergo comparative genomic analysis alongside international strains and local isolates (ICMP 7320, CM1, and CO1) to strengthen and expand the findings of this research, in alignment with Objective 3. Without these genomic insights, growers will continue to battle a poorly characterised threat, potentially relying on management strategies whose effectiveness has not been formally evaluated against the resistance-evading pathogen variants identified here.

Chapter 5

7. Conclusion

The findings of this research are consistent with a significant shift in phytosanitary regulations that the New Zealand tomato industry is currently navigating. While *F. fulva* was historically regarded as a manageable secondary pathogen, it appears to be evolving into a more significant biosecurity concern, with the effector-loss patterns observed here consistent with a genetic potential for resistance evasion, and symptom presence across all four resistant cultivars sampled suggesting that resistance breakdown may be more widespread than previously recognised — confirming its national extent would necessitate systematic surveillance across a wider range of cultivars sites and growing regions. As established in Objective 1, the presence of symptomatic leaf mould across all sampled previously resistant "Ff: A-E" cultivars indicates that the *Cf* genes carried by the four resistant cultivars sampled in this survey did not provide reliable protection under the field conditions encountered here, though whether this holds across the full suite of commercially deployed Cf genes nationally would require broader surveillance to confirm.

The environmental analysis conducted for Objective 3 highlights that high-tech climate control alone cannot serve as a panacea for disease prevention. Even in advanced glasshouses, the physical realities of thermal mass, the morning transition, and hydraulic feedback create microclimate patches that the pathogen exploits. This technical vulnerability is compounded by the socio-economic constraints of the New Zealand market, where the isolation from international economies of scale and the prohibitive cost of high-tech infrastructure leave many growers with limited environmental management options.

Furthermore, while the complete genomic characterisation outlined in Objective 2 is ongoing, this study has provided a more comprehensive overview of the *F. fulva* situation in New Zealand by generating isolates and high-quality genome assemblies, albeit limited to date, to bridge the current knowledge gap. The continued sequencing of these domestic strains remains paramount; identifying the specific races of the

fungus active in New Zealand will allow the industry to move beyond anecdotal observations towards a more technical approach to disease management, while supporting future breeding efforts to create resilient cultivars to this pathogen.

Ultimately, strengthening New Zealand's Integrated Pest Management (IPM) strategy requires a dual approach: the introduction of novel *Cf* resistance genes that are not yet overcome by local populations, and a rigorous refinement of environmental strategies that account for the specific microclimate risks identified in this report. By aligning genomic insights with practical management improvements, the industry can develop a more resilient framework to safeguard tomato production against the escalating pressure of *F. fulva*.

7.1. Genome Sequencing Conclusions

This study characterised 20 candidate effector genes across three New Zealand *F. fulva* isolates — ICMP 7320 (1980s), CM1 (isolated in 2022) and CO1 (isolated in 2025) — from whole-genome sequence data, using a reproducible bioinformatic pipeline, and placed the results in context by systematic cross-reference to 970 mutation observations extracted from 21 primary papers (see Appendix VI). The principal conclusions are as follows.

The effector repertoire is largely conserved, with change concentrated in the *Avr* genes. When examining 60 effector–isolate combinations, the majority of effector sequences were identical to the reference; discrete changes — six missense substitutions, two truncations, and six absence events — were confined to seven effectors, most of which were *Avr* genes. Sequence divergence was therefore the exception across the panel.

The molecular evidence is consistent with predicted breakdown of several *Cf* resistance genes in New Zealand, though sequence data alone cannot confirm loss of recognition. Because an effector change may be enough to cause resistance breakdown but sequence data alone cannot establish that it is — the change could be causal, incidental, or affect an effector the plant does not target — the following are predictions supported by sequence evidence and, where available, published

functional data, rather than causal relationships demonstrated in this study. *Avr9* was absent from all three isolates, consistent with loss of *Cf-9* effectiveness across the sampled population. In CM1 and CO1 *F. fulva* isolates, *Avr2* was truncated, *Avr9B* was absent, and Avr6 carried the C30Y substitution — the last of which has published complementation evidence for breaking Cf-6 — consistent with predicted evasion of *Cf-2*, *Cf-9B* and *Cf-6* by the recent lineage. In ICMP 7320 isolate, *Avr4E* was absent, consistent with predicted *Cf-4E* evasion. By contrast, *Avr5* was intact in all three isolates, so no Cf-5 breakdown is predicted in the sampled population. This suggests *Cf-5* may retain effectiveness against the New Zealand isolates examined here and could have short-term utility. However, *Avr5* loss and mutation have been reported as resistance-breaking in several international populations (Iida et al., 2015; Mesarich et al., 2014; Mesarich et al., 2023), so *Cf-5* is not intrinsically durable; its effectiveness in New Zealand may reflect the limited local sampling and the absence, so far, of selection pressure from deployed *Cf-5*. Both mutation within the existing population and incursion of *Avr5*-mutant strains from overseas remain plausible routes by which *Cf-5* could be overcome, and this risk reinforces the argument (section [6.8.4.]) that *Cf-5* would be more durably deployed as one component of a gene stack than alone.

CM1 and CO1 isolates are consistent with the presence of a single clonal lineage. CM1 and CO1, collected approximately three years apart from different commercial glasshouses, were identical across all 20 effector genes at the protein level. This identity across many independent loci in physically and temporally separated isolates indicates clonal spread of a single lineage rather than convergent independent mutations, consistent with the predominance of asexual reproduction in *F. fulva*. The ICMP 7320 isolate exhibited a distinct effector profile, indicating a separate lineage; whether the recent lineage displaced it, coexists with it, or represents a separate introduction cannot be resolved from three isolates alone.

One change is novel; the remainder have precedent in the literature. Of the non-synonymous changes present in the New Zealand isolates, only Ecp4 V127G was absent from all 21 surveyed papers and is reported here for the first time; its functional significance is unknown. The remaining substitutions occur at previously described positions, and the absence and truncation events align with well-documented routes of effector loss. Except for Ecp4 V127G, therefore, no individual change was

molecularly novel. Two features are nonetheless distinctive to New Zealand in the surveyed literature: Ecp4 V127G, which is novel outright; and complete deletion of the *Avr9B* locus, which — although deletion is itself a common mechanism — has to date been reported only in New Zealand strains, elsewhere being replaced by point or indel mutations (de la Rosa et al., 2024; Schol et al., 2025). Beyond these, the particular combination of changes carried by the recent clonal lineage was not described as a single profile in any of the surveyed sources, though each component change has international precedent.

The genome-sequencing results are consistent with independent prior data. For the one isolate previously genotyped at the effector loci (ICMP 7320), the whole-genome calls reproduced the PCR-amplicon results of Mesarich et al. (2018) across all nine genes examined in that study. They extended the characterisation of this strain to the *Avr* genes and to *Ecp4* for the first time. This cross-method concordance supports the reliability of the effector genotypes reported here.

The effectors recognised by the recently identified *Cf-Ecp* resistances are conserved in the New Zealand population, so those resistances are predicted to be effective. This is arguably the most directly applied finding of the study. The apoplastic effectors Ecp8, Ecp9-1, Ecp10-1, Ecp11-1, Ecp13, Ecp14-1, Ecp15, Ecp16 and Ecp17 — recognised, in wild tomato accessions, by the newly characterised *Cf-Ecp* resistances (*Cf-Ecp8*–*Cf-Ecp17*) — were intact and identical to the reference in all three isolates, and *Ecp12* was intact in the two currently circulating isolates (carrying a substitution only in the ICMP 7320 isolate). Because these effectors remain present and unmutated, the pathogen would still be recognised, and the corresponding *Cf-Ecp* resistances are therefore predicted to be effective against the sampled New Zealand population. The strong conservation of the Ecp effectors — here and in the wider literature — is consistent with these proteins being less dispensable to the pathogen than some Avr effectors, a property that, if confirmed, would make recognition of them comparatively durable and make them attractive deployment targets.

This effectiveness, however, is contingent and not guaranteed against future change or incursion. Variants of some of these effectors have been reported overseas — for example, Ecp11-1 (Phe119Val), Ecp14-1 (Lys148Glu) and Ecp12 (Gly124Arg)

(Mesarich et al., 2018) — none of which were present in the currently circulating New Zealand isolates. Critically, whether any of these variants actually abolishes recognition by its cognate *Cf-Ecp* resistance has not been determined: they are sequence variants of unknown functional consequence. Their existence nonetheless shows that these effectors *can* vary, and the incursion of an overseas strain carrying such an allele is a plausible route by which a deployed *Cf-Ecp* resistance could be challenged. The risk cannot be quantified without functional testing of these variants against the corresponding resistances, and this — together with border biosecurity to limit incursion — is an important direction for protecting any *Cf-Ecp* genes deployed in New Zealand.

On balance, pyramiding these resistances remains the most defensible strategy, and the biology of *F. fulva* strengthens rather than weakens that case. Given how readily *F. fulva* effectors mutate under selection, no single *Cf-Ecp* gene deployed alone should be expected to remain durable indefinitely. The pathogen's low level of sexual reproduction, however, is a decisive and favourable factor: because resistance-breaking mutations arising independently in different effectors cannot readily be combined into a single genotype through recombination, a largely clonal pathogen must accumulate every required mutation within one lineage, sequentially and independently, to defeat a pyramid — a substantially higher evolutionary barrier than overcoming genes one at a time. Pyramiding several *Cf-Ecp* genes that recognise conserved, likely-indispensable effectors therefore represents the most durable use of these new resistances. Two caveats temper this: even asexually, a large clonal population under sustained selection can accumulate escape mutations over time, as the sequential breakdown of the two-gene *Cf-9* (*Milky Way*) locus illustrates (de la Rosa et al., 2024); and incursion could import a strain in which multiple breaking mutations are already assembled. Pyramiding thus raises the barrier considerably but does not remove it, and is most effective when combined with diversified deployment, biosecurity, and ongoing molecular surveillance of the kind demonstrated here.

7.2. Limitations

The central limitation is that resistance breakdown was inferred from sequence data, not demonstrated; functional confirmation (inoculation assays of differential lines carrying different *Cf* resistance genes) was outside the scope of this study. The gene-absence calls (*Avr9*, *Avr9B*, *Avr4E*) rest on the effector not being detected in the genome assembly — that is, on absence of a matching sequence rather than on positive characterisation of a deletion — so they require confirmation of the deletion boundaries by targeted or long-read analysis to distinguish true loss from assembly gaps or divergent, unrecognised alleles. Furthermore, this study examined effector coding sequences only; promoter and other regulatory regions were not investigated, so changes affecting effector *expression* rather than protein sequence would not have been detected, and an effector scored as intact could in principle still be functionally altered through mis- or non-expression. With three isolates, the study supports description rather than population-level or temporal-trend inference. No mating-type data were generated for the sampled isolates, so questions of sexual reproduction and population structure remain open. Finally, the literature comparison rests on LLM-extracted metadata, which is a faithful record of the extraction rather than an independent reading of the primary sources and requires the stated verification.

A further limitation concerns Objective 3. Hypothesis 3 was originally framed as a testable statistical hypothesis regarding the relative effectiveness of different management strategies. However, this study did not collect grower-level management-practice data (e.g. spray programme composition, IPM adoption or other agronomic variables) linked to disease outcomes and no such analysis was undertaken. Therefore, Hypothesis 3 as originally stated could not be evaluated with the data collected here. The personal communications cited in section [6.6.] (A. Hutchinson; D. Cohen) are included as anecdotal industry perspectives on management effectiveness and disease severity and should not be read as evidence of a tested effect. Consequently, neither claim that management effectiveness has diminished nor that the pathogen has become more aggressive was assessed empirically within this study. Objective 3's contribution is therefore qualitative: the genomic and field findings are interpreted alongside the published literature to

generate applied recommendations rather than validated against a formally tested hypothesis.

7.3. Future Directions

The most immediate and tractable priorities are: functional validation of the predicted resistance-breaking changes — in particular the *Avr2* truncation and the Ecp4 V127G change — on the corresponding differential lines; deletion-boundary sizing for the *Avr9*, *Avr9B* and *Avr4E* absences to confirm the loss events and their extent; and mating-type locus typing of the sampled isolates, which is achievable from the existing genome assemblies and would directly address whether both mating types, and hence the potential for sexual recombination, are present in the New Zealand population. Broader sampling across glasshouses and time points would test whether the clonal lineage identified here is representative of the wider New Zealand population and would allow the temporal and epidemiological questions to be addressed with the statistical support that three isolates cannot provide.

8. References

Amitrano, C., Arena, C., Rouphael, Y., De Pascale, S., & De Micco, V. (2019). Vapour pressure deficit: The hidden driver behind plant morphofunctional traits in controlled environments. *Annals of Applied Biology*, *175*(3), 313–325. https://doi.org/10.1111/aab.12544

Australian Press Association New Zealand. (2012). Heinz to source Bay tomatoes after Oz exit. *The New Zealand Herald*. https://www.nzherald.co.nz/business/companies/manufacturing/heinz-to-source-bay-tomatoes-after-oz-exit/BIY5YI2HQVZXGLOIIYJMWALLQE/

Asano, S., Yoshida, K., & Hirayama, Y. (2024). Sensitivity of tomato leaf mould–causing *Fulvia fulva* to seven succinate dehydrogenase inhibitor (SDHI) fungicides in Nara Prefecture, Japan and high efficacy of isofetamid in controlling SDHI-resistant isolates. *Journal of Phytopathology*, *172*(1), e13243. https://doi.org/10.1111/jph.13243

Babadoost, M. (2011). Leaf mold (*Fulvia fulva*), a serious threat to high tunnel tomato production in Illinois. *Acta Horticulturae*, *914*, 87–90. https://doi.org/10.17660/ActaHortic.2011.914.14

Bahoch, S., Elaasri, A., Chafiki, S., Elame, F., Wifaya, A., Mayad, E. hassan, Bouharroud, R., & Qessaoui, R. (2025). Biocontrol potential of rhizobacteria against *Passalora fulva* and *Tuta absoluta*: A sustainable approach for tomato protection. *Plants*, *14*(17). https://doi.org/10.3390/plants14172672

Bayer Vegetables New Zealand. (2026a). *DR0603TC*. https://www.vegetables.bayer.com/nz/en-nz/products/tomato/details.html/tomato_dr0603tc_new_zealand_deruiter_all_high-tech_glasshouse_all.html

Bayer Vegetables New Zealand. (2026b). *DR0607TC*. https://www.vegetables.bayer.com/nz/en-nz/products/tomato/details.html/tomato_dr0607tc_new_zealand_deruiter_all_grehig_all.html

Bayer Vegetables New Zealand. (2026c). *Grandice*. https://www.vegetables.bayer.com/nz/en-nz/products/tomato/details.html/tomato_grandice_new_zealand_deruiter_fresh_market_grehig_all.html

Bayer Vegetables New Zealand. (2026d). *Marinice*. https://www.vegetables.bayer.com/nz/en-nz/products/tomato/details.html/tomato_marinice_new_zealand_deruiter_all_high-tech_glasshouse_all.html

Bayer Vegetables New Zealand. (2026e). *Merlice*. https://www.vegetables.bayer.com/nz/en-nz/products/tomato/details.html/tomato_merlice_new_zealand_deruiter_all_high-tech_glasshouse_all.html

Bernal-Cabrera, A., Martínez-Coca, B., Herrera-Isla, L., Ynfante-Martínez, D., Peteira-Delgado, B., Portal, O., Leiva-Mora, M., & de Wit, P. J. G. M. (2021). The first report on the occurrence race 9 of the tomato leaf mold pathogen *Cladosporium fulvum* (syn. *Passalora fulva*) in Cuba. *European Journal of Plant Pathology*, *160*(3), 731–736. https://doi.org/10.1007/s10658-021-02261-4

Bolton, M. D., van Esse, H. P., Vossen, J. H., de Jonge, R., Stergiopoulos, I., Stulemeijer, I. J. E., van den Berg, G. C. M., Borrás-Hidalgo, O., Dekker, H. L., de Koster, C. G., de Wit, P. J. G. M., Joosten, M. H. A. J., & Thomma, B. P. H. J. (2008). The novel *Cladosporium fulvum* lysin motif effector *Ecp6* is a virulence factor with orthologues

in other fungal species. *Molecular Microbiology*, *69*(1), 119–136. https://doi.org/10.1111/j.1365-2958.2008.06270.x

Cock, P. J. A., Antao, T., Chang, J. T., Chapman, B. A., Cox, C. J., Dalke, A., Friedberg, I., Hamelryck, T., Kauff, F., Wilczynski, B., & de Hoon, M. J. L. (2009). Biopython: Freely available Python tools for computational molecular biology and bioinformatics. *Bioinformatics*, *25*(11), 1422–1423. https://doi.org/10.1093/bioinformatics/btp163

Cohen, D. (2024). ToBRFV detected in Australia. *Tomatoes New Zealand*. https://www.tomatoesnz.co.nz/latest-news/tobrfv-detected-in-australia/ - :~:text=This is not currently in,employees between sites should stop

Colvin, S., Jolibois, E., Ramezani, H., Garcia Badaracco, A., Dorsey, T., Montague, D., Matveenko, S., Trylesinski, M., Runkle, S., & Hewitt, D. (2026). *Pydantic validation* (Version v2) [Computer software]. https://github.com/pydantic/pydantic

Cotter, A., Dracatos, P., Beddoe, T., & Johnson, K. (2024). Isothermal detection methods for fungal pathogens in closed environment agriculture. *Journal of Fungi*, *10*(12). https://doi.org/10.3390/jof10120851

Dearlove, E. L., Chandler, D., Edgington, S., Berry, S. D., Martin, G., Svendsen, C., & Hesketh, H. (2024). Improved control of *Trialeurodes vaporariorum* using mixture combinations of entomopathogenic fungi and the chemical insecticide spiromesifen. *Scientific Reports*, *14*(1), 15259. https://doi.org/10.1038/s41598-024-66051-8

De Boeck, H. J., De Groote, T., & Nijs, I. (2012). Leaf temperatures in glasshouses and open-top chambers. *New Phytologist*, *194*(4), 1155–1164. https://doi.org/10.1111/j.1469-8137.2012.04117.x

De la Rosa, S., Schol, C. R., Ramos Peregrina, Á., Winter, D. J., Hilgers, A. M., Maeda, K., Iida, Y., Tarallo, M., Jia, R., Beenen, H. G., Rocafort, M., de Wit, P. J. G. M., Bowen, J. K., Bradshaw, R. E., Joosten, M. H. A. J., Bai, Y., & Mesarich, C. H.

(2024). Sequential breakdown of the *Cf-9* leaf mould resistance locus in tomato by *Fulvia fulva*. *New Phytologist*, *243*(4), 1522–1538. https://doi.org/10.1111/nph.19925

de Wit, P. J. G. M. (2016). Cladosporium fulvum Effectors: Weapons in the Arms Race with Tomato. *Annual Review of Phytopathology*, *54*, 1–23. https://doi.org/10.1146/annurev-phyto-011516-040249

De Wit, P. J. G. M., van der Burgt, A., Ökmen, B., Stergiopoulos, I., Abd-Elsalam, K. A., Aerts, A. L., Bahkali, A. H., Beenen, H. G., Chettri, P., Cox, M. P., Datema, E., de Vries, R. P., Dhillon, B., Ganley, A. R., Griffiths, S. A., Guo, Y., Hamelin, R. C., Henrissat, B., Kabir, M. S., & Jashni, M. K. (2012). The genomes of the fungal plant pathogens *Cladosporium fulvum* and *Dothistroma septosporum* reveal adaptation to different hosts and lifestyles but also signatures of common ancestry. *PLOS Genetics*, *8*(11), 1–22. https://doi.org/10.1371/journal.pgen.1003088

Department of Agriculture, Fisheries and Forestry. (2024). *2024-54: Horticulture – Suspension of tomato exports to New Zealand*. Australian Government. https://www.agriculture.gov.au/biosecurity-trade/export/controlled-goods/plants-plant-products/ian/2024/2024-54

Dixon, M. S., Jones, D. A., Keddie, J. S., Thomas, C. M., Harrison, K., & Jones, J. D. G. (1996). The Tomato *Cf-2* Disease resistance locus comprises two functional genes encoding leucine-rich repeat proteins. *Cell*, *84*(3), 451–459. https://doi.org/10.1016/S0092-8674(00)81290-8

Doyle, J. J., & Doyle, J. L. (1987). A rapid DNA isolation procedure for small quantities of fresh leaf tissue. *Phytochemical Bulletin*, *19*, 11–15. https://worldveg.tind.io/record/33886/

Du, J., & Vleeshouwers, V. G. A. A. (2014). The do's and don'ts of effectoromics. *Methods in Molecular Biology*, *1127*, 257–268. https://doi.org/10.1007/978-1-62703-986-4_19

Energy Efficiency & Conservation Authority. (2026). *Innovative technology for transition to a low-carbon greenhouse industry*. Energy Efficiency & Conservation Authority - EECA. https://www.eeca.govt.nz/assets/EECA-Resources/Co-funding/technology-scan-for-TomatoesNZ_innovative-technology-for-transition-to-a-low-carbon-greenhouse-industry.pdf

Enya, J., Ikeda, K., Takeuchi, T., Horikoshi, N., Higashi, T., Sakai, T., Iida, Y., Nishi, K., & Kubota, M. (2009). The first occurrence of leaf mold of tomato caused by races 4.9 and 4.9.11 of *Passalora fulva* (syn. *Fulvia fulva*) in Japan. *Journal of General Plant Pathology*, *75*(1), 76–79. https://doi.org/10.1007/s10327-008-0134-0

Enza Zaden New Zealand. (n.d.). *Tomato*. https://www.enzazaden.com/nz/products-and-services/our-local-varieties/tomato

Feix, A. S., Cruz-Bustos, T., Ruttkowski, B., & Joachim, A. (2023). *In vitro* cultivation methods for coccidian parasite research. *International Journal for Parasitology, ApicoWplexa 2022: 6th International Meeting on Apicomplexan Parasites in Farm Animals*, *53*(9), 477–489. https://doi.org/10.1016/j.ijpara.2022.10.002

Flor, H. H. (1971). Current status of the gene-for-gene concept. *Annual Review of Phytopathology*, *9* (Volume 9, 1971), 275–296. https://doi.org/10.1146/annurev.py.09.090171.001423

Gül, E., Karakaya, A., & Ergül, A. (2024). The race distribution of the *Fulvia fulva* populations and mutations in the *Avr* genes in Turkey. *Journal of Phytopathology*, *172*(1), e13273. https://doi.org/10.1111/jph.13273

Gullino, M. L., Pugliese, M., Gilardi, G., & Garibaldi, A. (2018). Effect of increased CO_2 and temperature on plant diseases: A critical appraisal of results obtained in studies carried out under controlled environment facilities. *Journal of Plant Pathology*, *100*(3), 371–389. https://doi.org/10.1007/s42161-018-0125-8

Hane, J. K., Paxman, J., Jones, D. A. B., Oliver, R. P., & de Wit, P. (2020). "CATAStrophy," a Genome-informed trophic classification of filamentous plant pathogens – how many different types of filamentous plant pathogens are there? *Frontiers in Microbiology*, *10*. https://doi.org/10.3389/fmicb.2019.03088

Heuvelink, E., & Dorais, M. (2005). Crop growth and yield. In E. Heuvelink (Ed.), *Tomatoes* (pp. 85–144). CABI Publishing. https://doi/10.1079/9780851993966.0085

Holliday, P., & Mulder, J. (1976). *Fulvia fulva*. [Descriptions of fungi and bacteria]. *Descriptions of Fungi and Bacteria*, (49), Sheet-487. https://doi.org/10.1079/DFB/20056400487

Horticulture New Zealand. (2021). *Reforming industrial allocation in the New Zealand Emissions Trading Scheme*. https://www.hortnz.co.nz/assets/Environment/National-Env-Policy/Climate-Change/HortNZ-submission-on-ETS-IA-review-17-Sept-2021.pdf

Horticulture New Zealand. (2024). *Submission on proposed regulatory regime for carbon capture, utilisation and storage*. Ministry of Business, Innovation & Employment. https://www.mbie.govt.nz/dmsdocument/30452-horticulture-nz-proposed-regulatory-regime-for-carbon-capture-utilisation-storage-submission-pdf

Hunter, J. D. (2007). Matplotlib: A 2D graphics environment. *Computing in Science & Engineering*, *9*(3), 90–95. https://doi.org/10.1109/MCSE.2007.55

Iida, Y., Iwadate, Y., Kubota, M., & Terami, F. (2010). Occurrence of a new race 2.9 of leaf mold of tomato in Japan. *Journal of General Plant Pathology*, *76*(1), 84–86. https://doi.org/10.1007/s10327-009-0207-8

Iida, Y., van't Hof, P., Beenen, H., Mesarich, C., Kubota, M., Stergiopoulos, I., Mehrabi, R., Notsu, A., Fujiwara, K., Bahkali, A., Abd-Elsalam, K., Collemare, J., & de Wit, P. J. G. M. (2015). Novel mutations detected in avirulence genes overcoming tomato *Cf* resistance genes in isolates of a japanese population of *Cladosporium fulvum*. *PLOS ONE*, *10*(4), e0123271. https://doi.org/10.1371/journal.pone.0123271

Jones, J. D. G., & Dangl, J. L. (2006). The plant immune system. *Nature*, *444*(7117), 323–329. https://doi.org/10.1038/nature05286

Jones, J. B., Jones, J. P., Stall, R. E., & Zitter, T. A. (Eds.). (1991). *Compendium of tomato diseases*. APS Press. https://www.cabidigitallibrary.org/doi/full/10.5555/19912313548

Jones, D. A., Thomas, C. M., Hammond-Kosack, K. E., Balint-Kurti, P. J., & Jones, J. D. (1994). Isolation of the tomato *Cf-9* gene for resistance to *Cladosporium fulvum* by transposon tagging. *Science*, *266*(5186), 789–793. https://doi.org/10.1126/science.7973631

Jones, D., Dickinson, M., Balint-Kurti, P., Dixon, M., & Jones, J. (1993). Two complex resistance loci revealed in tomato by classical and RFLP mapping of the *Cf-2*, *Cf-4*, *Cf-5*, and *Cf-9* genes for resistance to *Cladosporium fulvum*. *Molecular Plant-Microbe Interactions - MPMI*, *6*, 348–348. https://10.1094/MPMI-6-348

Katoh, K., & Standley, D. M. (2013). MAFFT Multiple Sequence Alignment Software version 7: improvements in performance and usability. *Molecular Biology and Evolution*, *30*(4), 772–780. https://doi.org/10.1093/molbev/mst010

Kawaguchi, A., & Suenaga-Kanetani, H. (2014). Spatiotemporal distribution of tomato plants naturally infected with leaf mold in commercial greenhouses. *Journal of General Plant Pathology*, *80*(5), 430–434. https://doi.org/10.1007/s10327-014-0539-x

Koukounaras, A. (Ed.). (2021). *Advanced Greenhouse Horticulture*. Multidisciplinary Digital Publishing Institute - MDPI. https://doi.org/10.3390/books978-3-0365-0351-6

Kubota, M., Morishima, M., & Iida, Y. (2015). First occurrence of tomato leaf mold caused by the novel races 2.5.9 and 4.5.9 of *Passalora fulva* in Japan. *Journal of General Plant Pathology*, *81*(4), 320–323. https://doi.org/10.1007/s10327-015-0592-0

Kruijt, M., DE Kock, M. J. D., & de Wit, P. J. G. M. (2005). Receptor-like proteins involved in plant disease resistance. *Molecular Plant Pathology*, *6*(1), 85–97. https://doi.org/10.1111/j.1364-3703.2004.00264.x

Laugé, R., Dmitriev, A. P., Joosten, M. H. A. J., & De Wit, P. J. G. M. (1998). Additional resistance gene(s) against *Cladosporium fulvum* present on the *Cf-9* introgression segment are associated with strong PR protein accumulation. *Molecular Plant-Microbe Interactions - MPMI*, *11*(4), 301–308. https://doi.org/10.1094/MPMI.1998.11.4.301

Laugé, R., Goodwin, P. H., de Wit, P. J., & Joosten, M. H. (2000). Specific HR-associated recognition of secreted proteins from *Cladosporium fulvum* occurs in both host and non-host plants. *The Plant Journal: For Cell and Molecular Biology*, *23*(6), 735–745. https://doi.org/10.1046/j.1365-313x.2000.00843.x

Lazar, N., Mesarich, C. H., Petit-Houdenot, Y., Talbi, N., Li de la Sierra-Gallay, I., Zélie, E., Blondeau, K., Gracy, J., Ollivier, B., Blaise, F., Rouxel, T., Balesdent, M.-H., Idnurm, A., van Tilbeurgh, H., & Fudal, I. (2022). A new family of structurally conserved fungal effectors displays epistatic interactions with plant resistance proteins. *PLOS Pathogens*, *18*(7), 1–27. https://doi.org/10.1371/journal.ppat.1010664

Li, G., Tang, L., Zhang, X., Dong, J., & Xiao, M. (2018). Factors affecting greenhouse microclimate and its regulating techniques: A review. *IOP Conference Series: Earth and Environmental Science*, *167*(1), 012019. https://doi.org/10.1088/1755-1315/167/1/012019

Li, S., Zhao, T., Li, H., Xu, X., & Li, J. (2015). First report of races 2.5 and 2.4.5 of *Cladosporium fulvum* (syn. *Passalora fulva*), causal fungus of tomato leaf mold disease in China. *Journal of General Plant Pathology*, *81*(2), 162–165. https://doi.org/10.1007/s10327-015-0577-z

Liao, C.-J., Hailemariam, S., Sharon, A., & Mengiste, T. (2022). Pathogenic strategies and immune mechanisms to necrotrophs: Differences and similarities to biotrophs and hemibiotrophs. *Current Opinion in Plant Biology*, *69*, 102291. https://doi.org/10.1016/j.pbi.2022.102291

Lucentini, C. G., Medina, R., Franco, M. E. E., Saparrat, M. C. N., & Balatti, P. A. (2021). *Fulvia fulva* [syn. *Cladosporium fulvum*, *Passalora fulva*] races in Argentina are evolving through genetic changes and carry polymorphic *avr* and *ecp* gene sequences. *European Journal of Plant Pathology: Published in Cooperation with the European Foundation for Plant Pathology*, 1–18. https://doi.org/10.1007/s10658-020-02181-9

Luderer, R., Takken, F. L. W., de Wit, P. J. G. M., & Joosten, M. H. A. J. (2002). *Cladosporium fulvum* overcomes Cf-2-mediated resistance by producing truncated AVR2 elicitor proteins. *Molecular Microbiology*, *45*(3), 875–884. https://doi.org/10.1046/j.1365-2958.2002.03060.x

Merilo, E., Yarmolinsky, D., Jalakas, P., Parik, H., Tulva, I., Rasulov, B., Kilk, K., & Kollist, H. (2018). Stomatal VPD response: There is more to the story than ABA. *Plant Physiology*, *176*(1), 851–864. https://doi.org/10.1104/pp.17.00912

Mesarich, C. H., Barnes, I., Bradley, E. L., de la Rosa, S., de Wit, P. J. G. M., Guo, Y., Griffiths, S. A., Hamelin, R. C., Joosten, M. H. A. J., Lu, M., McCarthy, H. M., Schol, C. R., Stergiopoulos, I., Tarallo, M., Zaccaron, A. Z., & Bradshaw, R. E. (2023). Beyond the genomes of *Fulvia fulva* (syn. *Cladosporium fulvum*) and *Dothistroma septosporum*: New insights into how these fungal pathogens interact with their host plants. *Molecular Plant Pathology*, *24*(5), 474–494. https://doi.org/10.1111/mpp.13309

Mesarich, C. H., Griffiths, S. A., van der Burgt, A., Ökmen, B., Beenen, H. G., Etalo, D. W., Joosten, M. H. A. J., & de Wit, P. J. G. M. (2014). transcriptome sequencing uncovers the *Avr5* Avirulence gene of the tomato leaf mold pathogen *Cladosporium fulvum*. *Molecular Plant-Microbe Interactions - MPMI*, *27*(8), 846–857. https://doi.org/10.1094/MPMI-02-14-0050-R

Mesarich, C. H., Ökmen, B., Rovenich, H., Griffiths, S. A., Wang, C., Karimi Jashni, M., Mihajlovski, A., Collemare, J., Hunziker, L., Deng, C. H., van der Burgt, A., Beenen, H. G., Templeton, M. D., Bradshaw, R. E., & de Wit, P. J. G. M. (2018). Specific hypersensitive response–associated recognition of new apoplastic effectors from *Cladosporium fulvum* in wild tomato. *Molecular Plant-Microbe Interactions - MPMI*, *31*(1), 145–162. https://doi.org/10.1094/MPMI-05-17-0114-FI

Meyer, U., & Gärber, U. (2021). Bestimmung der in Deutschland vorkommenden pathotypen des erregers der samtfleckenkrankheit an tomate, *Fulvia fulva*. *Journal für Kulturpflanzen*, *73*(1–2). https://doi.org/10.5073/JfK.2021.01-02.04

Ministry for Primary Industries. (2024). *Biosecurity New Zealand takes action in response to Australia tomato virus find* [Press release]. https://www.mpi.govt.nz/news/media-releases/biosecurity-new-zealand-takes-action-in-response-to-australia-tomato-virus-find

Möller, E. M., Bahnweg, G., Sandermann, H., & Geiger, H. H. (1992). A simple and efficient protocol for isolation of high molecular weight DNA from filamentous fungi, fruit bodies, and infected plant tissues. *Nucleic Acids Research*, *20*(22), 6115–6116. https://doi.org/10.1093/nar/20.22.6115

National Center for Biotechnology Information. (2016). *Passalora fulva isolate PT1 18S ribosomal RNA gene, partial sequence; internal transcribed spacer 1, 5.8S ribosomal RNA gene, and internal transcribed spacer 2, complete sequence; and 28S ribosomal RNA gene, partial sequence* (GenBank Accession No. KX943038). U.S. National Library of Medicine. https://www.ncbi.nlm.nih.gov/nuccore/KX943038

Neo, D. C. J., Ong, M. M. X., Lee, Y. Y., Teo, E. J., Ong, Q., Tanoto, H., Xu, J., Ong, K. S., & Suresh, V. (2022). Shaping and tuning lighting conditions in controlled environment agriculture: a review. *ACS Agricultural Science & Technology*, *2*(1), 3–16. https://doi.org/10.1021/acsagscitech.1c00241

Nichols, M. A., & Bussel, W. T. (1980). The History of Process Tomato Production in New Zealand. *Acta Hortic.*, (100), 71–74. https://doi.org/10.17660/ActaHortic.1980.100.9

Novak, A., Ćosić, J., Vrandečić, K., Jurković, D., Plavec, J., Križanac, I., & Ivić, D. (2021). Characterization of tomato leaf mould pathogen, *Passalora fulva*, in Croatia. *Journal of Plant Diseases and Protection*, *128*(4), 1041–1049. https://doi.org/10.1007/s41348-020-00419-6

Novak, A., Kajić, V., & Masten Milek, T. (2011). Distribution of tomato leaf mold (*Passalora fulva* (Cooke) U. Braun and Crous, syn. *Cladosporium Fulvum*) in Croatia. *Acta Horticulturae*, (914), 117–119. https://doi.org/10.17660/ActaHortic.2011.914.20

Ökmen, B., Bachmann, D., & de Wit, P. J. G. M. (2019). A conserved GH17 glycosyl hydrolase from plant pathogenic Dothideomycetes releases a DAMP causing cell death in tomato. *Molecular Plant Pathology*, *20*(12), 1710–1721. https://doi.org/10.1111/mpp.12872

Parniske, M., Hammond-Kosack, K. E., Golstein, C., Thomas, C. M., Jones, D. A., Harrison, K., Wulff, B. B., & Jones, J. D. (1997). Novel disease resistance specificities result from sequence exchange between tandemly repeated genes at the *Cf-4/9* locus of tomato. *Cell*, *91*(6), 821–832. https://doi.org/10.1016/S0092-8674(00)80470-5

Paull, RobertE. (1999). Effect of temperature and relative humidity on fresh commodity quality. *Postharvest Biology and Technology*, *15*(3), 263–277. https://doi.org/10.1016/S0925-5214(98)00090-8

Pei, T., Hao, A., Lu, M., Zhang, H., Li, D., Xu, X., & Zhao, T. (2026). Fine mapping and functional verification of the Cf-19 gene controlling leaf mold disease resistance in tomato. *Theoretical and Applied Genetics*, *139*(4), 95. https://doi.org/10.1007/s00122-026-05203-y

Richard, B., Qi, A., & Fitt, B. D. L. (2022). Control of crop diseases through Integrated Crop Management to deliver climate-smart farming systems for low- and high-input crop production. *Plant Pathology*, *71*(1), 187–206. https://doi.org/10.1111/ppa.13493

Rivas, S., & Thomas, C. M. (2005). Molecular interactions between tomato and the leaf mold pathogen Cladosporium fulvum. *Annual Review of Phytopathology*, *43*, 395–436. https://doi.org/10.1146/annurev.phyto.43.040204.140224

Rooney, H. C., Van't Klooster, J. W., Van Der Hoorn, R. A., Joosten, M. H., Jones, J. D., & de Wit, P. J. (2005). Cladosporium Avr2 inhibits tomato Rcr3 protease required for Cf-2-dependent disease resistance. *Science*, *308*(5729), 1783–1786. https://doi.org/10.1126/science.1111404

Sievers, F., Wilm, A., Dineen, D., Gibson, T. J., Karplus, K., Li, W., Lopez, R., McWilliam, H., Remmert, M., Söding, J., Thompson, J. D., & Higgins, D. G. (2011). Fast, scalable generation of high-quality protein multiple sequence alignments using Clustal Omega. *Molecular Systems Biology*, *7*, 539. https://doi.org/10.1038/msb.2011.75

Soumpourou, E., Iakovidis, M., Chartrain, L., Lyall, V., & Thomas, C. M. (2007). The Solanum pimpinellifolium Cf-ECP1 and Cf-ECP4 genes for resistance to Cladosporium fulvum are located at the Milky Way locus on the short arm of chromosome 1. *TAG. Theoretical and Applied Genetics. Theoretische Und Angewandte Genetik*, *115*(8), 1127–1136. https://doi.org/10.1007/s00122-007-0638-6

Stanghellini, C., van 't Ooster, A., & Heuvelink, E. (2019). *Greenhouse horticulture: Technology for optimal crop production*. Wageningen Academic Publishers. https://research.wur.nl/en/publications/greenhouse-horticulture-technology-for-optimal-crop-production-2/

Steele, M. (2025). Wattie's NZ taking fewer tomatoes, corn, beetroot until demand increases. *Radio New Zealand*. https://www.rnz.co.nz/news/country/575996/wattie-s-nz-taking-fewer-tomatoes-corn-beetroot-until-demand-increases

Stergiopoulos, I., Groenewald, M., Staats, M., Lindhout, P., Crous, P. W., & De Wit, P. J. G. M. (2007). Mating-type genes and the genetic structure of a world-wide collection of the tomato pathogen *Cladosporium fulvum*. *Fungal Genetics and Biology*, *44*(5), 415–429. https://doi.org/10.1016/j.fgb.2006.11.004

Sudermann, M. A., McGilp, L., Vogel, G., Regnier, M., Jaramillo, A. R., & Smart, C. D. (2022). The diversity of *Passalora fulva* isolates collected from tomato plants in U.S. high tunnels. *Phytopathology*, *112*(6), 1350–1360. https://doi.org/10.1094/PHYTO-06-21-0244-R

Syngenta. (2026). *Tomato/tomaten brochure 2026*. https://www.syngentavegetables.com/sites/g/files/kgtney786/files/media/document/2025/09/18/Syngenta%20Tomaten%20brochure%202026_NL_EN.pdf

Tarallo, M., McDougal, R. L., Chen, Z., Wang, Y., Bradshaw, R. E., & Mesarich, C. H. (2022). Characterization of two conserved cell death elicitor families from the Dothideomycete fungal pathogens *Dothistroma septosporum* and *Fulvia fulva* (syn. *Cladosporium fulvum*). *Frontiers in Microbiology*, *13*, 964851. https://doi.org/10.3389/fmicb.2022.964851

Terranova Seeds New Zealand. (2026a). *ENDEAVOUR RZ*. https://terranovaseeds.co.nz/product-range/product/endeavour-rz/

Terranova Seeds New Zealand. (2026b). *GLORIETTE RZ*. https://terranovaseeds.co.nz/product-range/product/gloriette-rz/

Terranova Seeds New Zealand. (2026c). *SANTIANA RZ*. https://terranovaseeds.co.nz/product-range/product/santiana-rz/

Terranova Seeds New Zealand. (2026d). *SASSARI RZ*. https://terranovaseeds.co.nz/product-range/product/sassari-rz/

Thomma, B. P. H. J., Van Esse, H. P., Crous, P. W., & De Wit, P. J. G. M. (2005). *Cladosporium fulvum* (syn. *Passalora fulva*), a highly specialized plant pathogen as a model for functional studies on plant pathogenic *Mycosphaerellaceae*. *Molecular Plant Pathology*, *6*(4), 379–393. https://doi.org/10.1111/j.1364-3703.2005.00292.x

Tomatoes New Zealand. (2021). *Technology scan: Innovative technology for transition to a low-carbon greenhouse industry*. https://www.tomatoesnz.co.nz/dmsdocument/259-technscan-9jul21-fin-e-compressed-pdf

Tomatoes New Zealand. (2021). *Annual report*. https://www.tomatoesnz.co.nz/assets/TNZ-Annual-Report-2021-WEB-SP-Compressed.pdf

Tomatoes New Zealand. (2023). *Key Concerns*. https://www.tomatoesnz.co.nz/dmsdocument/289-tnz-key-concerns-2023-update-pdf

Tomatoes New Zealand. (2025). *Annual report & AGM Papers 2025*. https://www.tomatoesnz.co.nz/dmsdocument/404-tnz-2025-annual-report-web-dp-pdf

Tomatoes New Zealand.(2026a). *Industry overview*. https://www.tomatoesnz.co.nz/industry/industry-overview/

Tomatoes New Zealand. (2026b). *Industry statistics: Export data*. https://www.tomatoesnz.co.nz/industry/statistics/

Tomatoes New Zealand. 2026c). *Latest briefing on Pepino Mosaic Virus and ToBRFV*. https://www.tomatoesnz.co.nz/latest-news/latest-briefing-on-pepino-mosaic-virus-and-tobrfv/

Tomatoes New Zealand. (2026d). *Statistics*. https://www.tomatoesnz.co.nz/industry/statistics/

Tomatoes New Zealand. (2026e). *Tomatoes NZ representing commercial fresh tomato growers in New Zealand*. https://www.tomatoesnz.co.nz/

Torres, D. E., Oggenfuss, U., Croll, D., & Seidl, M. F. (2020). Genome evolution in fungal plant pathogens: Looking beyond the two-speed genome model. *Fungal Biology Reviews*, *34*(3), 136–143. https://doi.org/10.1016/j.fbr.2020.07.001

Te Puni Kōkiri - Tupu. (2026). *Growing covered tomato crops in NZ*. https://www.tupu.nz/en/fact-sheets/tomatoes-covered-cropping/

United States Department of Agriculture - Foreign Agricultural Service. (2025). *Retail foods annual – Wellington, New Zealand (NZ2025-0012)*. https://apps.fas.usda.gov/newgainapi/api/Report/DownloadReportByFileName?fileName=Retail%20Foods%20Annual_Wellington_New%20Zealand_NZ2025-0012.pdf

Van der Beek, J., Verkerk, R., Zabel, P., & Lindhout, P. (1992). Mapping strategy for resistance genes in tomato based on RFLPs between cultivars: *Cf9* (resistance to *Cladosporium fulvum*) on chromosome 1. *Theoretical and Applied Genetics*, *84*(1), 106–112. https://doi.org/10.1007/BF00223988

Van den Burg, H. A., Harrison, S. J., Joosten, M. H. A. J., Vervoort, J., & de Wit, P. J. G. M. (2006). Cladosporium fulvum *Avr4* protects fungal cell walls against hydrolysis by plant chitinases accumulating during infection. *Molecular Plant-Microbe Interactions - MPMI*, *19*(12), 1420–1430. https://doi.org/10.1094/MPMI-19-1420

Van Esse, H. P., Bolton, M. D., Stergiopoulos, I., de Wit, P. J. G. M., & Thomma, B. P. H. J. (2007). The chitin-binding *Cladosporium fulvum* effector protein *Avr4* is a virulence factor. *Molecular Plant-Microbe Interactions - MPMI*, *20*(9), 1092–1101. https://doi.org/10.1094/MPMI-20-9-1092

Van Esse, H. P., Thomma, B. P. H. J., van 't Klooster, J. W., & de Wit, P. J. G. M. (2006). Affinity-tags are removed from *Cladosporium fulvum* effector proteins expressed in the tomato leaf apoplast. *Journal of Experimental Botany*, *57*(3), 599–608. https://doi.org/10.1093/jxb/erj044

Van Esse, H. P., Van't Klooster, J. W., Bolton, M. D., Yadeta, K. A., Van Baarlen, P., Boeren, S., Vervoort, J., De Wit, P. J. G. M., & Thomma, B. P. H. J. (2008). The *Cladosporium fulvum* virulence protein Avr2 inhibits host proteases required for basal defense. *Plant Cell*, *20*(7), 1948–1963. https://doi.org/10.1105/tpc.108.059394

Van Kan, J. A., Van den Ackerveken, G., & De Wit, P. (1991). Cloning and characterization of cDNA of avirulence gene *avr9* of the fungal pathogen *Cladosporium fulvum*, causal agent of tomato leaf mold. *Molecular Plant-Microbe Interactions - MPMI*, *4*(1), 52–59. https://doi.org/10.1094/mpmi-4-052

Veronesi, E. R., Saville, D. J., van Koten, C., Wratten, S. D., & Goldson, S. L. (2022). Potential of the mirid bug, *Engytatus nicotianae*, for the biological control of the tomato-potato psyllid in greenhouses. *Crop Protection*, *156*, 105941. https://doi.org/10.1016/j.cropro.2022.105941

Veronesi, E. R., Wratten, S. D., van Koten, C., & Goldson, S. L. (2025). Potential of the mirid bug *Engytatus nicotianae*, and the parasitic wasp *Tamarixia triozae* for the biological control of the tomato-potato psyllid; a cage greenhouse assay. *New Zealand Journal of Crop and Horticultural Science*, *53*(1), 155–162. https://doi.org/10.1080/01140671.2022.2152843

Videira, S. I. R., Groenewald, J. Z., Nakashima, C., Braun, U., Barreto, R. W., de Wit, P. J. G. M., & Crous, P. W. (2017). *Mycosphaerellaceae*—chaos or clarity? *Studies in Mycology*, *87*, 257–421. https://doi.org/10.1016/j.simyco.2017.09.003

Vogrincic, S. (2024). *A crop on the cusp of ruin by leaf mould and the return of psyllid yellows*. Grower2Grower. https://www.grower2grower.co.nz/a-crop-on-the-cusp-of-ruin-by-leaf-mould-and-the-return-of-psyllid-yellows/

Vogrincic, S. (2026). *Combating leaf mould and powdery mildew in greenhouse tomatoes 2026*. Grower2Grower. https://www.grower2grower.co.nz/combating-leaf-mould-and-powdery-mildew-in-greenhouse-tomatoes-2026/

Vogrincic, S. (2018). *February, the weather bombs*. Grower2Grower. https://www.grower2grower.co.nz/february-the-weather-bombs/

Vogrincic, S. (2020). *Leaf Mould – Cladosporium*. Grower2Grower. https://www.grower2grower.co.nz/leaf-mould-cladosporium/

Watanabe, H., Horinouchi, H., Muramoto, Y., & Ishii, H. (2017). Occurrence of azoxystrobin-resistant isolates in *Passalora fulva*, the pathogen of tomato leaf mould disease. *Plant Pathology*, *66*(9), 1472–1479. https://doi.org/10.1111/ppa.12701

Westerink, N., Brandwagt, B. F., De Wit, P. J. G. M., & Joosten, M. H. A. J. (2004). *Cladosporium fulvum* circumvents the second functional resistance gene homologue at the *Cf-4* locus *(Hcr9-4E*) by secretion of a stable avr4E isoform. *Molecular Microbiology*, *54*(2), 533–545. https://doi.org/10.1111/j.1365-2958.2004.04288.x

Wulff, B. B. H., Chakrabarti, A., & Jones, D. A. (2009). Recognitional specificity and evolution in the tomato-*Cladosporium fulvum* pathosystem. *Molecular Plant-Microbe Interactions - MPMI*, *22*(10), 1191–1202. https://doi.org/10.1094/MPMI-22-10-1191

Yoshida, K., Asano, S., Sushida, H., & Iida, Y. (2021). Occurrence of tomato leaf mold caused by novel race 2.4.9 of *Cladosporium fulvum* in Japan. *Journal of General Plant Pathology*, *87*(1), 35–38. https://doi.org/10.1007/s10327-020-00963-x

Zaccaron, A. Z., Chen, L.-H., Samaras, A., & Stergiopoulos, I. (2022). A chromosome-scale genome assembly of the tomato pathogen *Cladosporium fulvum* reveals a compartmentalized genome architecture and the presence of a dispensable chromosome. *Microbial Genomics*, *8*(4), 000819. https://doi.org/10.1099/mgen.0.000819

Zhang, X., Liu, H., Xie, X., Sun, M., Du, N., & Xue, D. (2025). Physiological and transcriptomic analysis of tomato leaf mold resistance gene *Cf-12* against *Cladosporium fulvum*. *Physiological and Molecular Plant Pathology*, *138*, 102692. https://doi.org/10.1016/j.pmpp.2025.102692

Appendix I: Tomato Leaf Mould Sampling Guidelines

Tomato Leaf Mould Sampling Guidelines

Sampling Kit:

- Resealable plastic bag x 3
- Disposable gloves x 6
- Hand sanitiser x 1
- Sampling form x 3
- Prepaid Postage Bag x 1

Important:

- **ONE SAMPLING BAG, ONE CULTIVAR.** Use one bag to sample the same cultivar (or area containing the cultivar). Avoid mixing leaves from different cultivars/areas in the same bag.
- **SANITISE HANDS BETWEEN AREAS OR CULTIVARS.**
- **PLEASE, SEND THE SAMPLES WITHIN 3 DAYS OF COLLECTION**. If samples cannot be dispatched the same day, keep the bags open and separated from each other, in a well-ventilated area to allow leaves to dry.

Sampling Steps:

1. Thoroughly **wash your hands** before sampling.
2. Identify an area within your glasshouse with clear Leaf Mould symptoms.
3. Check **ONLY** the lower canopy (bottom leaves) and select 1 to 3 leaves with clear Leaf Mould symptoms. Leaves from the same area could come from the same plant or neighbour plants within 5 m.
4. Put your **disposable gloves** on and rub the **hand sanitiser** across your covered hands juts before removing the selected leaves.
5. Remove the whole leaf (breaking it from the main stem) and place it into one Resealable plastic bag. Purge some air and seal the bag.
6. Complete the **Sampling Form** and place it into the **resealable plastic bag** together with the leaves.
7. **DISCARD** your Disposable gloves and thoroughly wash your hands or use the Hand sanitiser.
8. If more than 1 cultivar or area is sampled, repeat steps 3 to 7.

Questions? Please contact Francis Ferrada-Hartley / **mob**: 022 647 6548 or 021 227 8411 / **email**: francisco.ferradasotelo.1@uni.massey.ac.nz

Appendix II: Leaf Mould (*Fulvia fulva*) 2024 Project Symptoms Guideline

TE KUNENGA KI PŪREHUROA MASSEY UNIVERSITY

TomatoesNZ

What do Leaf Mould symptoms look like?

The underside of the leaf:

Check for olive-greenish to brown velvety spots of mould.

Spots of mould may also be white.



Leaf surface:

Diffused green-yellowish spots on the early infection, turning into yellow as the disease progresses.



Which part of the crop to scout?

Lower canopy, as the oldest leaves are first infected.

Questions? Please contact Francis Ferrada-Hartley / **mob**: 022 647 6548 or 021 227 8411 / **email**: francisco.ferradasotelo.1@uni.massey.ac.nz

Appendix III: Factsheet – Tomato Leaf Mould

FACTSHEET

TomatoesNZ

Tomato Leaf Mould

Species: *Fulvia fulva* (ex *Cladosporium fulvum*)

Description

Tomato leaf mould disease, caused by the fungus *Fulvia fulva*, mainly affects glasshouse tomatoes.

Leaf mould disease almost exclusively affects the leaves, causing indirect yield losses. However, on rare occasions, the disease can also affect fruits, blossoms, and stems. In this case, there is a direct loss in yield.

Symptoms

What does the disease look like?

The disease presents itself as velvety olive-green to brown spots of mould on the underside of the leaf.

Diffuse light-yellow spots are often visible on the upper and lower leaf surfaces during early infection by the fungus. These spots frequently turn more yellow as the disease progresses.

Which part of the crop is affected?

The disease is predominantly found on the lower leaf canopy, as the oldest leaves are typically infected first.

Disease Facts

How is the disease spread?

The spores of the fungus spread from plant to plant (leaf to leaf) by overhead irrigation or spray, wind, workers, tools and possibly insects.

What conditions favour disease?

Development of the disease is favoured when relative humidity is at 85% or higher.

Management

What are the options?

- Open canopy to increase airflow.
- Remove affected leaves.
- Consider the removal of severely affected plants and surrounding plants.
- Dispose of all infected plant material.
- Clean and sterilise tools and equipment used in the glasshouse.
- Avoid cross-contamination between infected and healthy crops.
- Use chemical fungicides.
- If possible, adjust environmental settings to: increase ventilation and maintain RH below 85%.
- Maintain a higher glasshouse temperature than outside to avoid condensation on leaves.

What about resistant varieties?

Plant leaf mould-resistant tomato varieties (denomination Pf:A-E or Ff:A-E) whenever possible. This may reduce the incidence of the disease. However, infection may still occur, since resistant varieties are only effective against selected races of the fungus.





Figures 1, 2 and 3: Tomato leaf mould symptoms on the leaf's underside. Photo: Francis Ferrada-Hartley.





Figure 4: Tomato leaf mould symptoms on the leaf's upper side. Photo: Francis Ferrada-Hartley.

In collaboration with:

TE KUNENGA KI PŪREHUROA
MASSEY UNIVERSITY

Information compiled by Francis Ferrada-Hartley,
francisco.ferradaortelo.1@massey.ac.nz

For further questions, please contact the author of this factsheet or Tomatoes NZ

Appendix IV: Leaf Mould (*Fulvia fulva*) 2024 Project Sampling Form

TE KUNENGA KI PŪREHUROA MASSEY UNIVERSITY

TomatoesNZ

Leaf Mould (*Fulvia fulva*) 2024 Project

Sampling Form

(Please complete and attach a copy of this form with each submitted sample).

Date of sampling		
Sampling location (e.g., City, Region)		
Cultivar name		
Crop age (weeks)		
Crop developmental stage (Please select one)	Seedling	
	Vegetative/growing phase	
	Early production phase	
	Mid production phase	
	Late production phase	
	End of the crop	

PLEASE, SEND THE SAMPLES WITHIN 3 DAYS OF COLLECTION. If samples cannot be dispatched the same day, keep the bags open and separated from each other, in a well-ventilated area to allow leaves to dry.

Would you like to be acknowledged for supporting this research?
Please provide the following information:

Name: _____

Company: _____

Questions? Please contact Francis Ferrada-Hartley / **mob**: 022 647 6548 or 021 227 8411 / **email**: francisco.ferradasotelo.1@uni.massey.ac.nz

Appendix V: Statement on the Use of Large Language Model and Generative Artificial Intelligence

In accordance with Massey University's academic integrity regulations, this statement discloses the use of Generative AI tools during the preparation and redaction of this research project. These tools were utilised ethically as a collaborative framework for code improvement and debugging; planning, exploration, and linguistic refinement. The tools utilised are listed below:

- **Google Gemini (Paid Tier):** Utilised for structural planning, conceptual exploration of Integrated Pest Management (IPM) frameworks, and improving the flow and technical clarity of drafted text.
- **Anthropic Claude (Paid Tier):** Used to improve, debug and support Python script coding created to perform the bioinformatic pipeline.
- **OpenAI ChatGPT (Paid Tier):** Utilised to extract metadata from selected peer-reviewed papers (see subsection [4.8.8.]).
- **Google NotebookLM (Paid Tier):** Employed for synthesising literature tracking and thematic analysis across a corpus of peer-reviewed research papers.
- **Grammarly (Paid Tier):** Used for advanced spelling, grammatical correction, and ensuring consistency in professional tone.

Appendix VI: Code Availability

All custom Python scripts developed for the bioinformatic analyses in this thesis — covering intron excision, sequence alignment, variant calling and effector-integrity classification, generation of the conservation and divergence figures, and the literature cross-reference filter — are available from the author upon request.